ANALYSIS OF HIGH VOLTAGE CURRENT TRANSFORMER UNDER DETERIORATING AND FAILED INSULATION

BY

VUSUMUZI SAMUEL MAHLASELA

Bsc (Eng)

Submitted in partial fulfillment of the requirements for the degree of Master of Science in Engineering, in the School of Electrical, Electronic and Computer Engineering, University of KwaZulu Natal, South Africa

Supervisors: Prof A M Chol

Prof A A Jimoh

March 2006

ABSTRACT

Data pertaining to the number of failed high voltage current transformers installed in transmission substations by Eskom has been collected for a period from 1982 to 2000. The collected data was populated into a database. The data was then analysed and the single phase faulting was identified as the most dominant failure mode. The failure mode identified formed a cornerstone to the model that was developed. This model in turn served as the means for analysis and critical probing into the behaviour of this equipment. All possible scenarios that could lead to insulation failure within a CT were investigated.

For all the scenarios considered, the steady and transient equations relating the state variables of the model have been developed and analysed. For the implementation of the model, the model parameters were determined through laboratory experiments. Model implementation was performed in Matlab© for steady state analysis and Simplorer© for transient analysis. The CT insulation was modeled as a parallel combination of resistance and capacitance. The model showed at which values of resistance and capacitance when the insulation is perfect, deteriorating and complete failure. The magnitudes of current and voltage at which the insulation breakdown takes place have been demonstrated. This helps to explain why the failures experienced by Eskom were so catastrophic.

ACKNOWLEDGEMENTS

I would like to thank Eskom for the financial support which they provided for this work to be realized and University of KwaZulu Natal HVDC Centre for affording me the opportunity to carry out this research work.

In addition, I would like to thank the following people:

My family for their support, patience and their best wishes

Prof AM Chol and Prof AA Jimoh for their leadership while carrying out this work

God for making everything possible

TABLE OF CONTENTS

APPENDICES

LIST OF FIGURES AND TABLES

TABLE

LIST OF SYMBOLS AND ABBREVIATIONS

The commonly used symbols and notations adopted in this dissertation are listed below. Other symbols used in the text are explained where they first occur.

Acronyms

CT	Current Transformer
HV	High Voltage
kV	Kilo Volts

Current transformer model parameters

R_{ins}	insulation resistance
C_{ins}	insulation capacitance
Z_p	primary impendance
n	inter-turn ratio
m	inter-turn ratio
I_{source}	supply current in the primary windings
R_p	primary winding resistance
L_p	primary winding inductance
I_{mag}	magnetizing current
L_m	magnetising inductance
R_m	magnetizing resistance
R_s	secondary winding resistance
L_s	secondary winding inductance
R_{burden}	burden resistance
L_{burden}	burden inductance
I_{sec}	secondary current

I_{ins}	insulation current
Z_m	magnetizing impedance
Z_s	secondary winding impedance

CHAPTER ONE

INTRODUCTION

1.0 INTRODUCTION

The restructuring of the electricity market worldwide, especially in European and American countries has changed the way things were done due to competition in the market. The electricity market in these countries has been dominated by regional or national monopolies. During the past few years, this picture has been changing significantly and it is soon going to hit South African shores. Eskom, the South African utility has enjoyed a national monopoly since its inception, but in the next few years this picture will change drastically due to privatization.

The privatization of the electricity utilities has put utilities under severe pressure to reduce cost in order to be competitive. The trend towards free competition and privatization with the related demand on return on investments, results in a cost consciousness among utilities [1],[2]. Planned maintenance has been seen as a contributor to high cost investment with very little return on investment. The objectives of planned maintenance are to avoid failures by ensuring the plant is in good condition, minimizing the duration and/or the frequency of un-planned outages, preserving the long term integrity of assets, sometimes environment responsibility , safety responsibility and statutory requirements.

Before, much emphasis was placed on cost. Planned maintenance was a routine activity which every utility carried out as a necessity. The frequency of planned maintenance was determined from manufacturer specifications and recommendations, performance of the plant, environment which the plant is exposed to and sometimes 'thumb suck' rule from experienced personnel within the

organization. Planned maintenance is executed in the plant even if it was not required. This was done as prescribed by utilities standards although sometimes it was neither improving performance, nor reducing network outages but was for satisfying management of the utility. In most scenarios a breakdown of plant would occur after execution of the planned maintenance [3].

Experience has shown that planned maintenance is expensive and it does not guarantee the prevention of plant failure. This became a concern to all utilities because their high investment on planned maintenance results in little or no return, or in some cases total loss [4]. This is the case with the failures of current transformers in Eskom. The failure of a current transformer (CT) in a utility could result in a loss of revenue, network outages, damage to the adjacent equipments that could be up to millions of rands and pose a safety risk to the operating personnel [5]. Due to risks that equipment in the field are exposed to and the transformation in the electrical industry which require justification for any investment made, maintenance engineers worldwide had to come up with solutions to solve the problems. Economic pressure was forcing the industry to reduce maintenance while increasing reliability and availability of all equipment.

Eskom, South African utility has in excess of 1000 CTs in their transmission substations, which can amount to more than a billion rands in investment. Standards for maintaining these equipment in Eskom are available and management are enforcing them to be followed. The failure rate of CTs in Eskom's transmission substations has reached an alarming rate which any utility can not tolerate [4]. Planned maintenance is done as per standard,but this has not prevented the CTs failures. Causes of CT failures and modes of failures are not understood.

1.1 Problems Definition and Objectives

High voltage bushings and current transformers are among the most vulnerable power system's equipment because they are subjected to high dielectric and thermal stresses. Sudden failure of a current transformer in the transmission substation can cost a utility in excess of one million rands in damage and loss of revenue [5].

The failure pattern of current transformers in Eskom has generally been violent, catastrophic and in some instances near fatal. The nature of these failures makes it difficult in most cases for an Eskom investigation team to determine the root cause of the failure [5].The objectives of this work is to:

1. Develop a database and analysis of current transformers failures experienced by Eskom.

2. Use the database findings to develop and implement a current transformer model that will lead to the understanding of the phenomena and processes that leads to violent and sudden failure of CTs in HV substations.

1.2 Solution Methodology

In Eskom there has been some work done on the power transformer failures. The common modes of failures for the power transformer were determined by looking at the workshop records where failed transformers were dismantled to determine the root causes of failures. From the workshop records, a database was formed to determine dominant cause of failure.. In this study, the same approach has been taken to determine the most common mode failure that HV current transformers normally suffer.

The investigation records from Eskom CT Investigation Group were obtained to prepared CT failure database. The staff from the Investigation Group were interviewed for additional information which may be missing on the investigation report. After the analysis of the investigation reports and information from the interviews, a comprehensive database of failures experienced so far was prepared. Statistical methods were used to analyse the database prepared from the investigation reports.

After the analysis of the current transformer database a model was developed with the help of the results from the database and some background work done on this topic. All the possible scenarios that the HV CT can be exposed to, were then investigated using this model with the goal to determine the phenomena preceding the failure. Steady state and transient conditions were investigated, and the influence of changes in the insulation state of the device on its state variables became the focal points of the analyses. The steady state equations of the model were implemented in Matlab© software while transient equations were implemented in Simplorer© software.

1.3 Dissertation Layout

The First chapter is an introduction of the problem that Eskom is currently facing where CT failures experienced have been violent and investigation conducted were not conclusive, hence the objectives of this work was to develop and implement the current transformer model to contribute to the understanding of the phenomena and processes that leads to violent and sudden failure of CTs in HV substations.

Chapter Two highlights the description of CT failures database and reasons why it was done. Data is examined to determine the most common mode of failure of CTs in the transmission substation with the voltage rating from 88kV to 400kV.

Chapter 3 is devoted for model development. Results from the analysis of the database played an important role in the development of the model. Different scenarios that the CT in Eskom transmission substation can be exposed are considered in this chapter.

Implementation of the model is contained in Chapter Four. For this work steady state equations were developed and simulated using Matlab software. Transient analysis of the model was also done and the development of the corresponding equations. The analysis of the steady state and transient results are discussed

Chapter Five summarises all that has been achieved in this work and the further work that can be pursued on the same topic.

CHAPTER TWO

CURRENT TRANSFORMER FAILURES DATABASE

2.1 Introduction

Some information in high voltage current transformers in Eskom's 153 transmission substations are presented in Table 1. The total value of this plant is in excess of R700M [5]. Most of the current transformers that Eskom uses are hermetically sealed. Due to the seal, the quality of the high voltage paper and oil can not be easily evaluated, without breaking the seal, which can lead to introduction of moisture [6]. The quality of the seal deteriorates over the 30 years of service in the harsh South African weather conditions, where summer temperatures of 40 degrees are common, and moisture ingress and deterioration of the insulation quality is only a matter of time [6]. After deterioration of insulation, a violent or catastrophic failure will normally follow. The failure of one current transformer is normally accompanied by damage to the adjacent equipment, buildings, quality of supply due to voltage depressions and sometimes poses risk to Eskom personnel working in the vicinity of the equipment. To rectify the situation an outage is normally arranged for which the customers go without electricity for the duration of the outage.

Table 1: Eskom, Transmission installed current transformers [6]

	No of CTs	**No of Substations**
Total (400, 275,220, 132, 88,66 kV)	8886	135
Average per substation	66	

The failure of one CT does not cost less than one million rands per incident, which may prove costly for any utility [5]. The mentioned cost is for putting the system back to normal and excludes cost suffered by customer due to power loss and production lost in some instances. Eskom has to intervene to eliminate any risk associated with its plants, danger posed to personnel working in the vicinity of the equipment, quality of supply delivered to the customers and cost associated with the failure of current transformer. Eskom has tried to implement various methods to ensure that they correctly intervene before any failure.

2.2 Background to the development of the database

During the literature survey it was discovered that Eskom has done work on the power transformer failures. In the power transformer research work available databases were searched to get insight into the dominant failure mode [7]. In this study interrogation of historical records of the failed power transformer from the workshop was also carried out.

With this in mind it was decided to embark on the search of the available information on the CT failures because this would form a corner stone of this study. There was no existing database within Eskom with the information of the CTs failures with their failure mode and causes of such failures. After the investigation, staff in the Instrument Transformer Support Group were interviewed to determine the available information on CTs failures. It was discovered that this department is in charge of investigating any CT failures in Eskom country wide. They explained the whole procedure on how they get involved on investigating the CTs failures.

After discussion with the staff it was discovered that the post-mortem reports are not properly stored. There was no standardised source of storing this useful

information from the investigations. In this work it was decided to collect all the available information. This was done by spending 2 weeks with the Instrument Transformer Support Group. All the possible sources of post-mortem reports were thoroughly interrogated. When there was a doubt with the report, an interview was held with the author of that particular report to remove any uncertainties. Where the authors were not available for the interview because he or she has left Eskom, the Head of Department was interviewed.

The post-mortem reports were obtained from different sources like staff personal computers, unofficial filing cabinets in the Head of Department's office and desks of the staff personnel of this department. This was viewed as a deficiency from the information management point of view. There was no workshop where information could be searched about repairs they have done on the CTs. With all the information obtained from the Current Transformer Support Group a database was prepared as shown in Appendix A1.

From the literature it was discovered that generally the current transformer failures are due to the following problems [4]:

- Electric circuit faults(winding short circuits, insulation failure, bad joints, partial discharge)
- Magnetic circuit faults(circulating currents)
- Dielectric circuit faults (moisture in oil, paper) .
- Others fault includes transportation problems, faulty manufactured equipment.

Results of the database

Several databases (like Phoenix, Orion and Permac) exist within Eskom transmission department but they do not have details of CT failures. The existing databases consisted of the current transformer's asset information but lacked failure details. During the literature survey, post mortem Manual Reports were identified as the only source with CT failures. It was decided to collect these Manual Reports and conduct interviews to form a comprehensive database as can be seen in Appendix A1. The following results were obtained from Manual Reports and interviews and were used as the basis for this study. There could be more current transformer failures that Eskom has experienced but this information could be lost due to investigation teams not documenting the failure or capturing them into any source of data records.

Table 2: Current Transformers Failure records (from 1982-1999)

Voltage(kV)	No of failures
400	30
275	31
220	2
132	33
88	2

From the above records, manufacturers of the failed current transformers were as follows:

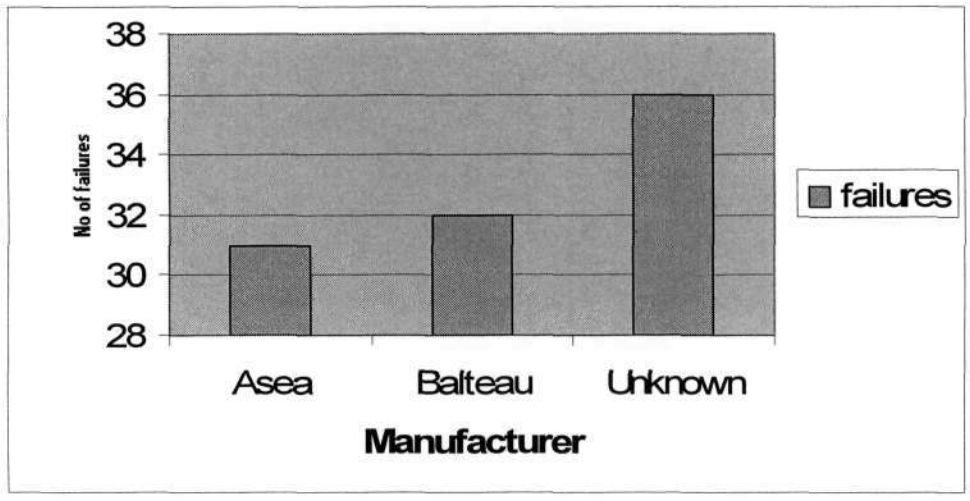

Fig.1: Current Transformers Failures classified according to manufacturer

Eskom has an installed database of 8886 CTs in their substations. From Fig.1 it can be noted that majority of failures has been dominated by Balteau manufactured CTs with 32 failures out 96 failures of the available information. Although the number of Balteau failures is a small percentage compared to the installed base but it should be closely monitored.

It was decided to use the available information to determine which month of the year are the failures dominant. The reason for the investigating seasons of the year was because of the temperature variations within season of the year. The failures distribution was as shown in Fig.2 which showed more failures were experienced in months during storm seasons. It can be concluded that temperature variation (seasonal variations also include precipitation and pressure) could be factor to the recorded failures of CTs.

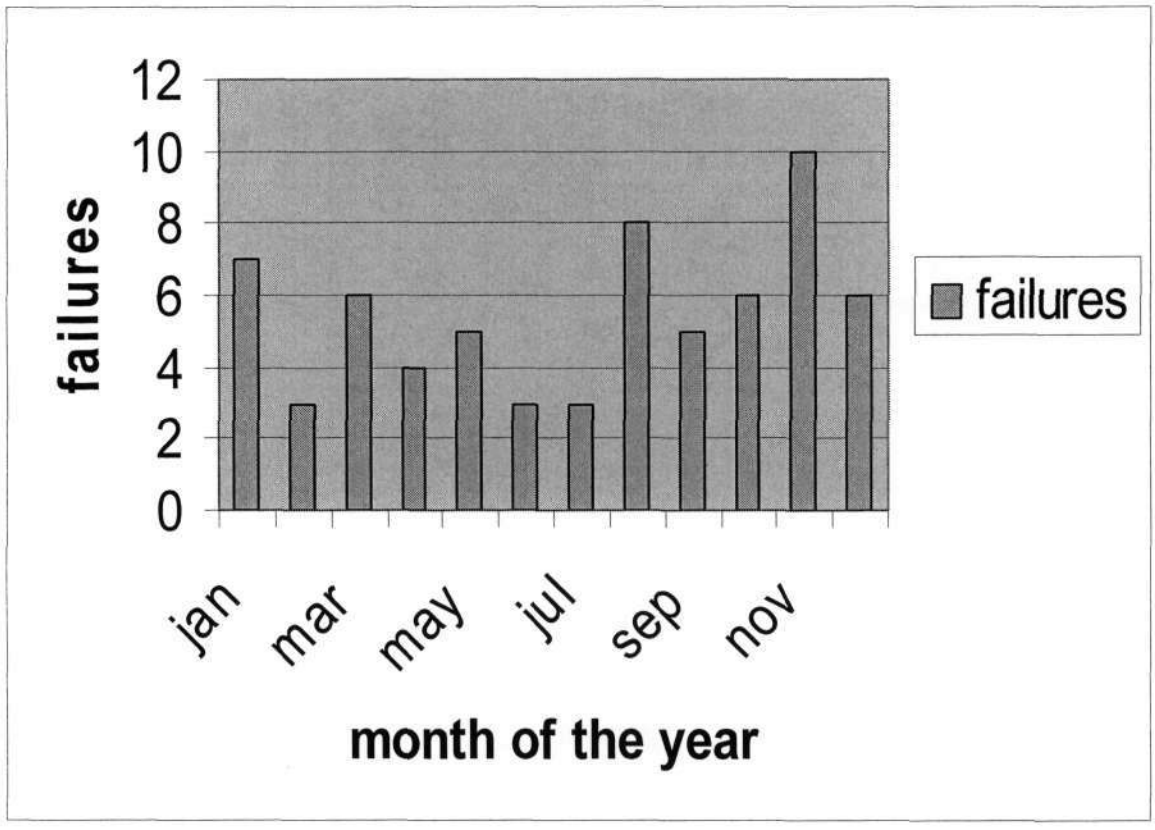

Fig.2: CT Failure distribution per month (Appendix A)

Fig.3 shows different types of current transformer design in the Eskom transmission substations. When the design of CT was not mentioned in the fault report then it was designated as unknown. From the available information top core CT design dominated failures experienced.

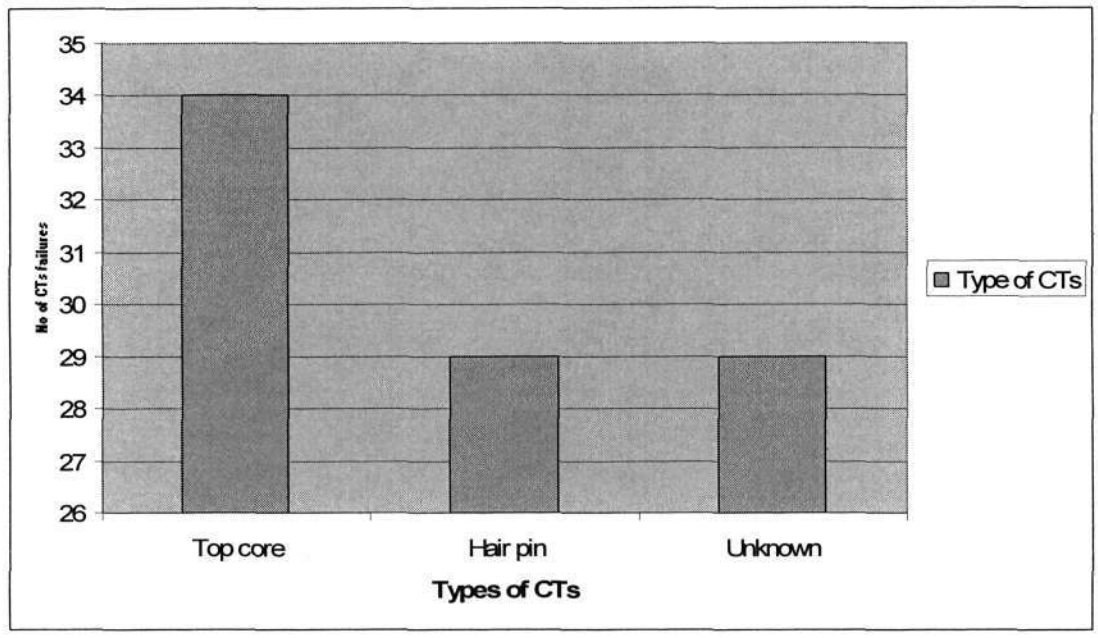

Fig.3: Design type distribution [Appendix A]

Table 3: Failure modes of CTs

Failure mode	Cause	Number
Insulation failure	Unspecified	24
Single phase faulted	Unspecified	58
Unknown	Unspecified	6
Pre-energisation	Unspecified	2
Star point fault	Unspecified	1
Tank rapture	Unspecified	1

Table 3 shows information extracted from the Manual reports. The dominant failure mode is single phase fault which could be due to insulation failure. Single

phase faults and insulation failure were the most dominant failures from the database, hence the investigation of insulation failure mode in the proceeding chapters of this dissertation.

2.4 Conclusion

Valuable information was collected and prepared into a database where information about current transformer failures in Eskom transmission networks to year 2000 can be obtained. Various analysis of the information forming the database has been presented. From the analysis the most affected design was identified. The database showed single phase fault failure as the dominant failure mode which could be related to insulation failure, hence strengthening why insulation failure was investigated during model development. A modified structure of the investigation report format could assist in identifying the causes of the failures and a modified investigation report can be viewed in Appendix A2. Continual update of the database prepared in this work, is encouraged.

CHAPTER THREE

Model Development

3.1 Introduction

Finding an engineering solution to a problem which is not well understood can be a difficult task. As described in the previous chapters, the nature of CT failures experienced by Eskom in their transmission substations has been impossible to determine the phenomena and processes leading to the violent nature of the failures. In this study it was decided to develop a current transformer model where possible causes of CTs failures can be simulated to acquire a better understanding of the failures experienced.

3.2 Background to the development of the model

Fig. 4 is a cut-away view of a typical current transformer showing the primary windings terminal which are normally connected directly to the HV line [8,9]. The insulator (normally porcelain material) isolates the inner part of the CT from moisture. As can be seen from Fig.4, there is no physical link between the primary current carrying conductor and secondary current carrying conductor. The link is through electromagnetic coupling through the core.

Insulation failure mode is what would be investigated in this work. The insulator was modelled as a parallel combination of resistance and capacitance which is regarded to be the practical representation [9] as shown in Fig.4.

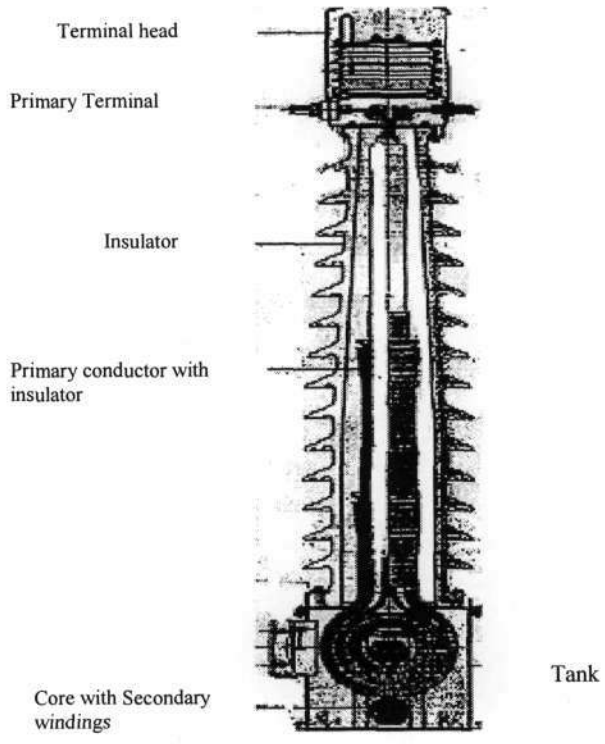

Fig.4 Hair Pin HV Current transformer [9]

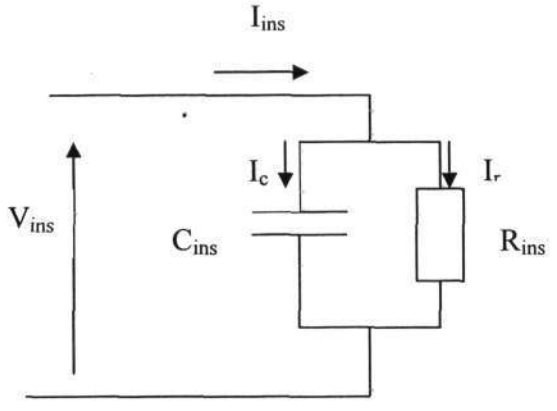

Fig.5 Equivalent circuit of a practical insulator

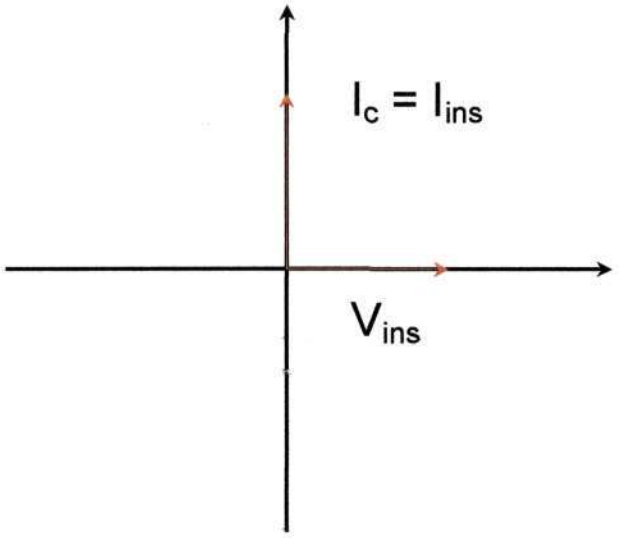

Fig.6: Phasor diagram of an ideal insulator ($R_{ins}=0$)

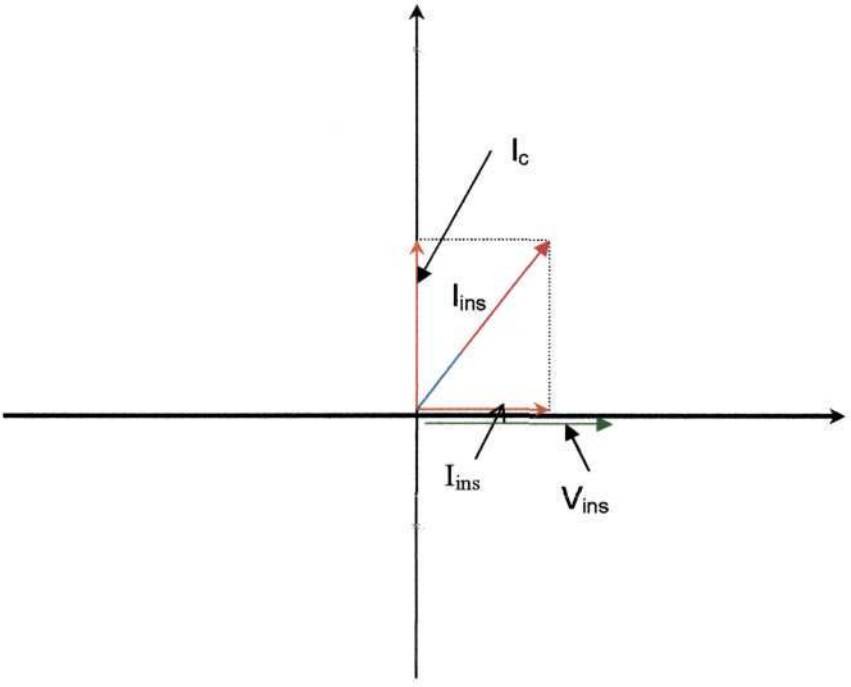

Fig.7: Phasor diagram of practical insulator

For an ideal insulator the angle between current and voltage is exactly 90 degrees (Fig 6). However, in a practical insulator, the angle is smaller than 90 degrees due to resistive current component (Fig 7). There are combinations of scenarios which

may lead to insulation deterioration or failure within the current transformer but this thesis will consider the following scenarios for the development of the CT model.

- Inter-turn failure within the primary winding
- Inter-turn failure within secondary winding
- Insulation failure between primary and secondary winding
- Insulation failure between secondary winding and the core
- Insulation failure between primary winding and the core
- Insulation failure between primary winding and the ground
- Insulation failure between secondary winding and the ground

It is, however, important to emphasis that all the scenarios mentioned above would not occur at the same time. A combination of these factors may, however ,deteriorate or fail concurrently or in a cascade form. For all the above mentioned scenarios, the CT model was initially developed ignoring the presence of a current controlled voltage breakdown due to the insulation deterioration or failure. Later on, this assumption was removed. Apart from being a model development necessity, this allowed for a better understanding of the roles played by the various parameters or state variables.

3.3 Model Development and Associated Equations

3.3.1 Models with Breakdown Voltage ignored

The following section will concentrate on model development and the associated equations when breakdown voltage is assumed to be absent.

3.3.1.1 Insulation breakdown within primary winding only

Inter-turn insulation breakdown may be represented as shown in Fig.8

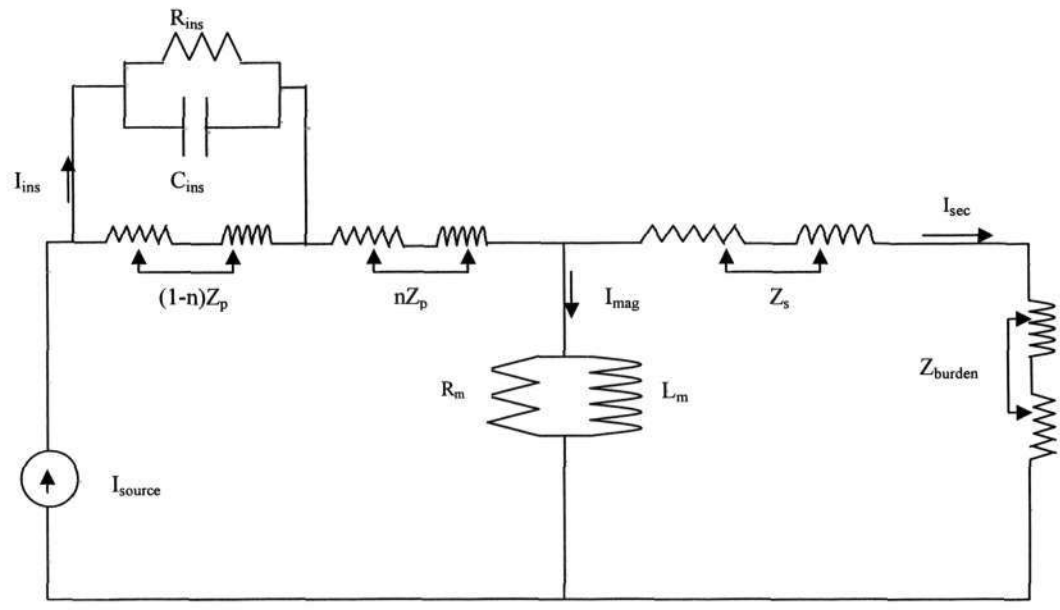

Fig.8: Inter-turn breakdown between primary winding

The primary function of the current transformer is to transform current magnitude, hence we decided to use current source as the main source for the model. The model consists of the primary windings labelled as Z_p. The primary windings consist of resistance and inductance. The primary windings have been divided into n turns to show that a failure or deterioration within primary windings can happen anywhere. The scenario presented in Fig.8 occurs when there is an insulation deterioration or failure within primary windings only. The insulation is represented as parallel combination of resistance and capacitance as shown in Fig.8. For a perfect insulator, an open circuit is presented by the insulator representation to the current flow of I_{ins}. When the insulator starts to deteriorate until failure, a short circuit is presented by the insulator representation to the current flow of I_{ins}. The magnetising windings which link primary and secondary windings are represented by parallel combination resistance (R_m) and inductance (L_m). The secondary windings of the CT model in Fig.8 are represented by resistance (R_s) and

inductance (L_s). The burden that is normally presented in the secondary of the CT is represented by series resistance (R_{burden}) and inductance (L_{burden}).

3.3.1.1.1 Steady State Equations

The steady state equations governing the model in Fig.8 are as follows;

$$I_{ins} = \frac{(1-n)Z_p}{(1-n)Z_p + Z_{ins}} I_{source} \quad (1)$$

Where I_{ins} is the insulation current

I_{source} is the source current and Z_p is the primary winding impedance given by

$$Z_p = R_p + jX_p \quad (2)$$

R_p is the primary winding resistance

X_p is the primary winding reactance

The insulation impedance may be expressed by

$$Z_{ins} = \frac{R_{ins}C_{ins}}{R_{ins} + C_{ins}} \quad (3)$$

R_{ins} is the insulation resistance

C_{ins} is the insulation capacitance

$$I_{sec} = \frac{Z_m}{Z_m + Z_{sb}} I_{source} \quad (4)$$

I_{sec} is the secondary current

$$Z_{sb} = R_s + R_{burden} + j(X_s + X_{burden}) \quad (5)$$

Z_{sb} is the combination of secondary winding impedance and the burden impedance

$$I_{mag} = \frac{Z_{sb}}{Z_m + Z_{sb}} I_{source} \quad (6)$$

I_{mag} is the magnetising current

Z_m is the magnetising impedance, which is

$$Z_m = \frac{(R_m)(j * X_m)}{R_m + j * X_m} \tag{7}$$

R_m is the magnetising winding resistance

X_m is the magnetising winding reactance

R_s is the secondary winding resistance

X_s is the secondary winding reactance

R_{burden} is the burden winding resistance

X_{burden} is the burden winding reactance

3.3.1.1.2 Transient State Equations

With the aid of mesh current analysis, starting from the left hand side of the circuit, the transient equations governing the model in Fig.8 may be formulated as follows. The loop equations were used to develop the following equations and the transient equations to follow in this dissertation. The loop currents are indicated as per Fig.9 and same principle was applied for the following transient equations in the dissertation.

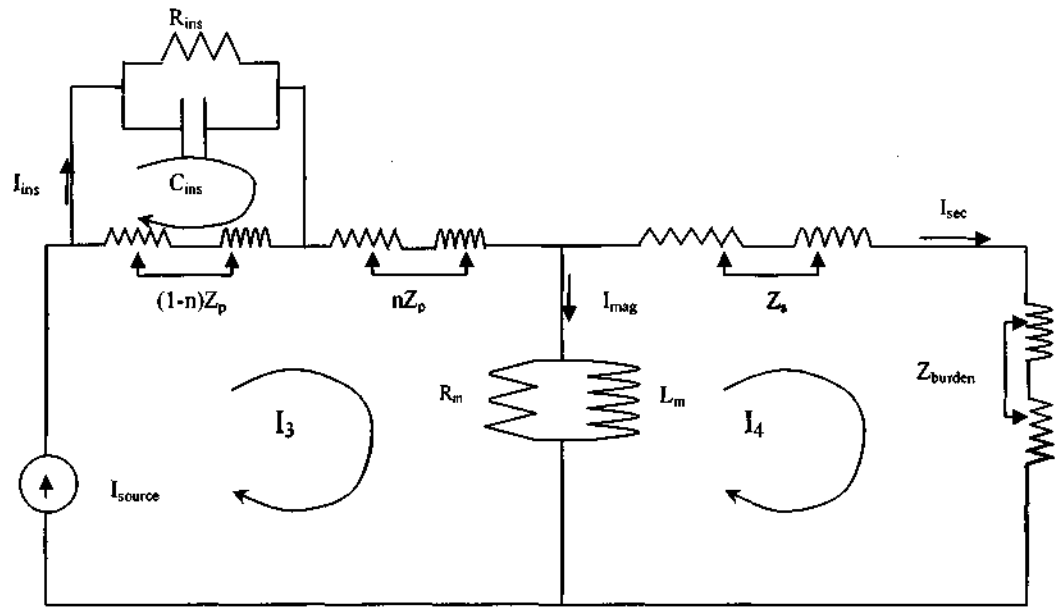

Fig.9: Inter-turn breakdown between primary winding

$$i_1 R_{ins} + \frac{1}{C_{ins}} \int_0^t (i_1 - i_2)dt = 0 \qquad \textbf{(8)}$$

$$\frac{1}{C_{ins}} \int_0^t (i_2 - i_1)dt + (i_2 - i_1)(1-n)R_p + (1-n)L_p \frac{d}{dt}(i_2 - i_1) = 0 \qquad \textbf{(9)}$$

$$(i_3 - i_2)(1-n)R_p + i_3(nR_p + R_m) + ((1-n)L_p \frac{d}{dt}(i_3 - i_2) + nL_p \frac{di_3}{dt} = 0 \qquad (10)$$

$$(L_s + L_{burden} + L_m)\frac{di_4}{dt} + i_4(R_s + R_{burden}) = 0 \qquad (11)$$

The state variables of the model can be calculated as follows;

$$I_{ins} = 2i_1 - i_2 \qquad (12)$$

$$I_{mag} = i_3 - i_4 \qquad (13)$$

$$I_{sec} = i_4 \qquad (14)$$

3.3.1.2 Insulation Breakdown between the Primary Winding and Ground

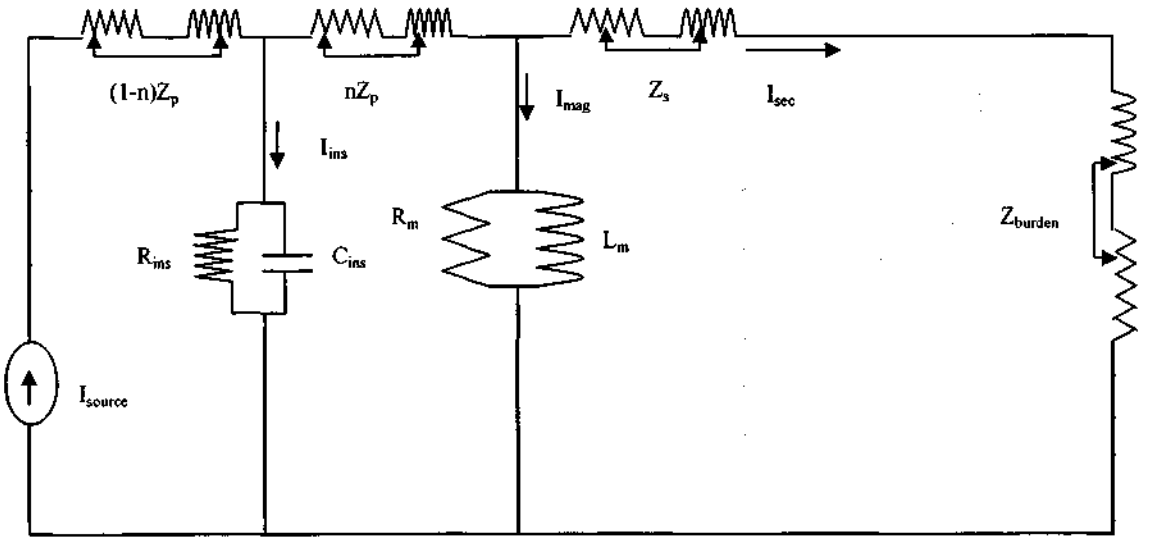

Fig .10: Insulation failure between Primary Winding and Ground

Under the condition of insulation breakdown between primary winding and ground, the model of the CT will be as shown in Fig.10, where the definition of parameters are the same as in section 3.1.1.

3.3.1.2.1 Steady state equations

The steady state equations governing the model in Fig.10 are as follows

$$I_{ins} = I_{source} \frac{Z_{eq}}{Z_{ins} + Z_{eq}} \qquad (15)$$

where Z_{eq} is the equivalent impedance of secondary, burden, magnetising and primary windings given as

$$Z_{eq} = nZ_p + \frac{Z_{sb}Z_m}{Z_{sb} + Z_m} \tag{16}$$

$$I_{mag} = I_{p2}\frac{Z_{sb}}{Z_{sb} + Z_m} \tag{17}$$

I_{p2} is the current flow through nZ_p which can be obtained using current divider rule

$$I_{sec} = I_{p2}\frac{Z_m}{Z_{sb} + Z_m} \tag{18}$$

3.3.1.2.2 Transient State Equations

Using the same analysis as in section 3.1.1.2, the transient equations governing the model in Fig 10 are as follows;

$$(1-n)(I_{source} - i_1)R_p + (1-n)L_p\frac{d}{dt}(I_{source} - i_1) + i_1R_{ins} = 0 \tag{19}$$

$$i_3(nR_p + R_m) + nL_p\frac{di_3}{dt} + \frac{1}{C_{ins}}\int_0^t i_2 dt = 0 \tag{20}$$

$$(L_{burden} + L_s + L_m)\frac{di_3}{dt} + i_3(R_s + R_{burden}) = 0 \tag{21}$$

3.3.1.3 Insulation breakdown within secondary winding

Inter-turn insulation breakdown in the secondary winding may be represented as shown in Fig. 11;

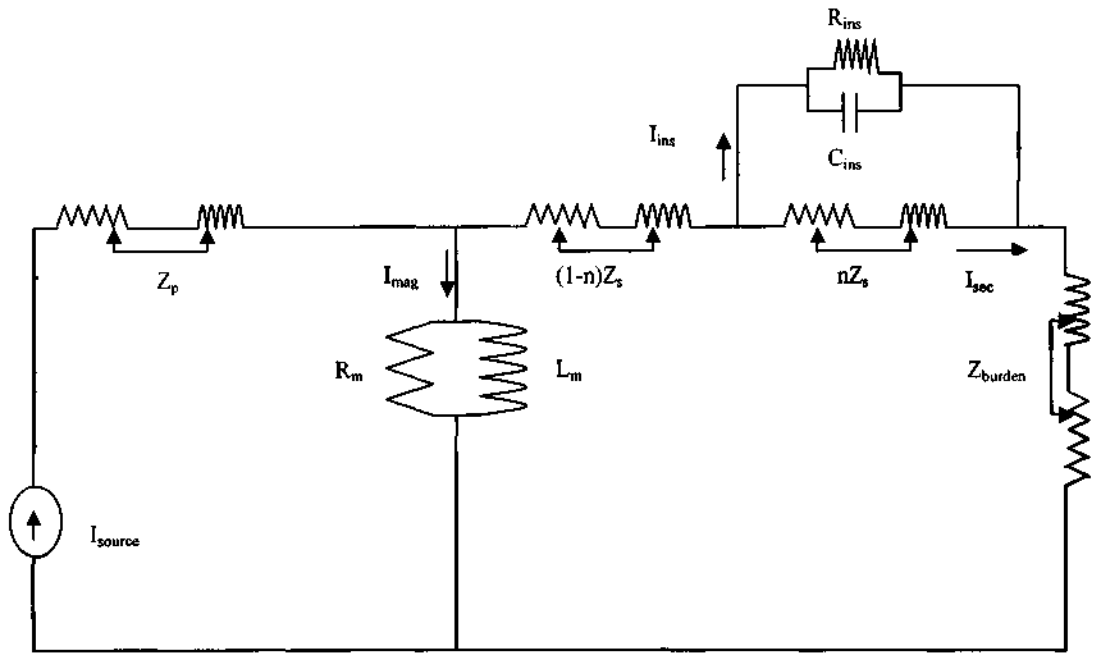

Fig.11: Inter-turn failure within Secondary Windings

The parameters description in Fig.11 is the same as the previous scenarios except that the secondary windings have been divided into n terms. N terms division of the secondary winding demonstrate different locations where insulation deterioration or failure can occur.

3.3.1.3.1 Steady State Equations

The steady state equations governing the model in Fig.11 are as follows;

$$I_{sec} = \frac{Z_m}{Z_m + (1-n)Z_s + Z_{equivalent}} I_{source} \quad (22)$$

$$I_{mag} = \frac{(1-n)Z_s + Z_{equivalent}}{Z_m + (1-n)Z_s + Z_{equivalent}} I_{source} \quad (23)$$

Where $Z_{equivalent}$ is the equivalent impedance of Z_{ins}, Z_s and Z_{burden} given as follows;

$$Z_{equivalent} = \frac{Z_{ins} n Z_s}{n Z_s + Z_{ins}} + Z_{burden} \quad (24)$$

$$I_{ins} = \frac{n Z_s}{Z_{ins} + n Z_s} I_{sec} \quad (25)$$

3.3.1.3.2 Transient State Equations

Using the same analysis as in section 3.1.1.2, the transient equations governing the model in Fig.11 are as follows.

$$(I_{source} - i_1)(R_p + R_m) + L_p \frac{d}{dt}(I_{source} - i_1) = 0 \quad (26)$$

$$(L_m + (1-n)L_s + L_{burden})\frac{di_2}{dt} + nL_s \frac{d}{dt}(i_2 - i_3) + i_2((1-n)R_s + + R_{burden}) + nR_s(i_2 - i_3) = 0 \quad (27)$$

$$ni_3 R_s + nL_s \frac{di_3}{dt} + \frac{1}{C_{ins}} \int_0^t (i_3 - i_4)\,dt = 0 \quad (28)$$

$$i_4 R_{ins} + \frac{1}{C_{ins}} \int_0^t (i_4 - i_3)\,dt = 0 \quad (29)$$

3.3.1.4. Insulation breakdown within secondary winding and ground

Model representing insulation breakdown within secondary winding and ground is as shown in Fig.12:

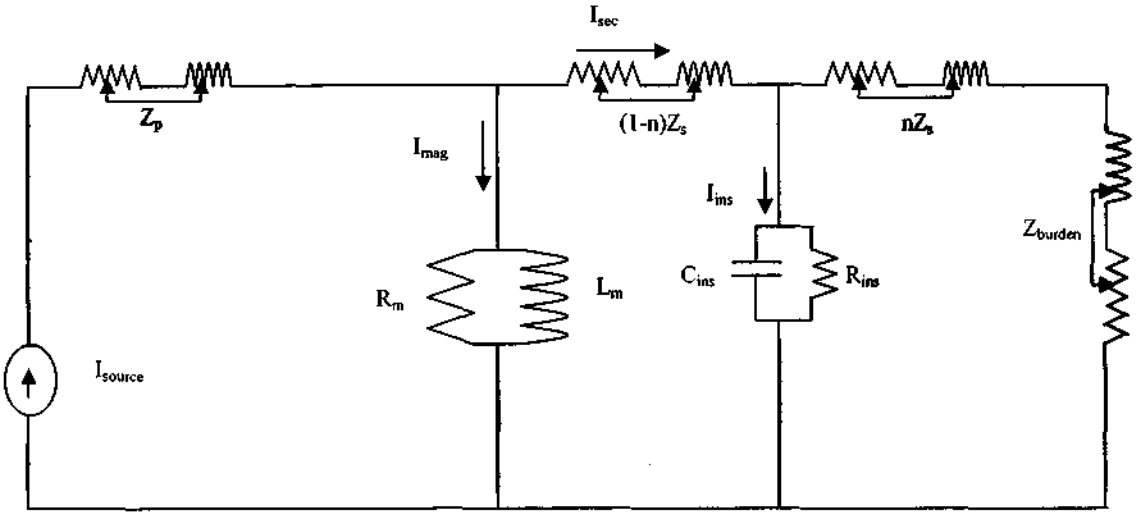

Fig.12: Insulation breakdown between Secondary and Ground

3.3.1.4.1 Steady State Equations

The equations governing the model in Fig.12 may be represented as follows;

$$I_{ins} = \frac{I_{sec}(nZ_s + Z_{burden})}{nZ_s + Z_{burden} + Z_{ins}} \tag{30}$$

$$\text{Where } I_{sec} = \frac{I_{source} Z_m}{Z_m + (1-n)Z_s + Z_{equivalent}} \tag{31}$$

$$Z_{equivalent} = \frac{(nZ_s + Z_{burden})Z_{ins}}{(NZ_s + Z_{burden}) + Z_{ins}} \tag{32}$$

$$I_{mag} = \frac{I_{source}((1-n)Z_s + Z_{equivalent})}{Z_m + (1-n)Z_s + Z_{equivalent}} \tag{33}$$

3.3.1.4.2 Transient State Equations

With the aid of mesh current analysis and applying the same methodology as above section, the transient equations for Fig.12 are as follows

$$(I_{source} - i_1)(R_p + R_m) + L_p \frac{d}{dt}(I_{source} - i_1) = 0 \quad (34)$$

$$(L_m + (1-n)L_s)\frac{di_2}{dt} + (1-n)i_2 R_s + \frac{1}{C_{ins}}\int_0^t (i_2 - i_3)dt = 0 \quad (35)$$

$$(R_{ins} + nR_s + R_{burden})i_3 + (L_s + L_{burden})\frac{di_3}{dt} = 0 \quad (36)$$

3.3.1.5 Insulation Failure between Primary and Secondary Windings

Model representing insulation breakdown between secondary and primary windings is as shown in Fig.13.

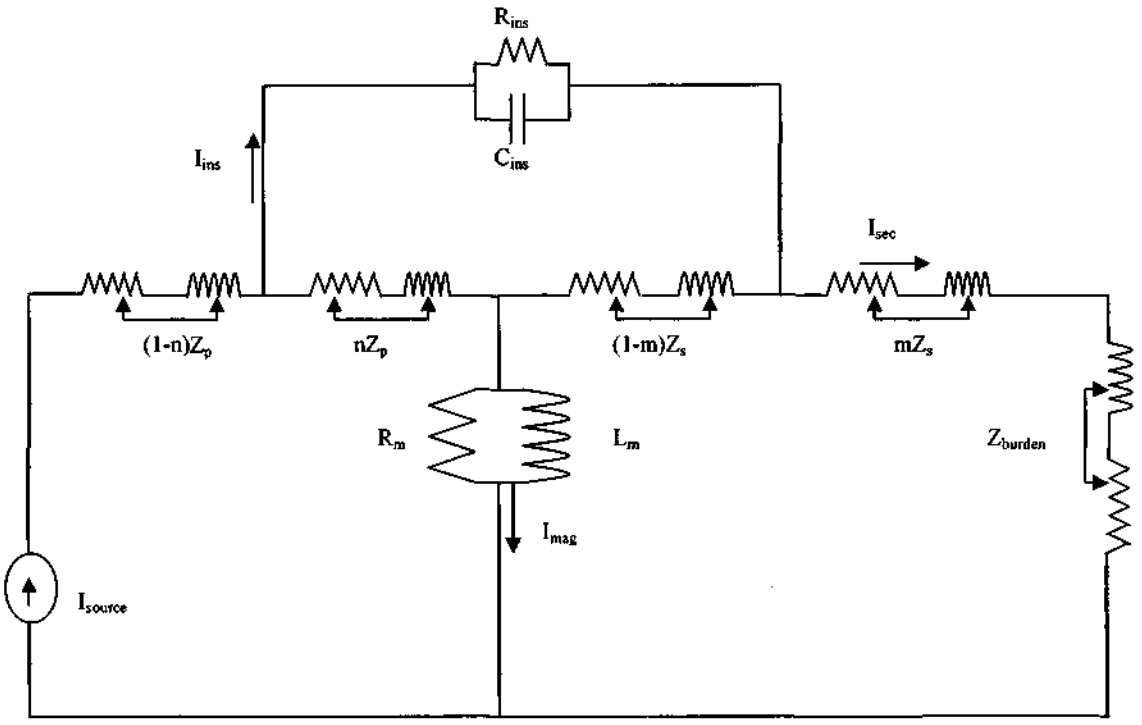

Fig.13: Insulation breakdown between Secondary and Primary Windings

3.3.1.5.1 Steady State Equations

Suppose mesh currents were defined as in section 3.2.1.1.2, then using mesh current analysis method in Fig.13, the following results were achieved;

$$i_1 = I_{source} \tag{37}$$

$$i_2 = \frac{Z_m i_1 + (1-m)Z_s i_3}{Z_m + (1-m)Z_s + mZ_s + Z_{burden}} \tag{38}$$

$$i_3 = \frac{(nZ_m Z_p + (1-n)(1-m)Z_p Z_s + m(1-n)Z_p Z_s)i_1 - (1-m)(n)Z_p Z_s}{(nZ_p + Z_{ins} + (1-m)Z_s)Z_m} \tag{39}$$

which leads to the following expressions

$$I_{ins} = i_2 \quad (40)$$

$$I_{mag} = i_1 + i_3 \quad (41)$$

$$I_{sec} = i_3 \quad (42)$$

3.3.1.5.2 Transient State Equations

The same definitions of mesh currents in section 3.3.1.5.1 were used to obtain the following equations for Fig.13.

$$((1-n)R_p(I_{source} - i_1) + i_1R_m + (i_1 - i_2)nR_p + (1-n)L_p\frac{d}{dt}(I_{source} - i_1) + nL_p\frac{d}{dt}(i_1 - i_2) = 0 \quad (43)$$

$$nR_p(i_2 - i_1) + (1-m)R_s)(i_2 - i_3) + nL_p\frac{d}{dt}(i_2 - i_1) + (1-m)L_s)\frac{d}{dt}(i_2 - i_3) + \frac{1}{C_{ins}}\int_0^t i_2 dt = 0 \quad (44)$$

$$(1-m)R_s(i_3 - i_2) + (mR_s + R_{burden})i_3 + (1-m)L_s(\frac{d}{dt}(i_3 - i_2) + (mL_s + L_{burden})\frac{di_3}{dt} = 0 \quad (45)$$

3.3.1.6 Insulation breakdown between Primary Winding and the Core

Model representing insulation breakdown between primary windings and the core is as shown in Fig.14. The magnetising winding has been divided into m terms for the same reason as section 3.1.3.

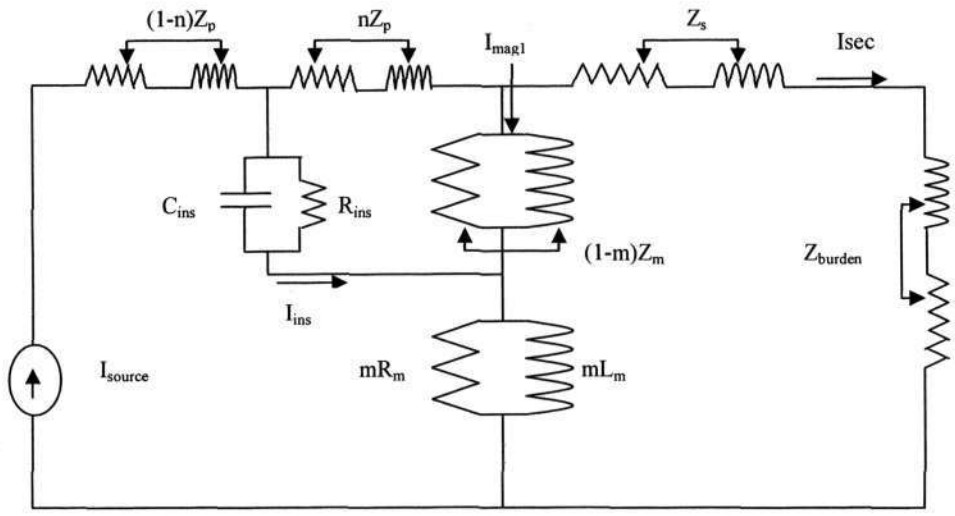

Fig.14: Insulation breakdown Primary Windings and Core

3.3.1.6.1 Steady State Equations

Using the mesh current analysis method, with the definition of mesh currents as in section 3.1.5.1, the mesh current values for Fig.14 are as follows;

$$i_1 = I_{source} \tag{46}$$

$$i_2 = \frac{Z_{ins} i_1 + (1-m) Z_m i_3}{nZ_p + Z_{ins} + (1-m) Z_m} \tag{47}$$

$$i_3 = \frac{nZ_{ins} Z_m i_1 + (1-n)(1-m) Z_p Z_m + (1-m) Z_{ins} Z_m + (1-m) nZ_m}{((1-m) Z_m + mZ_m + Z_s + Z_{burden}) Z_{ins} + (1-m)(m) Z_m^{\,2}} \tag{48}$$

This leads to the following expressions

$$I_{ins} = i_1 + i_2 \tag{49}$$

$$I_{mag1} = i_2 + i_3 \tag{50}$$

$$I_{mag2} = i_1 + i_3 \tag{51}$$

$$I_{sec} = i_3 \tag{52}$$

3.3.1.6.2 Transients State Equations

The same definitions of mesh currents in section 3.1.6.1 for Fig.14 were used to obtain the following equations.

$$((1-n)R_p(I_{source} - i_1) + mR_m i_1 + (1-n)L_p \frac{d}{dt}(I_{source} - i_1) + \frac{1}{C_{ins}}\int_0^t (i_1 - i_2)dt = 0 \tag{53}$$

$$(nR_p + (1-m)R_m + R_{ins})i_2 + (nL_p)\frac{di_2}{dt} = 0 \tag{54}$$

$$((1-m)L_m + mL_m + L_s + L_{burden})\frac{di_3}{dt} + (R_s + R_{burden})i_3 = 0 \tag{55}$$

3.3.1.7 Insulation failure between Secondary Winding and the Core

Model representing insulation breakdown between secondary winding and the core is as shown in Fig.15.

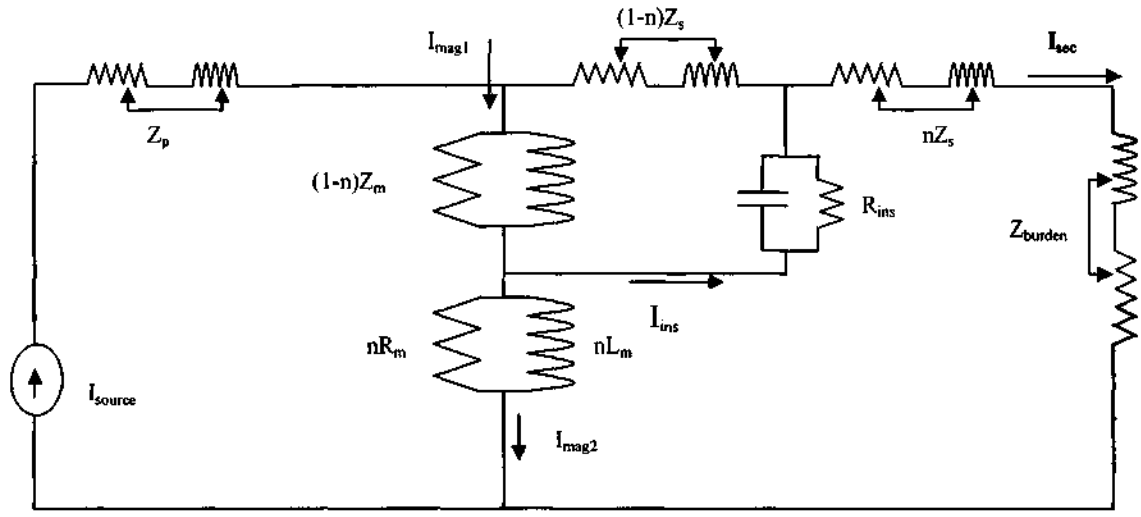

Fig.15: Insulation failure between secondary winding and the core

3.3.1.7.1 Steady State Equations

Using the mesh current analysis method, the mesh current values for Fig.15 are as follows

$$i_1 = I_{source} \tag{56}$$

$$i_2 = \frac{Z_{ins} i_3 + (1-n) Z_m i_1}{(1-n) Z_s + (1-m) Z_m + Z_{ins}} \tag{57}$$

$$i_3 = \frac{(m(1-m) Z_m^{\ 2} + Z_{ins} Z_p + (1-m) Z_m Z_{ins} + m Z_m Z_{ins}) i_1}{(n Z_s + Z_{burden} + m Z_m + Z_{ins})(1-m) Z_m + m Z_{ins} Z_m} \tag{58}$$

This leads to the following expressions

$$I_{mag1} = i_1 + i_2 \tag{59}$$

$$I_{mag2} = i_1 + i_3 \tag{60}$$

$$I_{ins} = i_2 + i_3 \tag{61}$$

$$I_{\sec} = i_3 \tag{62}$$

3.3.1.7.2 Transients State Equations

The same definitions of mesh currents in section 3.1.7.1 for Fig.15 were used to obtain the following equations;

$$((1-m)R_m + mR_m)i_1 + R_p(I_{source} - i_1) + ((1-m)L_m + mL_m)\frac{di_1}{dt} + L_m\frac{d}{dt}(I_{source} - i_1) = 0 \tag{63}$$

$$(1-n)R_s i_2 + ((1-m)L_m + (1-n)Z_s)\frac{di_2}{dt} + \frac{1}{C_{ins}}\int_0^t (i_2 - i_3)dt = 0 \tag{64}$$

$$(R_{ins} + nR_s + R_{burden})i_3 + (mL_m + nL_s + L_{burden})\frac{di_3}{dt} = 0 \tag{65}$$

3.3.1.8 Insulation failure between the Core and the Ground

Model representing insulation breakdown between the core and the ground is as shown in Fig.16:

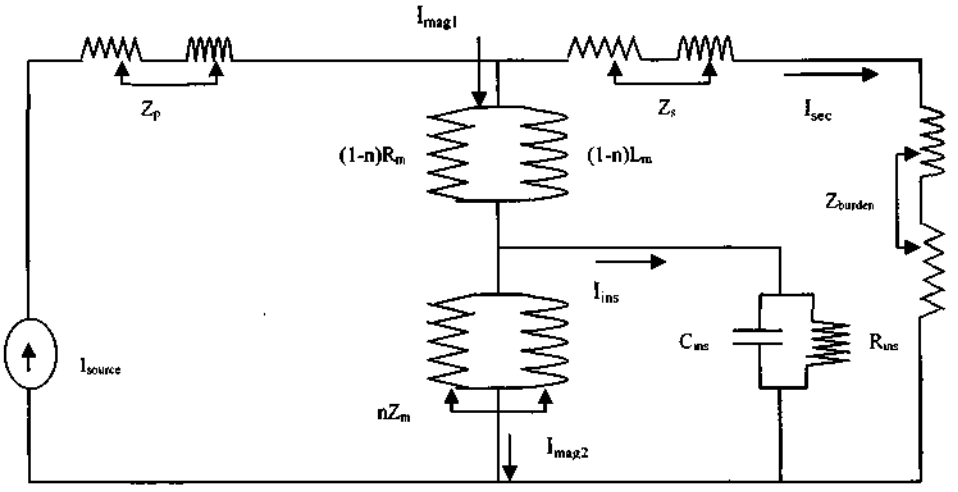

Fig.16 Insulation failure between the core and the ground

3.3.1.8.1 State Steady Equations

The equations governing the model in Fig.16 are as follows

$$I_{ins} = \frac{nI_{mag}Z_m}{nZ_m + Z_{ins}} \tag{66}$$

$$I_{mag} = \frac{I_{source}Z_{sb}}{Z_{equivalent} + Z_{sb}} \tag{67}$$

$$\text{where } Z_{equivalent} = (1-n)Z_m + \frac{nZ_{ins}Z_m}{nZ_m + Z_{ins}} \tag{68}$$

$$I_{sec} = \frac{I_{source}Z_{equivalent}}{Z_{sb} + Z_{equivalent}} \tag{69}$$

3.3.1.8.2 Transient State Equations

With the aid of mesh current analysis, the transient equations for Fig.16 are as follows;

$$((1-n)R_m + nR_m)i_1 + (I_{source} - i_1)R_p + L_p \frac{d}{dt}(I_{source} - i_1) = 0 \quad (70)$$

$$nL_m i_2 + \frac{1}{C_{ins}} \int_0^t (i_2 - i_3)dt = 0 \quad (71)$$

$$(R_{ins} + R_{burden} + R_s)i_3 + ((1-n)L_m + L_s + L_{burdem})\frac{di_3}{dt} = 0 \quad (72)$$

3.3.2 Model with Breakdown Voltage

3.3.2.1 Insulation Failure between Primary Winding and Ground with Breakdown Voltage present

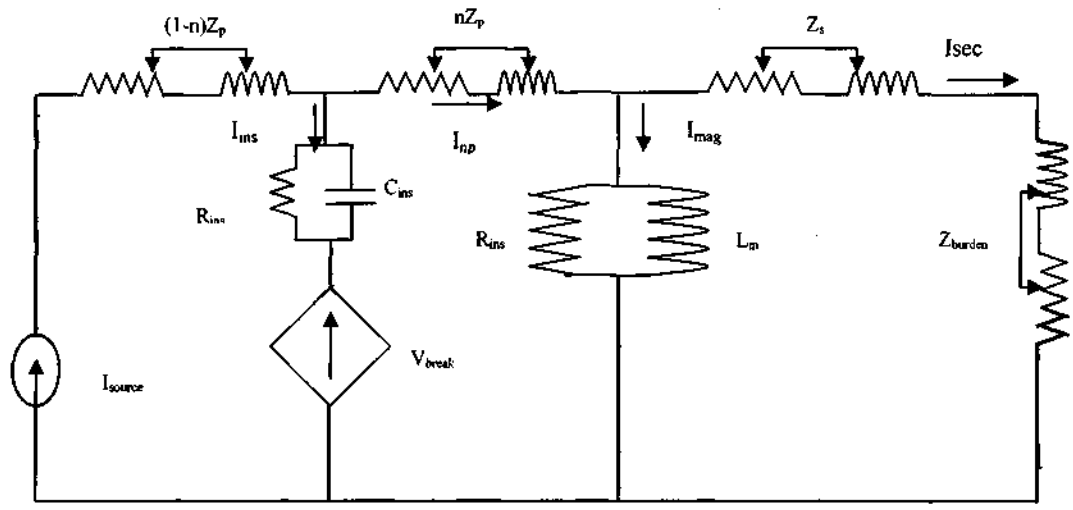

Fig.17: Insulation failure between Primary winding and Ground with Breakdown Voltage

Fig.17 represents insulation failure between the primary winding and ground with current controlled voltage source. Current controlled voltage source was chosen as breakdown voltage representation because the breakdown voltage is dependant on the insulation current flow. When the insulation is perfect, no breakdown voltage is expected to be generated. When the insulation is starting to deteriorate, a current flow through the insulator is expected, which would generate some voltage as per breakdown voltage expression in equation 84. When insulation is presenting a short circuit on Fig.16 (ie when I_{ins} is of high magnitude), breakdown voltage is expected to be at most severe. Only one scenario with breakdown voltage was investigated for this work. An opposite sign of V_{break} to the I_{ins} flow was chosen for this work because it was expected to oppose the current flow.

3.2.1.1 Steady State Equations

Since there were 2 sources present in Fig.17, a superposition principle was applied. A contribution of two sources was considered for obtaining the equations 80 to 94. A subscript one shows contribution when the current source was open circuited

(I_{ins}). A subscript two shows contribution when the voltage source was short circuited (I_{ins2}).

$$I_{ins} = i_{ins1} + i_{ins2} \tag{73}$$

Where $i_{ins1} = \frac{Z_e I_{np}}{Z_{ins} + Z_e}$ (74)

$$Z_e = nZ_p + \frac{Z_{sb} Z_m}{Z_{sb} + Z_m} \tag{75}$$

$$i_{ins2} = \frac{-V_{break}}{Z_{ins} + Z_e} \tag{76}$$

$$V_{break} = V_{primary} \frac{I_{ins}}{I_{ins\,max}} \tag{77}$$

$$I_{mag} = i_{m1} + i_{m2} \tag{78}$$

$$i_{m1} = \frac{Z_{sb} I_{np1}}{Z_{sb} + Z_m} \tag{79}$$

Where I_{np1} is the current through nZ_p

$$i_{m2} = \frac{Z_{sb} I_{np2}}{Z_{sb} + Z_m} \tag{80}$$

$$I_{sec} = i_{sec1} + i_{sec2} \tag{81}$$

$$i_{sec1} = \frac{Z_m I_{np1}}{Z_{sb} + Z_m} \tag{82}$$

$$i_{sec2} = \frac{Z_m I_{np2}}{Z_{sb} + Z_m} \tag{83}$$

3.2.1.2 Transients State Equations

With the aid of mesh current analysis, the following transient equations can be obtained using mesh current description as shown in Fig.17;

$$R_{ins}i_1 + (1-n)R_p(I_{source} - i_1) + (1-n)L_p\frac{d}{dt}(I_{source} - i_1) = -V_{break} \quad \textbf{(84)}$$

$$(nR_p + R_{ins})i_2 + nL_p\frac{di_3}{dt} + \frac{1}{C_{ins}}\int_0^t i_2 dt = V_{break} \quad \textbf{(85)}$$

$$(R_s + R_{burden})i_3 + (L_m + L_s + L_{burden})\frac{di_3}{dt} = 0 \quad \textbf{(86)}$$

3.4 Conclusion

A current transformer model with every possible different scenario which could lead to CT failure has been presented. Model development has been presented with assumption that breakdown voltage was absent, and then with breakdown voltage being present in the model. For the entire scenario presented in this work, state variables (I_{ins}, I_{mag} and I_{sec}) have been identified and investigated. The corresponding equations (steady and transient state) associated with all scenario models have been demonstrated in this chapter. The next step was to implement these models which will be discussed in details in the following chapter.

CHAPTER FOUR

MODEL IMPLEMENTATION AND ANALYSIS OF RESULTS

4.1 Introduction

In Chapter 3 a CT model is presented for analyzing how the condition of the insulation is affected when CT is in good condition, deteriorating and failing. Steady state and transient state equations has been formulated. The steady state equations were implemented in the *Matlab*© software programming package. The transient state equations developed in the previous chapter were not implemented like the Steady state equations. The software used (Simplorer©) for Transient implementation uses circuits parameters (resistor, inductance, capacitor current and voltage source) for modeling. Because of this system capability, Transient implementation was done by building circuit as per CT developed model.

It is normal research procedure to develop a method to determine model parameters and then prove these theoretical parameters with practical implementation. Once the parameters of the model have been verified practically, the next step would be to test model functionality in the laboratory set up. With this in mind, an attempt was made to obtain practical current transformer from Eskom for practical determination of model parameters and testing of the model.

4.2 Determination of the Model Parameters

To determine the model parameters, a 132 kV CT was obtained from Eskom. The specification of the CT can be obtained in Appendix B page B1. The tests that were performed were short circuit, open circuit and ratio test. The ratio test was performed to verify name plate values not to determine model parameters. Short circuit and open circuit were used to determine the model parameters. The circuit diagram used for performing open tests is as follows:

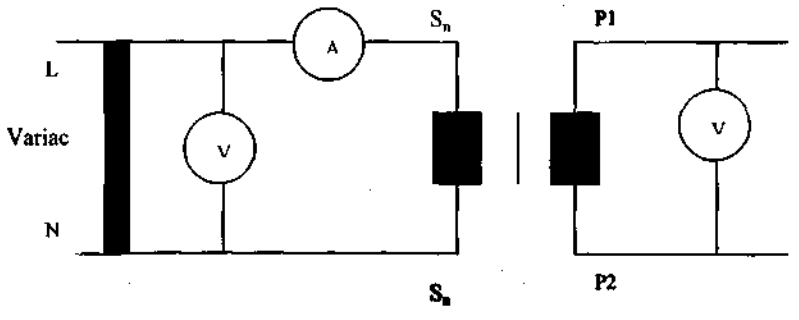

Fig.18: Open circuit test circuit diagram

CT secondary is never left open when there is current injection in the primary because the of the voltage rises that occurs on the secondary [10,11]. With this in mind, the open circuit test was done by injecting current on the secondary windings as can been seen on Fig.18. The power supply was obtained from the variable voltage source. The CT tested had multi ratio windings on the secondary which has been den0ted by S_n in the circuit diagram. The primary winding is denoted by P1 and P2 on the circuit diagram. The test voltage was varied from 0 to 750 V because of the available voltmeters that were limited to 750 V scale. The results were obtained by metering shown in Fig.18 and can be viewed in Appendix B page B3.

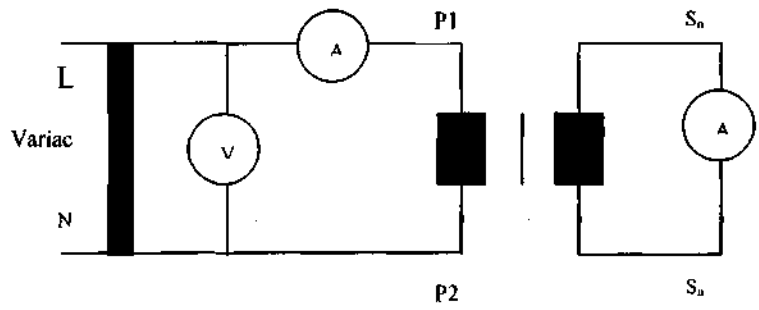

Fig.19: Short circuit test circuit diagram

For the short circuit test, the injection was performed on the primary windings. The power supply source was also provided through variable voltage source. The voltage was varied until some current was generated on the primary windings. The maximum primary current was limited to maximum 10 A because of the ammeters available that were limited 10 A scale .The readings obtained during practical implementation can be viewed in Appendix B page B3. The laboratory set up for determination of model parameters was as shown in Fig.19

Fig.20: Laboratory set up

The following are the model parameters that were used during model implementation. They were obtained from the laboratory experiments and methods used for calculating them can be obtained in Appendix B page B3. The open and short circuit values were obtain during laboratory and in turn these values were used to determine the following parameters.

$R_{secondary} = 54.8\ \Omega$

$R_{burden} = 10\Omega$

$X_{secondary} = 0.548\ \Omega$

$X_{magnetising} = 23\ 548\ \Omega$

$R_{magnetising} = 235.48\ \Omega.$

$X_{burden} = 0.01\ \Omega$

$X_{primary} = 0.00274\ \Omega$

$R_{primary} = 0.274\ \Omega$

4.3 Steady State Implementation

Ideally, a good insulator would be capacitive. In a perfect insulator, there would be no current flowing through the insulator because the value of insulation resistance would be infinity and there will be voltage across the capacitor. When the insulator starts to deteriorate, the value of resistance will be less than the infinity value and there will be varying voltage across the capacitor then some current will start to flow. When the value of resistance is approaching zero, maximum current is expected to flow in the insulator and breakdown of insulation will follow.

Since parallel representation of insulation was being investigated, it was going to be impossible to identify the influence of the individual insulation parameter if they were varied simultaneously. For all steady state implementation, one of insulation parameters is varied while the other For steady state implementation, the steady state equations developed in the previous chapter were implemented in Matlab© software. The following approach was adopted for model implementation in the steady state.

- Equations of the model were derived as per previous Chapter 3.
- Derived equations were solved by programming in Matlab to produce results which will be discussed in the following section and a sample of Matlab programs can be viewed in Appendix C.
- For the generation of the results one of the components of the insulator parameter (R_{ins} or C_{ins}) was kept constant while the other was varied . The process was then reserved where the insulator parameter that was kept constant was then varied. The range at which insulation resistance (R_{ins}) was varied is from 0 to 10^{19} ohms and the insulation capacitance (C_{ins}) is 10^{6} to 10^{-12} Farads. Data has been obtained pertaining to the following cases:

- R_{ins} is varied while C_{ins} is constant.
- C_{ins} is varied while R_{ins} is constant.
- Both C_{ins} and R_{ins} are varied.

the data enabled us to determine the condition of perfect insulation, deteriorating insulation and failed insulation.

- Introduction of inter-turn ratio n in the model helps in the insulation failure location identification within the winding. n was therefore varied from 0 to 1.
- In order to evaluate the influence of insulation breakdown on source voltage (ie source voltage overshoot), a separate model with current controlled voltage was introduced in Chapter 3. Same procedure as explained above was used for implementation..

4.4 Transients State Implementation

The model representation circuit diagram presented in the previous chapter were built in the Simplorer© software. Simplorer© is a simulation software for multi-domain designs in automotive, aerospace, power electronics, and electric drive systems and more information about the product can be obtained at this site (www.simplorer.com).When the circuit was built, different transient conditions were investigated. A sample of circuits used for transient implementation can be viewed in Appendix E. The software used for transient analysis is capable of performing transient analysis without using developed equations. The approach adopted for the model implementation in the transient state is :

- **Use of** Sinusoidal wave form as an input signal for all transient analysis.
- Use of values of Rins and Cins obtained in Steady State analysis.

4.5 Steady State Results and Discussions

4.5.1 Results and Discussions with Breakdown Voltage ignored

4.5.1.1 Insulation Breakdown within Primary Windings only

Fig.21 and Fig.22 shows the variation of insulation current with the insulation resistance and capacitance. For Fig. 21 the insulation resistance (R_{ins}) was varied, insulation capacitance (C_{ins}) was kept constant and the inter-turn ration ratio (n) was varied from 0 to 0.9. In Fig. 22 the process was reversed. From Fig.21, the resistance values of 10^{20} to 10^{4} ohms represent the perfect insulator and this corresponds with the current transformer when it is transforming the current into the acceptable level for the protection system to make a determination whether the system is normal or not. The values of resistance from 10^{3} to 10^{1} ohms show the region where the insulation is deteriorating and the value of 10^{0} shows the state where there is complete insulation failure. If during CT insulation failure there is a fault in the power system this will result in CT not being able to provide input to the protection system which can lead to extensive damage to the protected plant and corresponding CT.

From Fig.22, the capacitance values of 10^{-14} to 10^{0} Farads represent perfect insulator and this correspond with when the current transformer is transforming the current for protection system to make a determination whether the system is normal or not., while 10^{1} to 10^{3} represent deteriorating insulator and 10^{4} to 10^{7} represent a insulation which has deteriorated until complete failure. If during CT insulation failure there is a fault in the power system this will result in CT not being able to provide input to the protection system which can lead to extensive damage to the protected plant and corresponding CT. Other state variables ($I_{magnetising}$ and $I_{secondary}$) are not shown for this scenario because the results obtained are similar to those

discussed in Fig. 21 and 22 and can be viewed in Appendix C page C1. In Fig.23, both $C_{insulation}$ and $R_{insulation}$ are varied at the same time while the inter-turn ratio is kept constant and the same results were observed. In Fig. 24 & 25 the results are the same as in Fig. 21 and Fig. 22 while $C_{insulation}$, $R_{insulation}$ and inter-turn ratio (n) was varied. For the 3d plots, the 3 states presented by 2 d with family of curves were also revealed in the 3d plots in Fig.23, 24 and 25

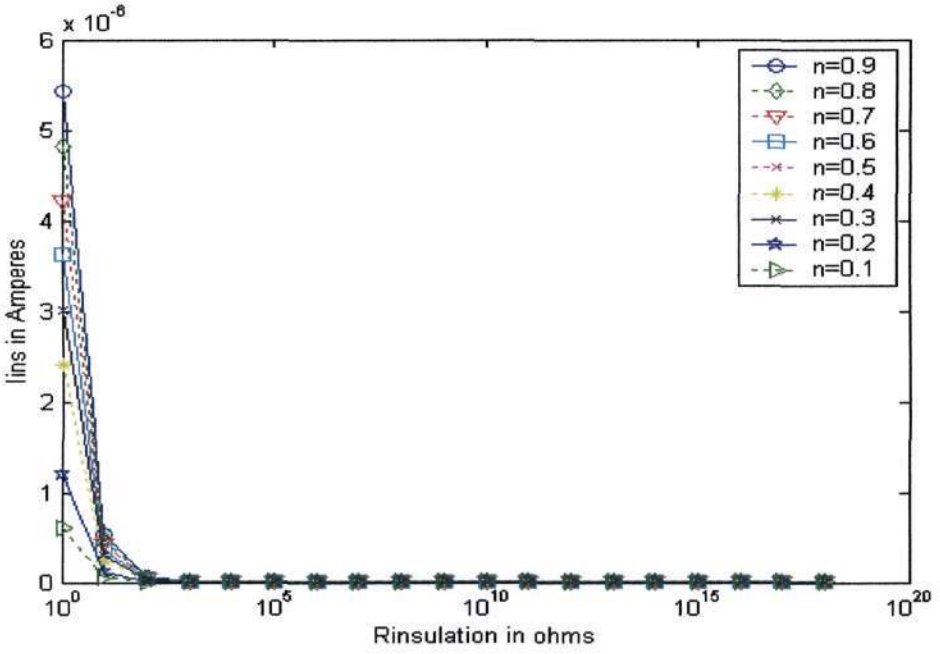

Fig.21: I_{ins} vs $R_{insulation}$

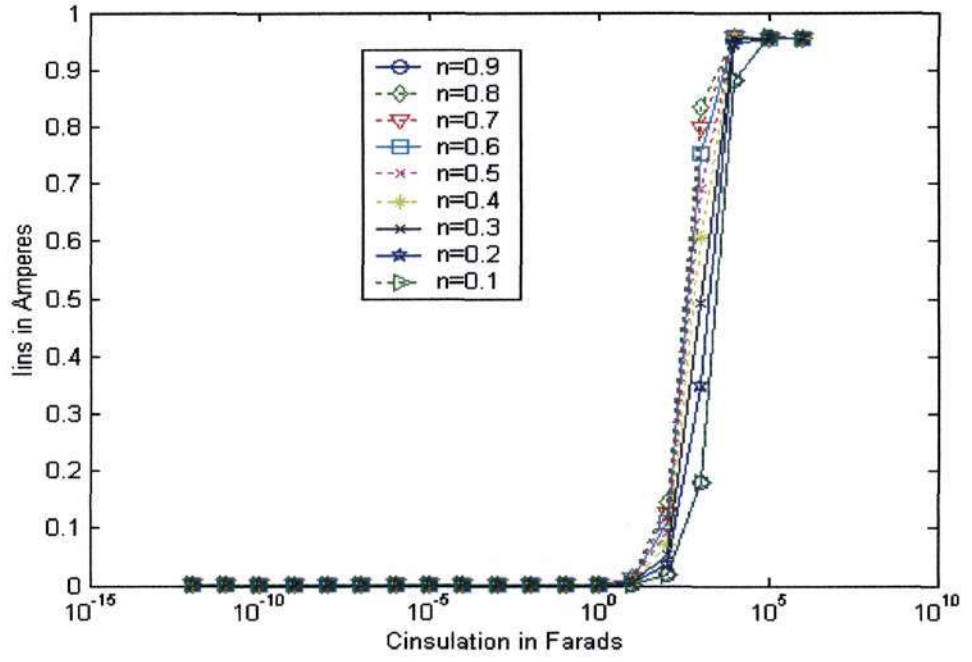

Fig.22: I_{ins} vs $C_{insulation}$

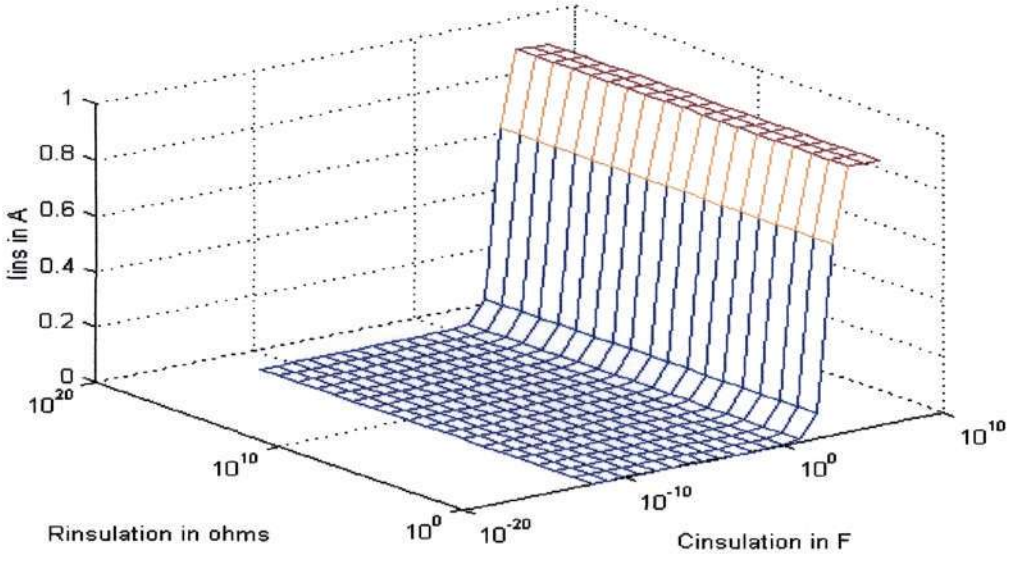

Fig.23: I_{ins} vs $R_{insulation}$ & $C_{insulation}$

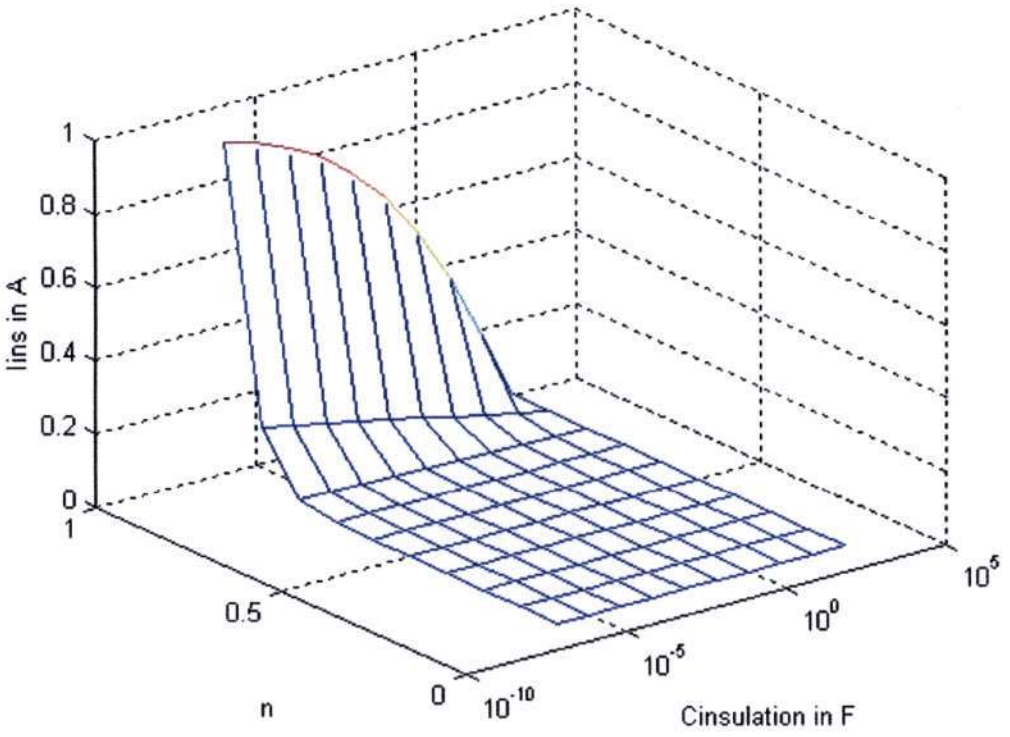

Fig.24: I_{ins} vs n and $C_{insulation}$

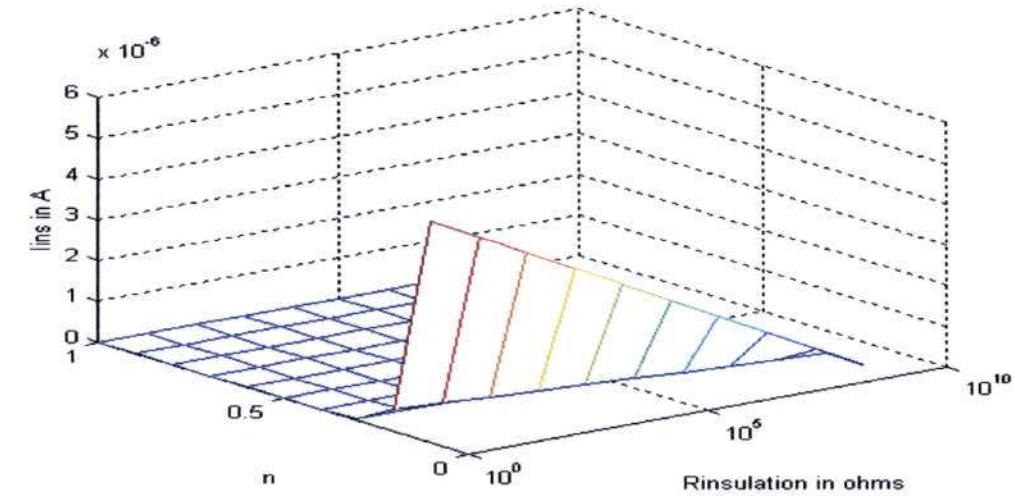

Fig.25: I_{ins} vs n and $R_{insulation}$

4.5.1.2 Insulation Breakdown within Primary Windings and Ground

The following results will demonstrate the changes in state variables when there is insulation degradation between the primary windings and ground.

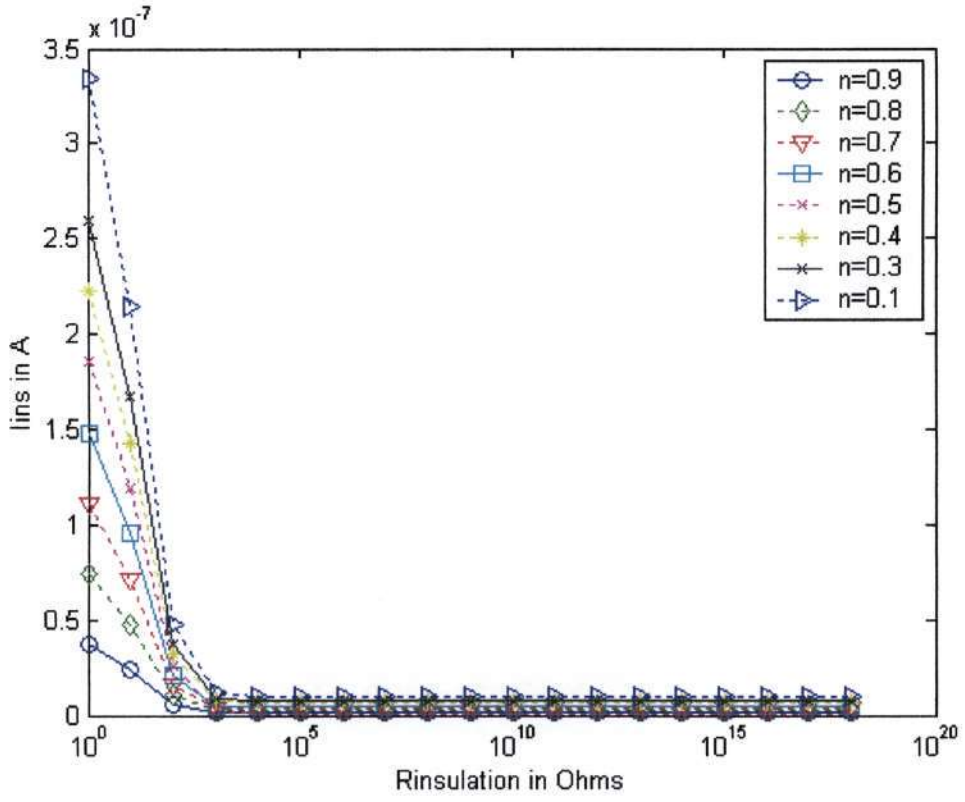

Fig.26: I_{ins} vs $R_{insulation}$

Fig.26 represents the insulation current (I_{ins}), when only the resistance component of the insulation was varied. From the figure three different insulation conditions can be easily identified. These conditions are when the insulation is perfect, deteriorating and complete failure. Same argument as in section 4.5.1.1 can be used about outcome of the protection system when these conditions of insulation are occurring. Other state variables ($I_{magnetising}$ and $I_{secondary}$) are not shown for this scenario because they have shown same results as Fig.26 but can be viewed in Appendix C. Same results were obtained when I_{ins}, $I_{magnetising}$ and $I_{secondary}$ are

plotted against insulation capacitance ($C_{insulation}$). The results in Fig 27 was when there is inter-turn ratio was kept constant.

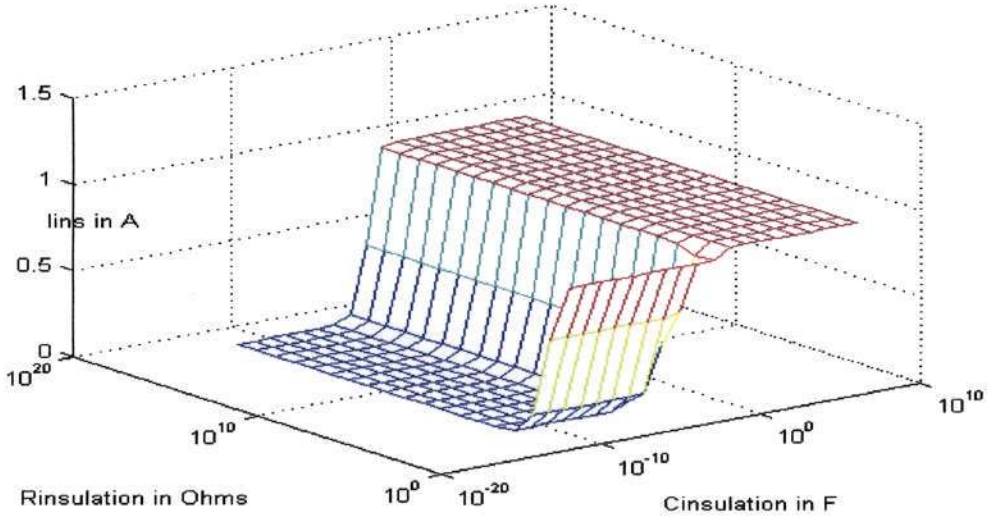

Fig.27: I_{ins} vs $R_{insulation}$ and $C_{insulation}$

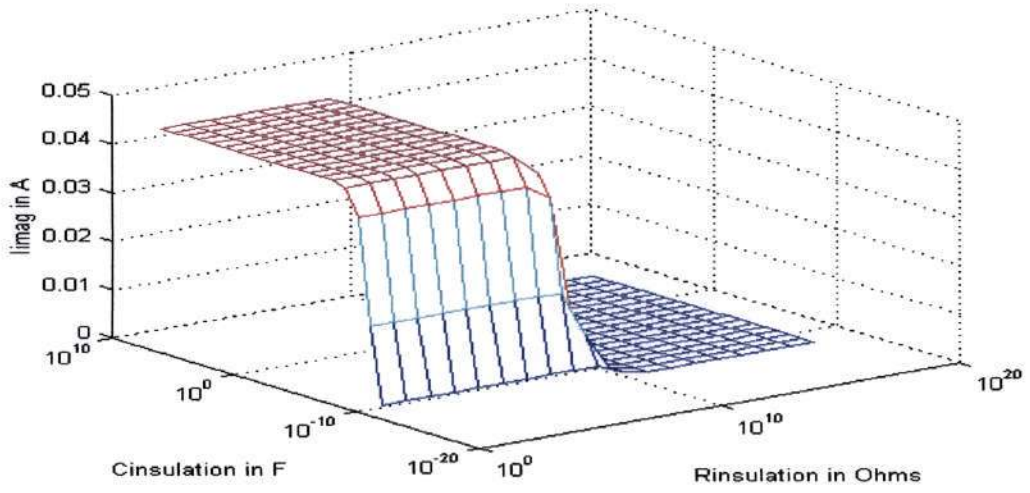

Fig.28: I_{mag} vs $R_{insulation}$ and $C_{insulation}$

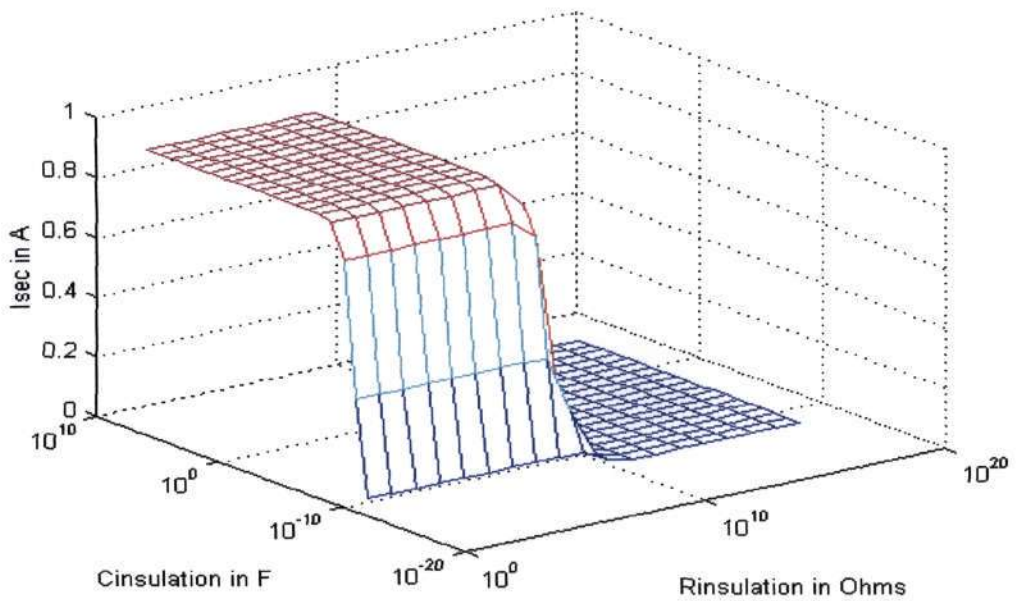

Fig 29: I_{sec} vs $R_{insulation}$ and $C_{insulation}$

Although it was decided in this work to vary the insulation parameters (R_{ins} and C_{ins}) independent to clearly identify the influence of the individual parameters but the study was also done when insulation parameters were varied concurrently for completeness as shown in Fig.27 to Fig.29. Although these results are not clear as when insulation parameters are varied independently but same result can be observed.

4.5.1.3 Insulation Breakdown within Secondary Windings

The following results will demonstrate the changes in state variables when there is insulation degradation within secondary windings only.

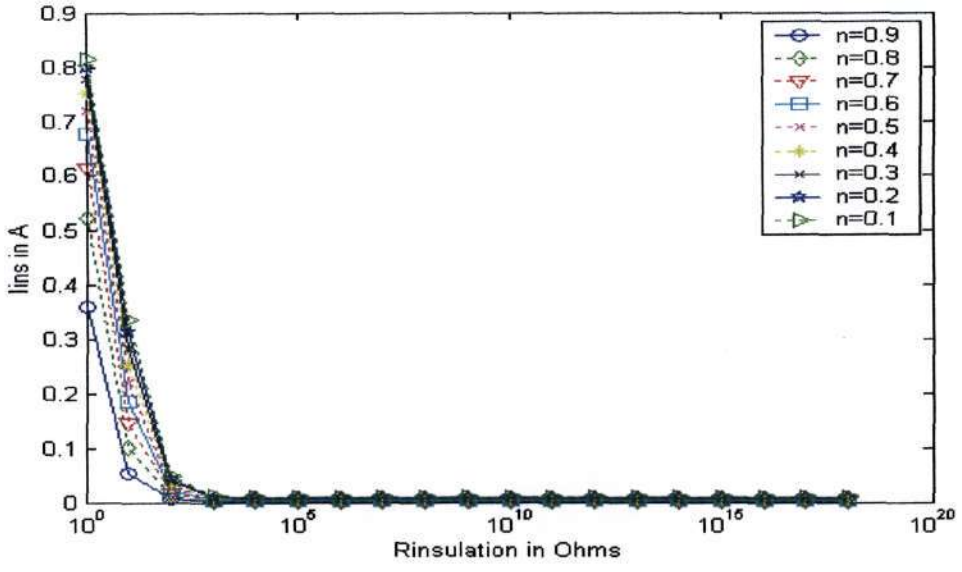

Fig.30: I_{ins} vs $R_{insulation}$

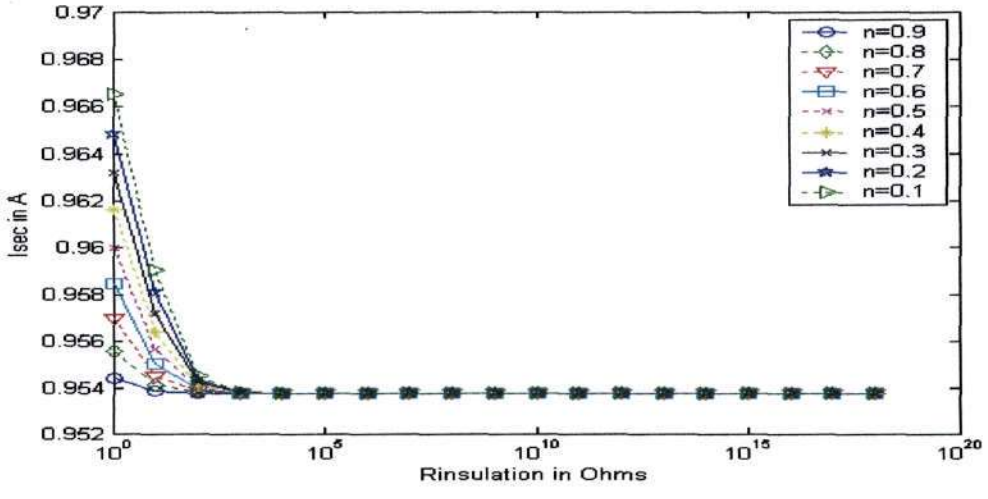

Fig.31: I_{sec} vs $R_{insulation}$

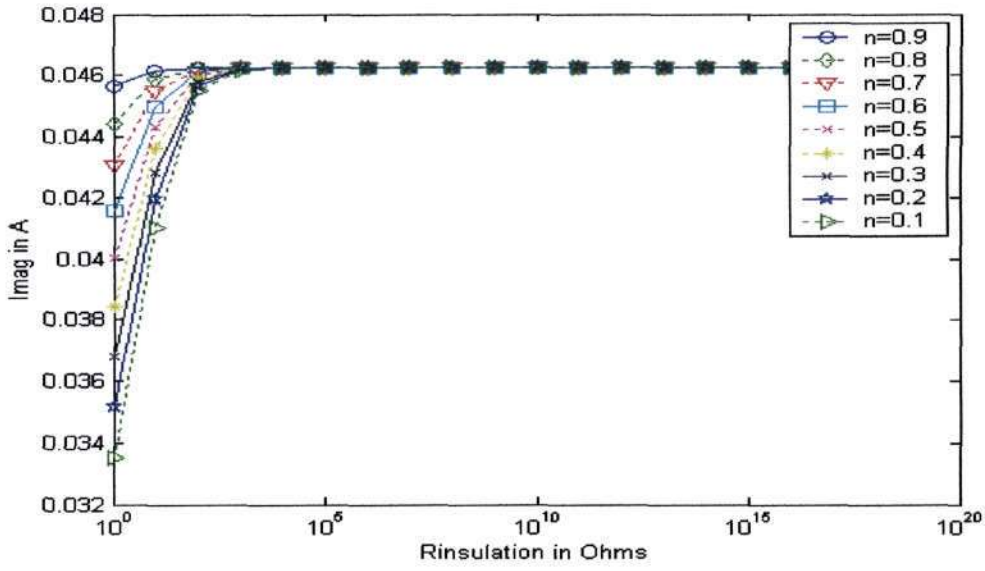

Fig.32: I_{mag} vs $R_{insulation}$

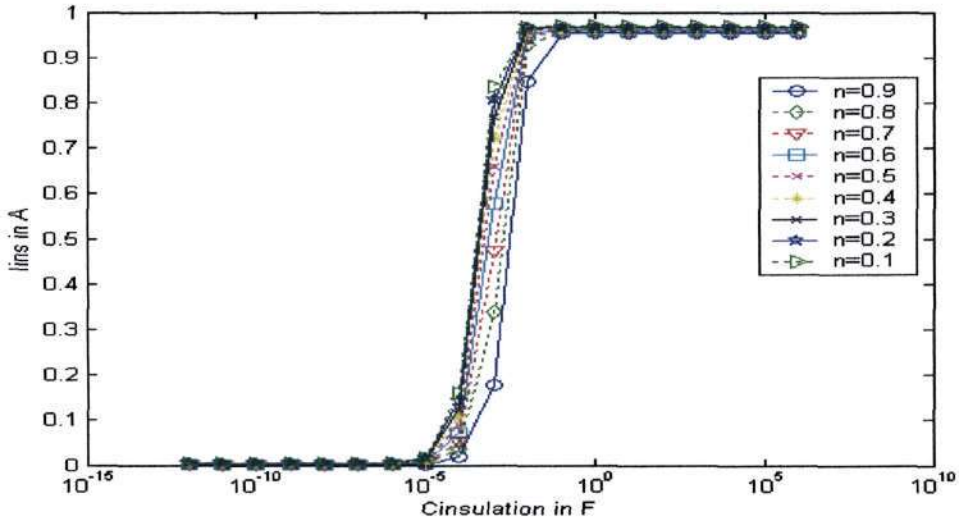

Fig.33: I_{ins} vs $C_{insulation}$

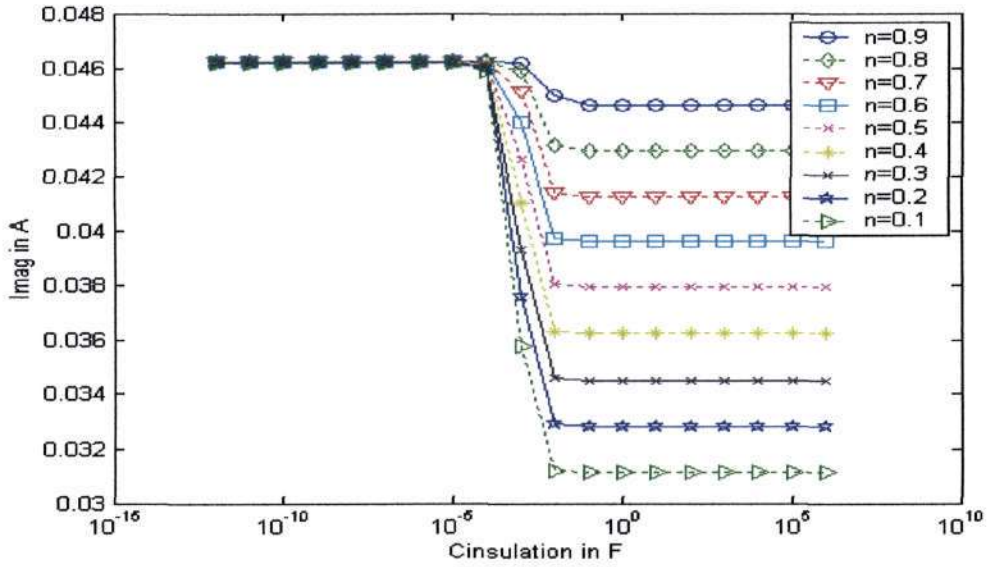

Fig.34: I_{imag} vs $C_{insulation}$

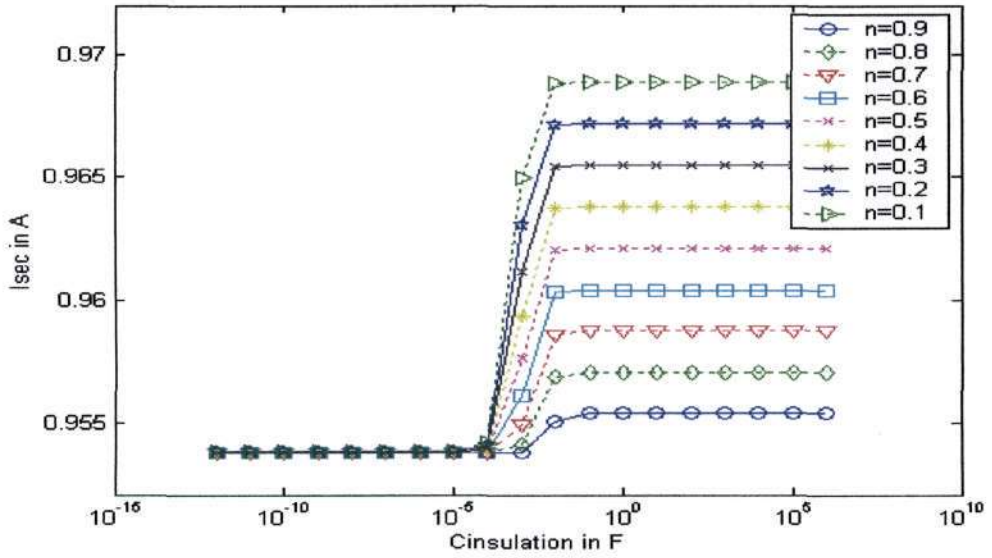

Fig.35: I_{sec} vs $C_{insulation}$

From Fig.30 to Fig.35, all the three states of insulation can be clearly observed. The same values of insulation capacitance and resistance as in above sections are also observable.

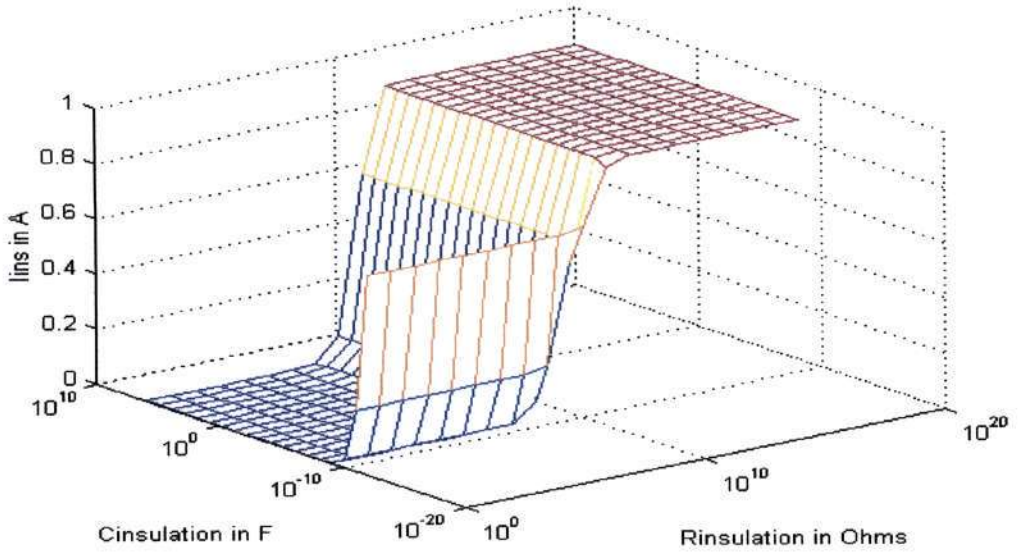

Fig.36: I_{ins} vs $R_{insulation}$ & $C_{insulation}$

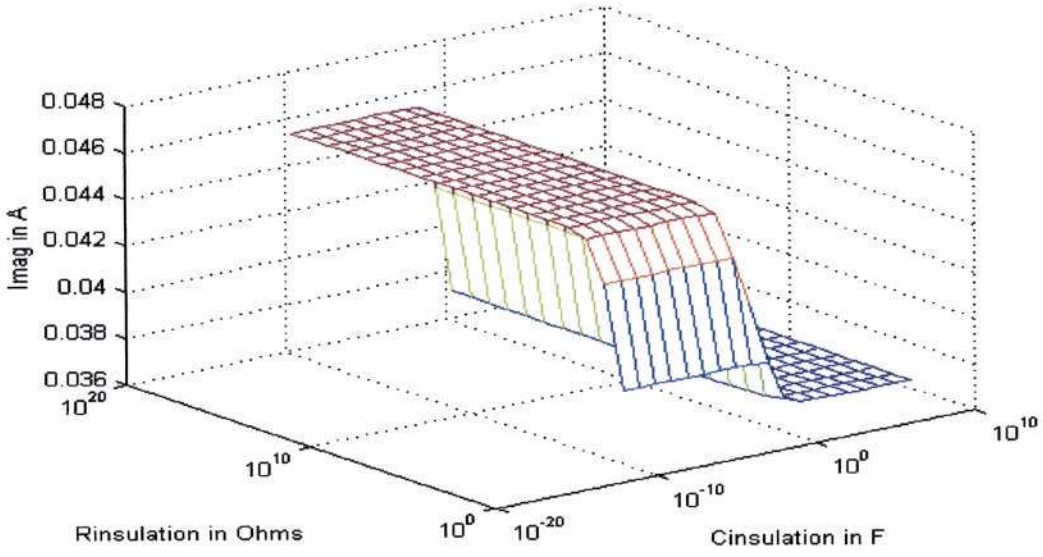

Fig.37: I_{imag} vs $R_{insulation}$ & $C_{insulation}$

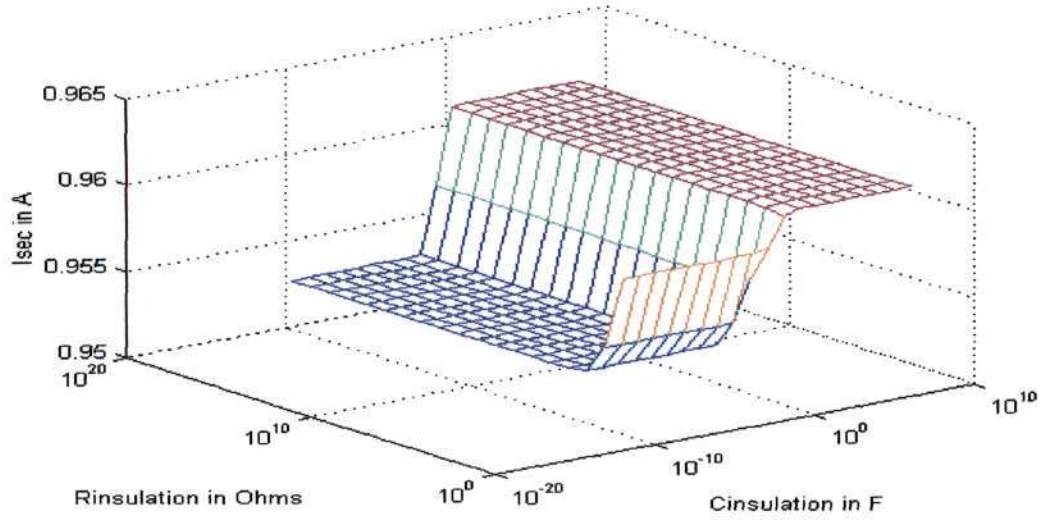

Fig 38: I_{sec} vs $R_{insulation}$ & $C_{insulation}$

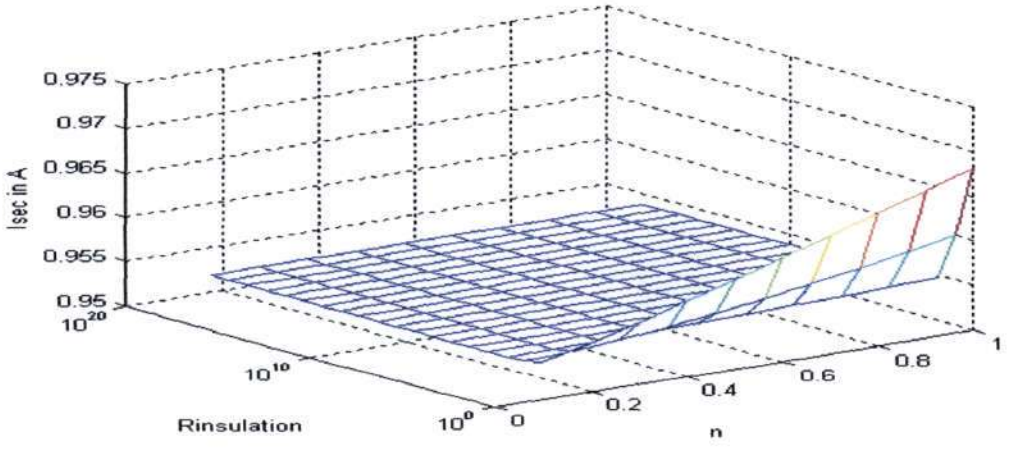

Fig.39: I_{sec} vs n&$R_{insulation}$

Fig.30 to Fig.35 plots were done in a 2 dimensional plot to show how insulation changes from perfect insulator to failing insulation. 3d plots in all scenarios were done to look at all possibility that might have been omitted in 2d plots. Fig.36 to Fig.39 has re-iterated what has been shown in 2d plots.

4.5.1.4 Insulation Failure between Primary and Secondary Windings

The following results will demonstrate the changes in state variables when there is insulation degradation between primary and secondary windings.

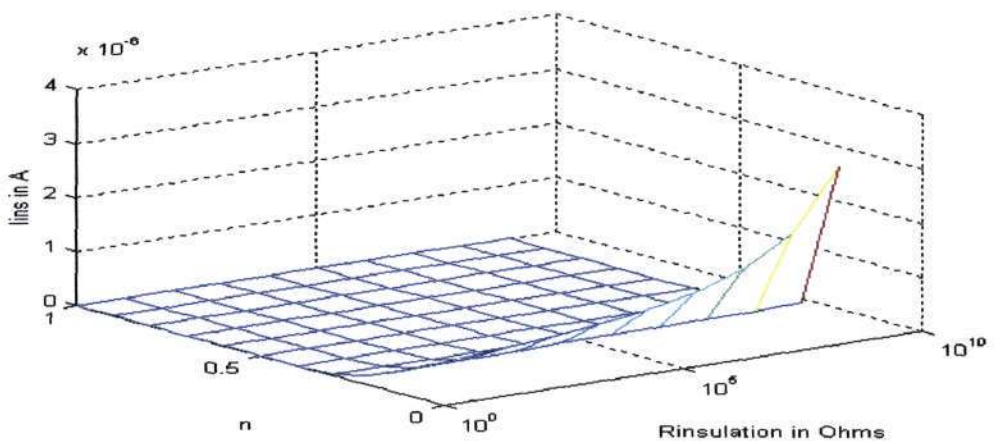

Fig.40: I_{ins} vs n&$R_{insulation}$

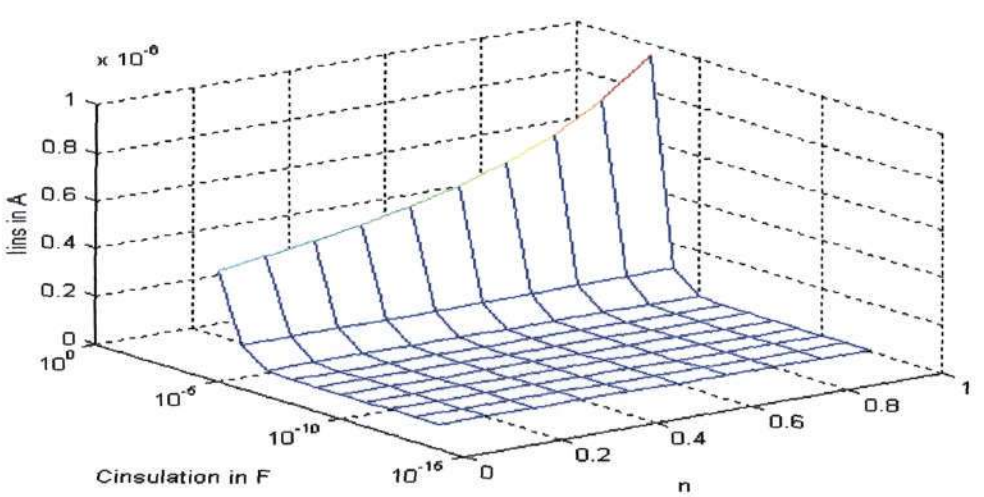

Fig.41: $I_{insulation}$ vs n&$C_{insulation}$

The families of curves for this scenario are not shown for this section but can be viewed in Appendix C. Fig.40 and Fig.41 have confirmed what has been observed in the previous section.

4.5.1.5 Insulation Failure between Secondary windings and Ground

The following results will demonstrate the changes in state variables when there is insulation degradation between the secondary windings and ground.

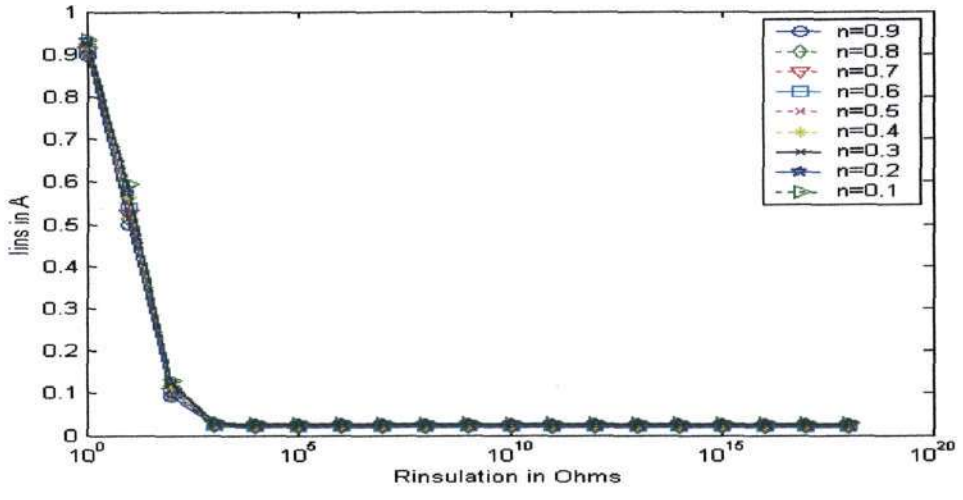

Fig.42: I_{ins} vs $R_{insulation}$

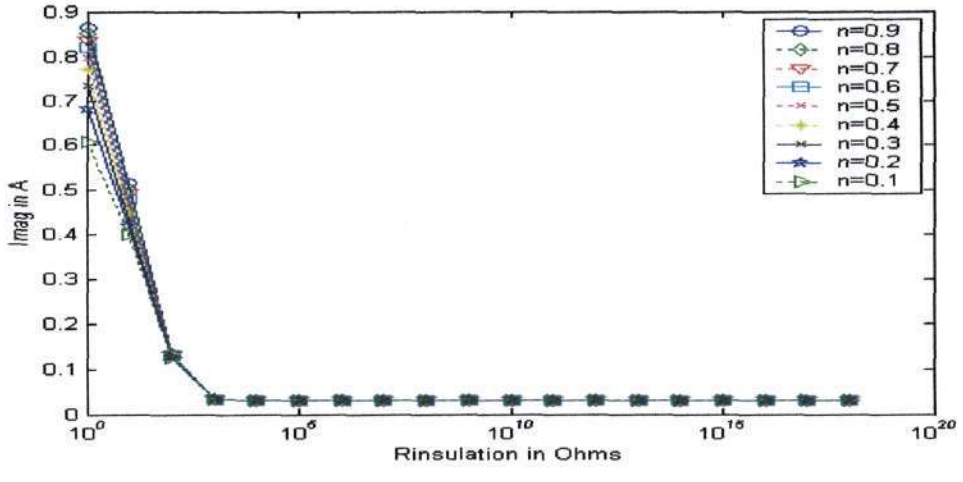

Fig.43: I_{mag} vs $R_{insulation}$

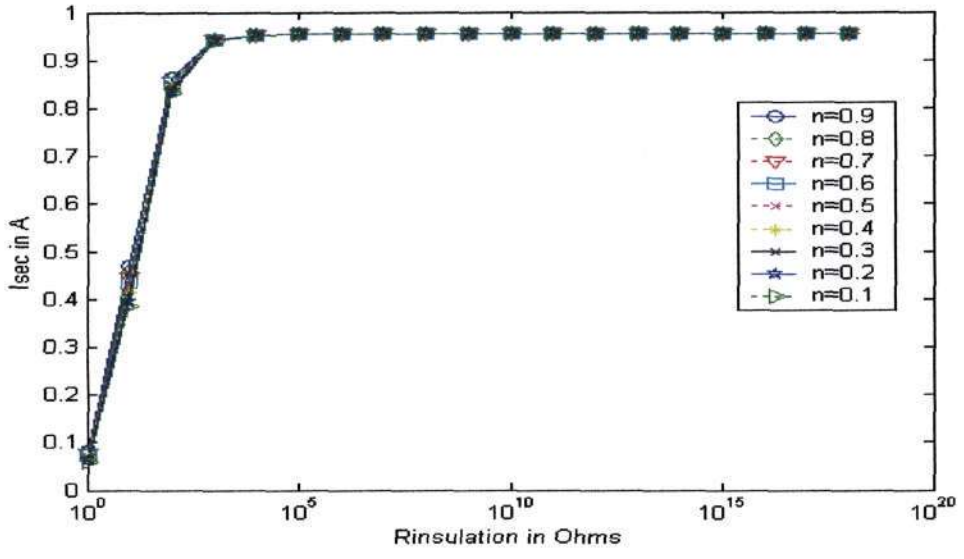

Fig.44: I_{sec} vs $R_{insulation}$

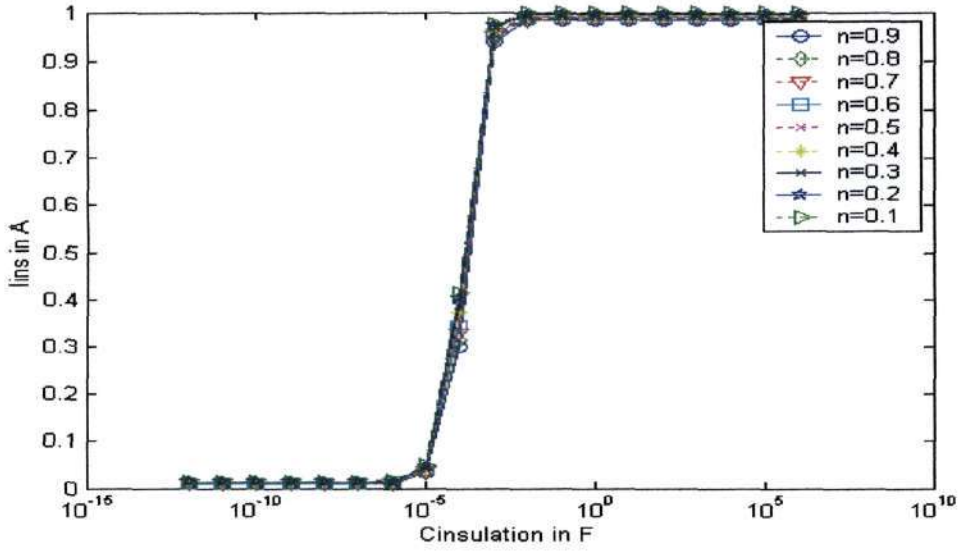

Fig.45: I_{ins} vs $C_{insulation}$

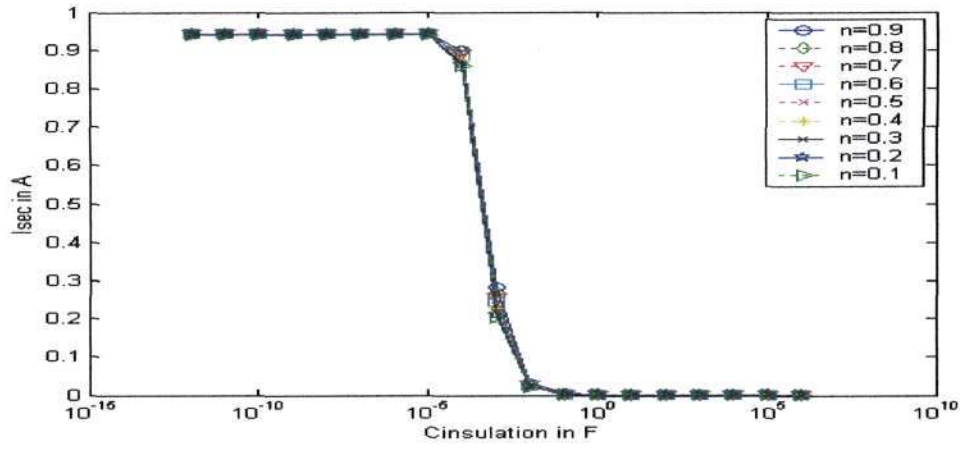

Fig.46: I_{ins} vs $C_{insulation}$

The graph presented in this section has just re-iterated what has been observed in the previous figures. The graphs clearly shows when the insulation is perfect, deteriorating and when it is failing completely. The 3 dimensional plots for the scenario under discussion can be viewed in the Appendix C.

4.5.1.6 Insulation failure between the core and ground

The results to follow will demonstrate the changes in state variables when there is insulation degradation between the core and ground.

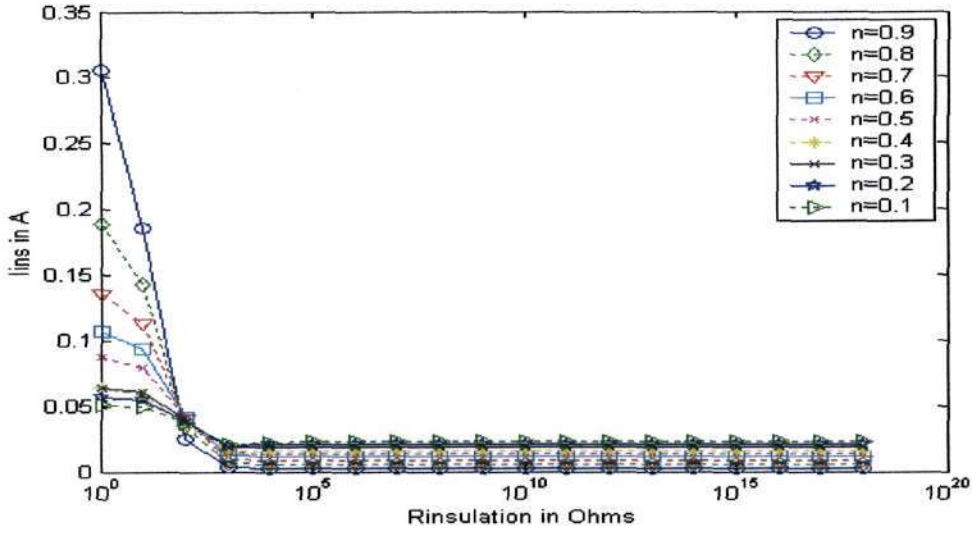

Fig.47: I_{ins} vs $R_{insulation}$

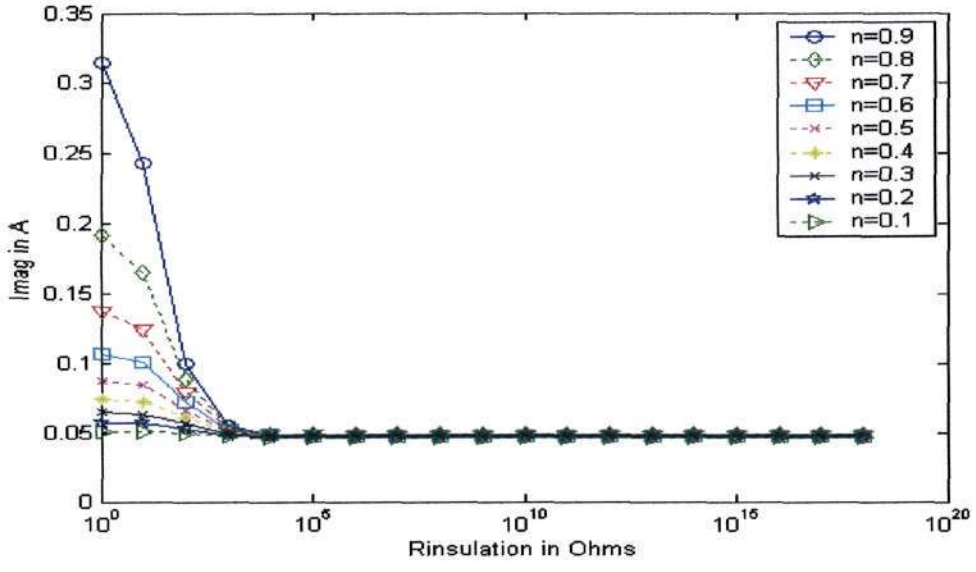

Fig 48: I_{mag} vs $R_{insulation}$

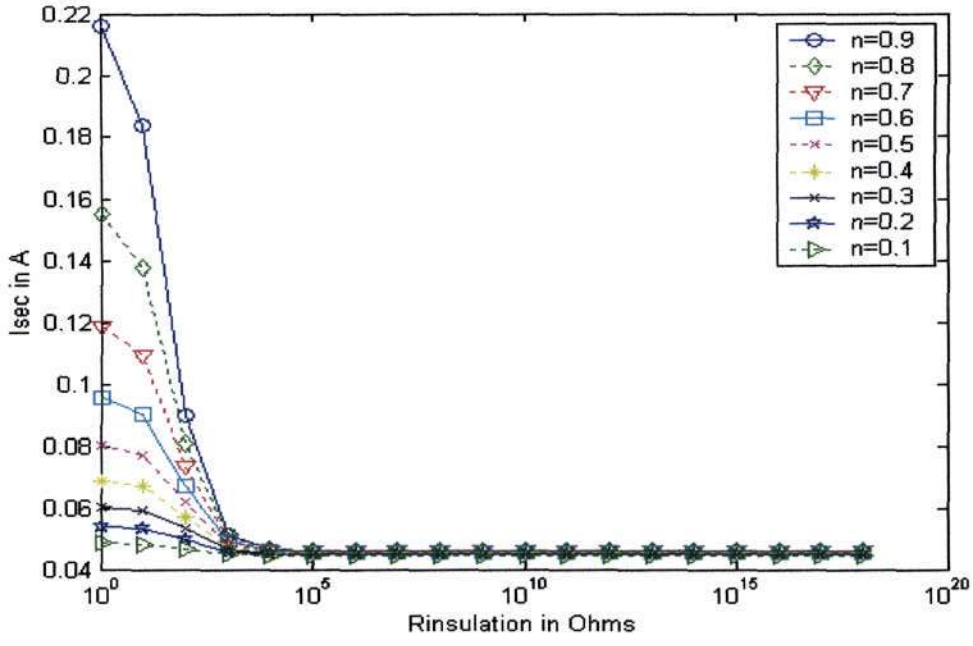

Fig.49: I_{sec} vs $R_{insulation}$

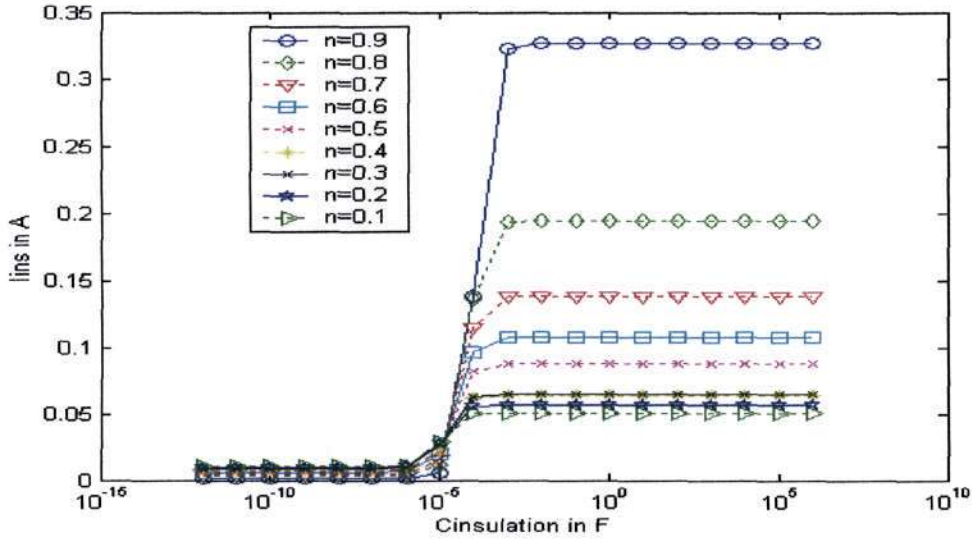

Fig.50:I_{ins} vs $C_{insulation}$

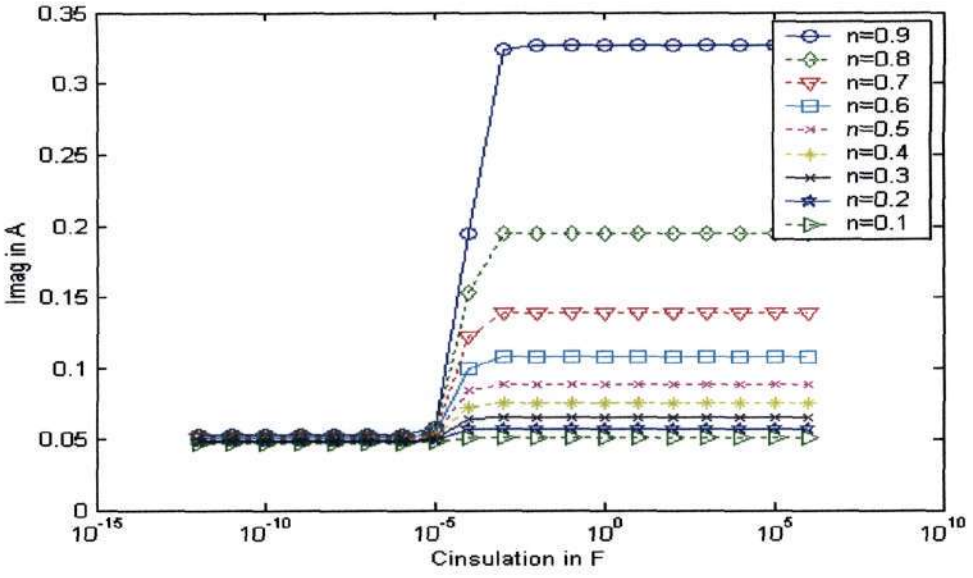

Fig.51:I_{mag} vs $C_{insulation}$

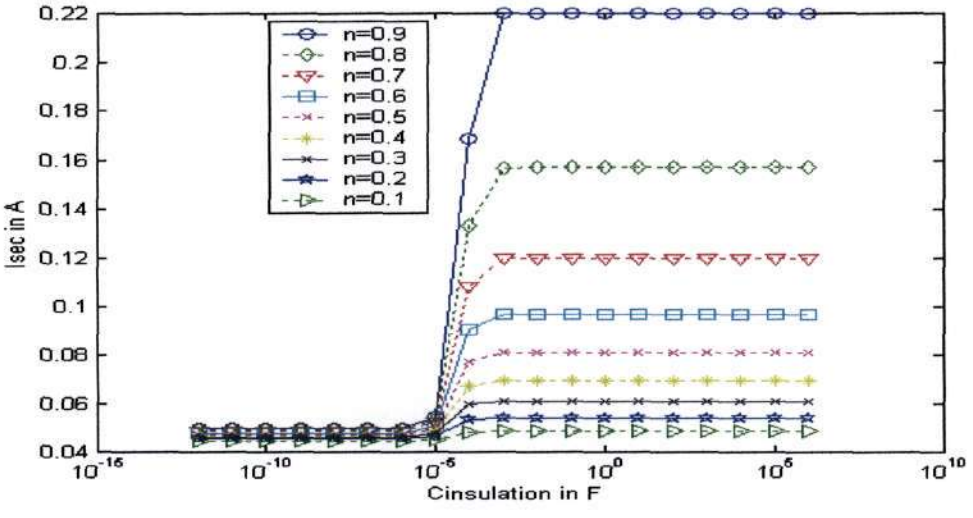

Fig.52: I_{sec} vs $C_{insulation}$

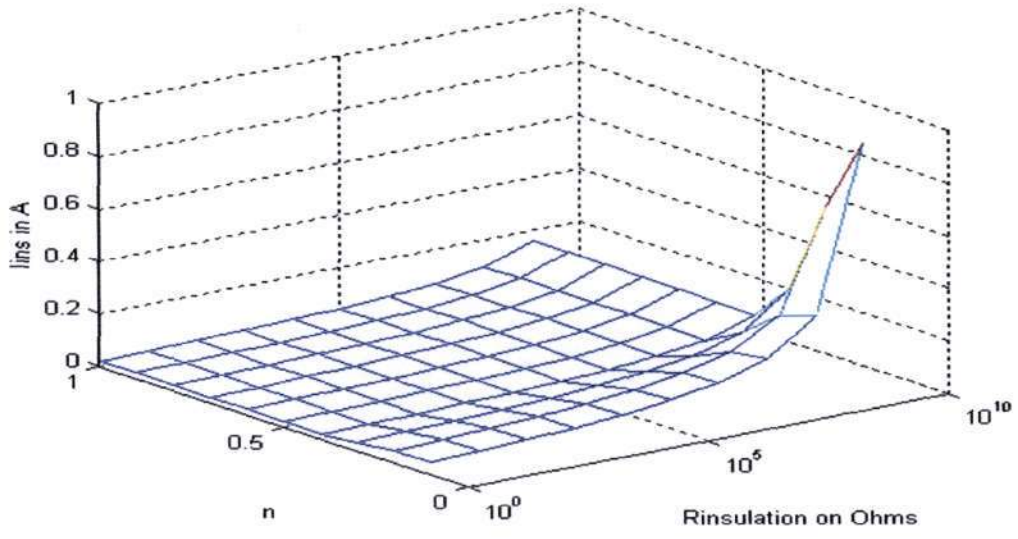

Fig.53: I_{ins} vs n&$R_{insulation}$

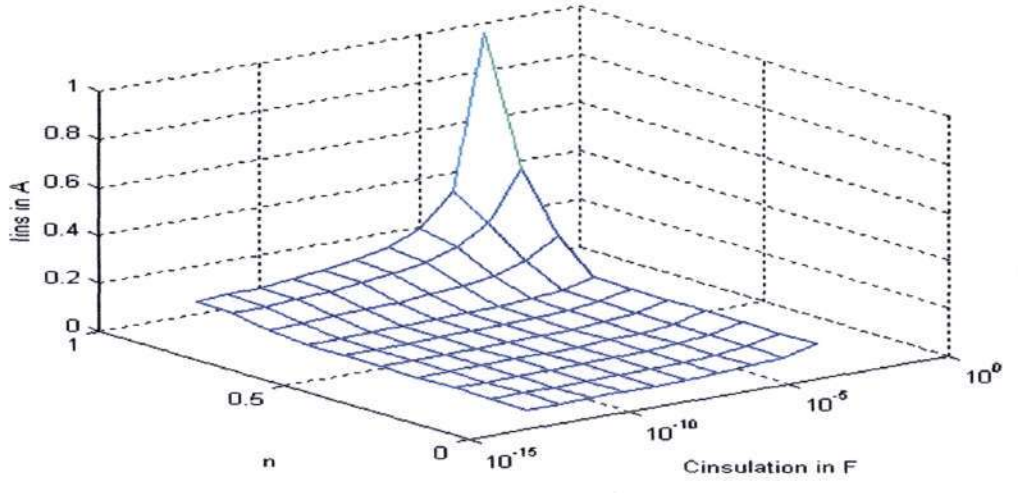

Fig.54: I_{ins} vs n&$C_{insulation}$

The families of curves graph have confirmed the regions where the insulation is perfect, deteriorating and complete. The 3d plots have also shown the same values of resistance and capacitance.

4.5.2 Results and Discussions when the Breakdown Voltage is present

4.5.2.1 Insulation failure between primary windings and ground with current controlled voltage source

The following results will demonstrate the changes in state variables when there is insulation degradation between the primary winding and ground. The current controlled voltage source was included to determine the influence of breakdown voltage. Real, Imaginary and Absolute values of the state variables were plotted on the same set of axis to determine the influence of the breakdown voltage.

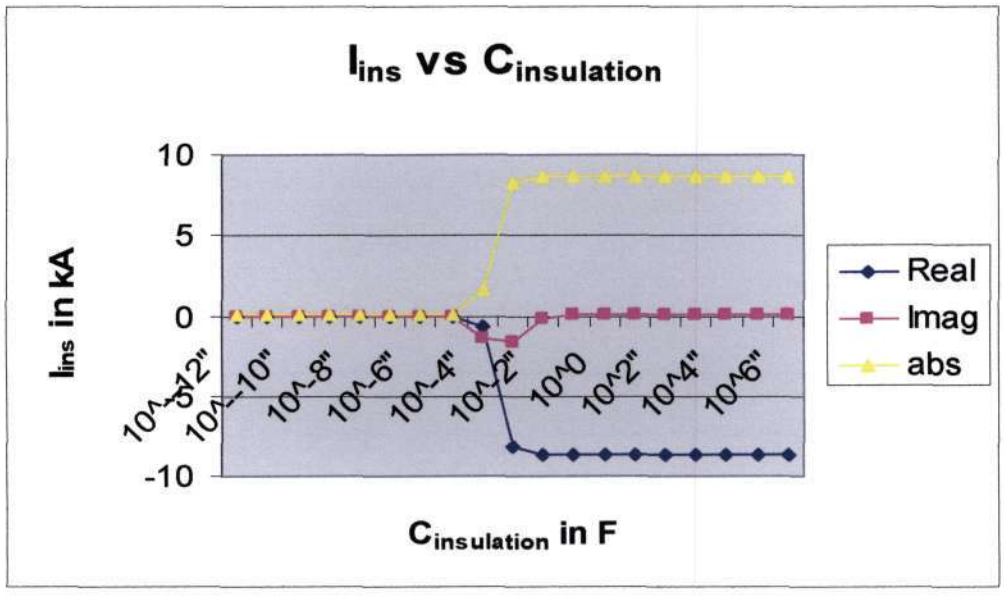

Fig.55:I_{ins} vs $C_{insulation}$

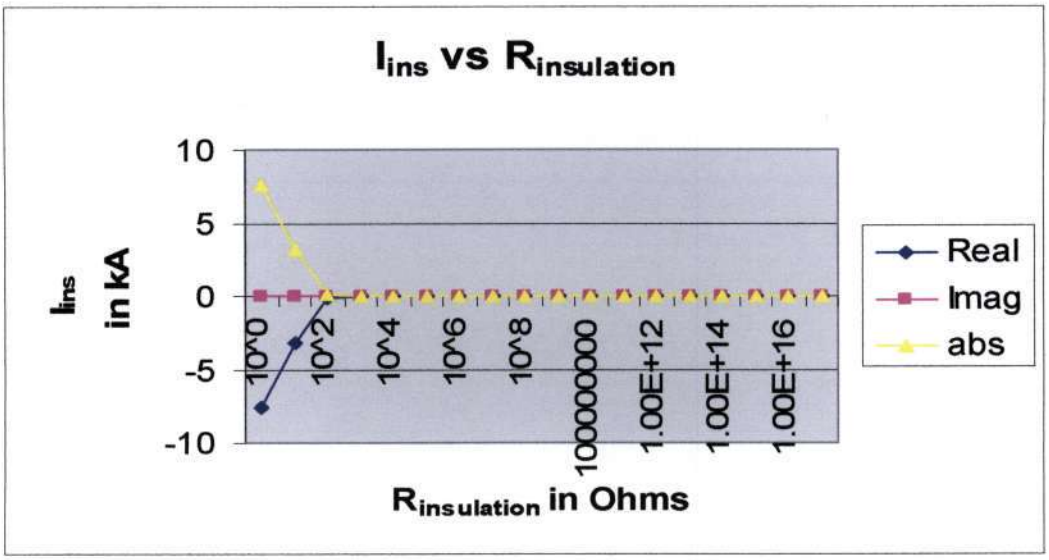

Fig.56:I_{ins} vs $R_{insulation}$

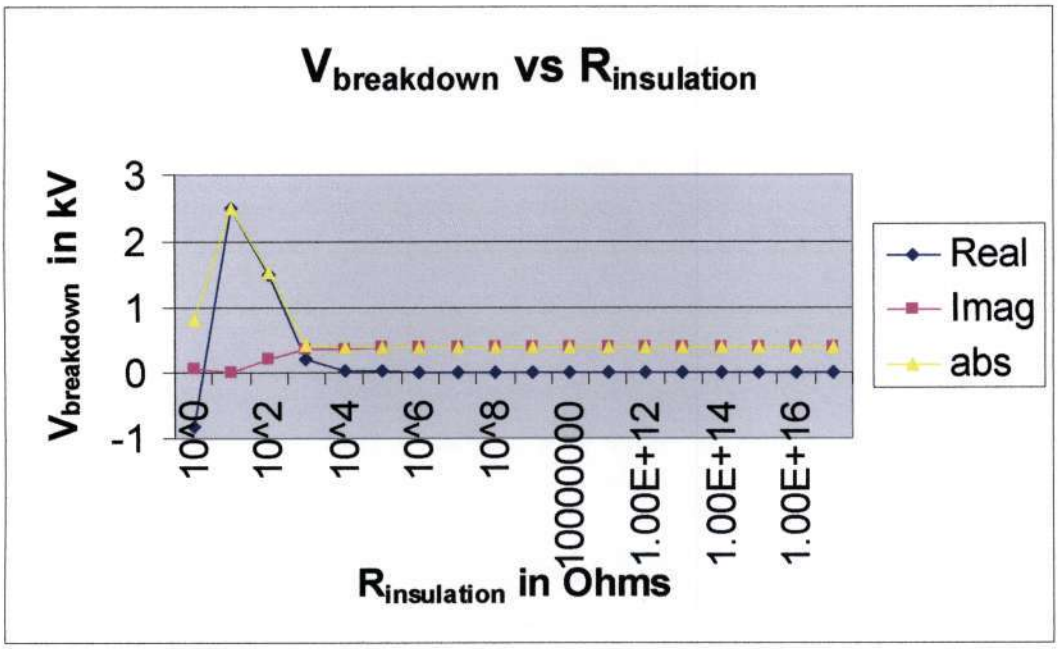

Fig.57: $V_{breakdown}$ vs $R_{insulation}$

With the breakdown voltage incorporated in the analysis the steady state results are as in Fig 55 to Fig 57. These reflect the same state change from good insulation to deteriorating and failed as observed in the previous results. Zero to very low voltage breakdown voltage leads to insignificant contribution to current flowing through the insulation. However, large voltage breakdown results in the large value of current contribution to the insulation current. In proportion this contribution of the breakdown voltage is quite significant that it causes proportionally large current to flow in the rest part of the device, thus resulting, on one hand, in the outright burn out of the device. On the other hand, large currents in the presence of magnetic fields produce large forces responsible for the violent nature of the failure of the device.

4.6 Transient Results and Discussions

The following results were obtained during transient analysis. All the scenarios presented in Chapter 3 have been considered for the transient analysis. The model circuit diagrams presented in the previous chapter was implemented for transient analysis. With the aid of Simplorer© simulation software the results of the transient analysis are as shown in Fig. 58 to Fig 62. A sinusoidal wave form was used as the input for the implemented scenarios with 1000 millimeters as the amplitude on the Y-axis and 40 milli-second on the X-axis. Fig. 59 has micro meters in the Y-axis. A scope to monitor the changes in the state variables was strategically placed within the circuit to see the influence on the state variables during transient state.

4.6.1 Insulation Failure between Primary Windings only

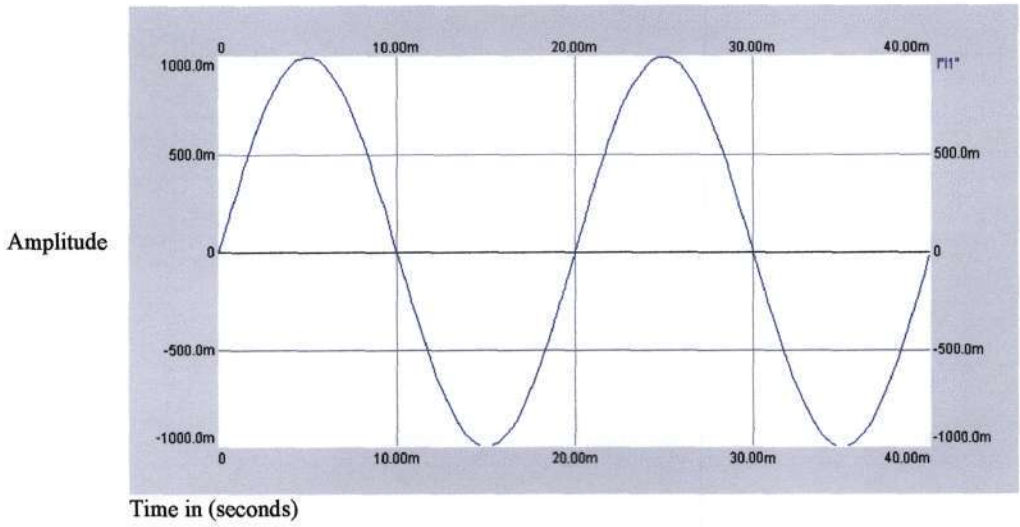

Fig.58: Input current

Fig.58 is the perfect sinusoidal wave form which was used as the input for all transient implementation. From the literature review if the output of state variables waveform came out as the Fig.58 then there was no transient influence on the model developed [11,12].

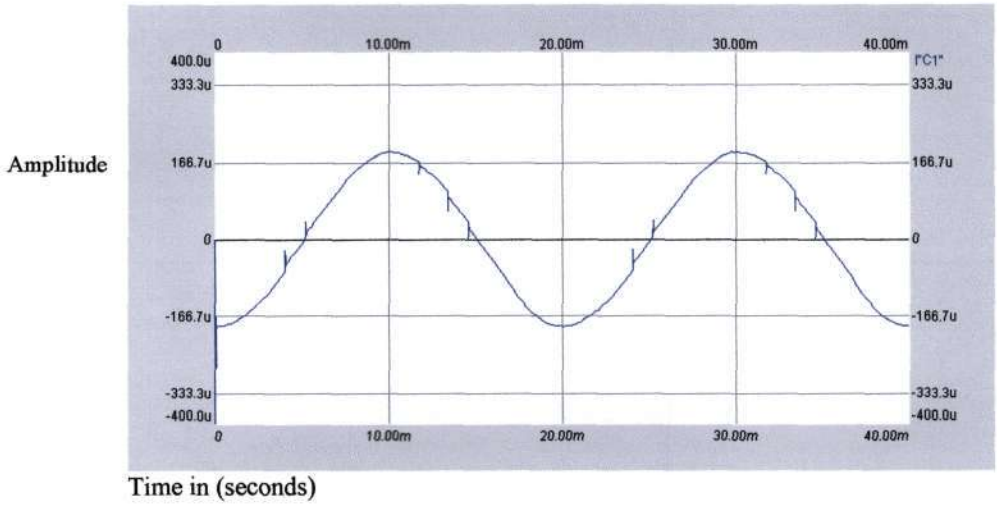

Fig.59: $I_{capacitor}$

4.6.2 Insulation Failure between Primary Windings and Core

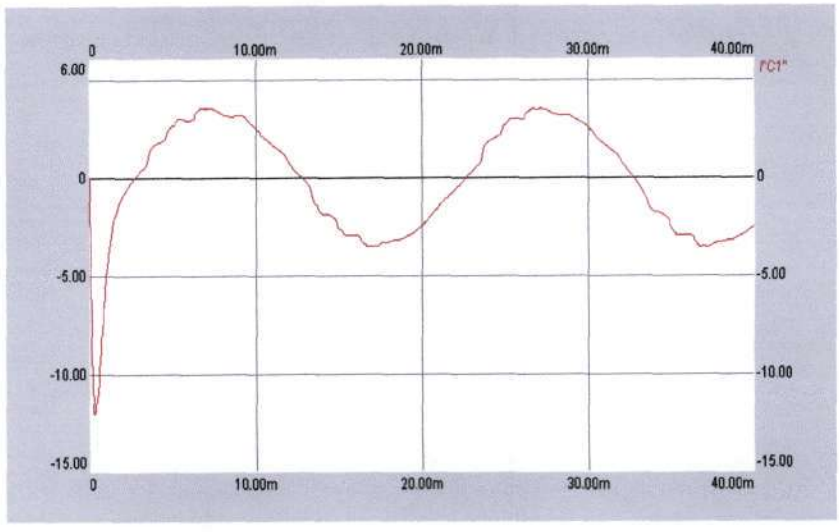

Fig.60: $I_{capacitor}$

4.6.3 Insulation Failure between Secondary Windings and Core

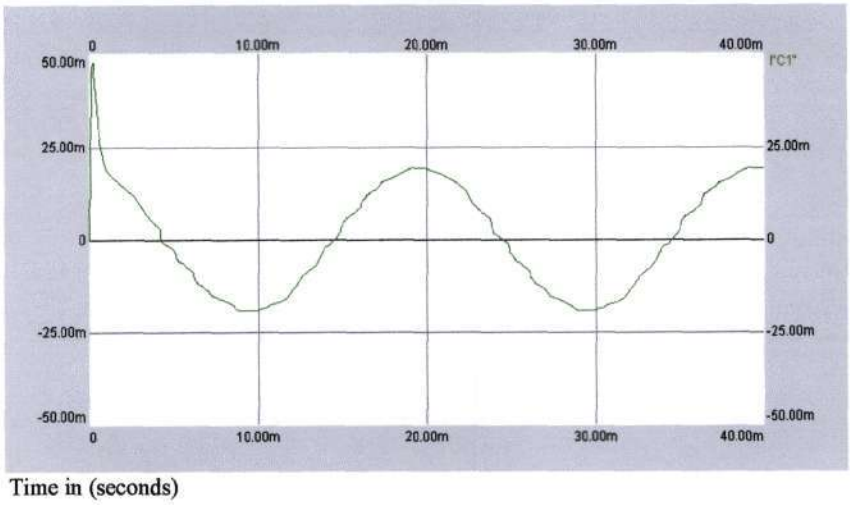

Fig.61: $I_{capacitor}$

4.6.4 Insulation Failure between Secondary Windings and Ground

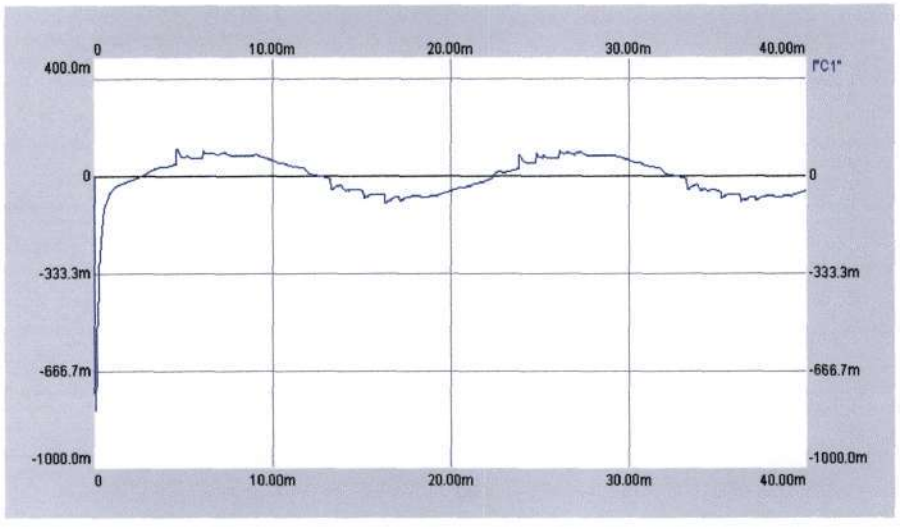

Amplitude

Time in (seconds)

Fig.62:$I_{capacitor}$

Fig.59 to Fig.62 are some of the result from Transient State implementation. These are waveforms of current quantities at various points of the device during the insulation deterioration. Of particular interest is the influence of insulation deterioration on the source, insulation, and the secondary current waveforms. Apart from expected glitches in the insulation current through the insulation capacitances there generally no significant influences on the current waveforms of the device. This implies that there is no significant production of harmonics due to failing insulation.

4.7 Conclusion

Parameters used in the developed models have been demonstrated in this chapter. Methodologies used in the transient and steady analysis of the models have been demonstrated. The insulation parameters (resistance and capacitance) have been varied to show the effects on the state variables of the model. Various analysis of the models have been done when the insulation breakdown voltage component was absent in the model, and then secondly when breakdown voltage was present. The Steady State analysis has shown how the insulation changes can lead to complete failure of the current transformer. The Transient State analysis did not have any influence on the process leading to the breakdown of insulation.

CHAPTER FIVE

CONCLUSION AND RECOMMENDATIONS

5.1 Current Transformer Failures Database

From the literature survey [6], the number of failed CTs within Eskom transmission's substations was quantified, which warranted the South African utility to eliminate risks associated with their plant. Available historical data from Eskom was extracted from manual reports, Orion, Permac and Phoenix databases which are recognized Eskom Transmission sources of information. Collected data from the above mentioned sources of information and discussion with field staff made formation of the database possible which can be viewed in the Appendix A1 section.

The failure rate of current transformer within transmission substation according to voltage levels as shown in Table 2 showed that 400, 275 and 132 kV CTs were the most affected equipment. The classification of failures according to the manufacturers showed that Asea and Balteau manufacturers were the most affected type of CTs. The database analysis showed it is possible that more CT failures were experienced in the months when storm conditions were prevailing because of the South Africa weather pattern. Top core design of the CT was identified as highest contributor to the failures experienced by Eskom in the period from 1982 to 2000.

It was also discovered that single phase fault was the dominant failure mode among the failures investigated which could lead to insulation failure. This finding created the need for the development of the model for the failure modes to be investigated in Chapter 3. All the information used to deduce the above conclusion was consolidated into the database which can be viewed in Appendix A1. The information in the database can be stored by Eskom personnel such that anyone

looking for this information can easily access it. This work is also proposing a new format of investigation report to be used by the investigation staff to document their post-mortem findings which can be viewed in Appendix A2.The new format of the investigation report can be compared to the old format which can be viewed in Appendix A3.

5.2 Model Development and Equations

From the database, a single phase fault was identified as the dominant failure mode. With this result in mind and discussion with field staff from Current Transformer support group, insulation failure was the failure mode investigated in this work. After literature survey, parallel representation of insulation was chosen instead of series representation and used in investigating the insulation as the failure mode. The theoretical understanding of the ideal insulation versus practical insulation has been presented in a graphical form.

A CT model with insulation being investigated has been developed. The CT model proposed in this work was base on power transformer model which has been widely developed and proven [11]. In this work all the possible scenario which may lead into insulation failure within CT were investigated. Seven different scenarios which may lead to insulation deterioration or failure within CT are identified and discussed.

For all seven scenarios which may lead to insulation failure, an associated steady state and transient state equations were developed in this work. Since CT function is to transform current, a current source was used as the main source in the CT model. Initially steady state and transient state equations were developed with current source as the only source. For completeness and better understanding a breakdown current control voltage source was introduced at the points of deteriorating or failed insulation. The associated steady state and transient state

equations with current source and breakdown voltage were also developed in this work. Method for determining this breakdown voltage with changing condition of insulation was derived.

5.3 Model Implementation and Results Analysis

The current transformer model investigating insulation failure mode was developed in Chapter 3. Before implementing the model, laboratory experiments were performed in this work to obtain the model parameters. The tests that were performed were short circuit test, ratio test and open circuit test. The assumptions made to determine model parameters were obtained during the consultation with Eskom Current Transformer Support Group. The steady state equations developed were implemented in Matlab©. The transient mathematical representation of the models were not implemented in Matlab© but circuit diagram of the CT models developed were implemented in Simplorer©. With the aid of the model the CT was subjected to varying operating conditions of interest, and these were analysed to establish the respective state variables behaviors. When the insulation breaks down, a rise in source voltage overshoot is expected due to nature of the processes and this has been accommodated in the developed model. Although the model parameters were determined before the analysis, however the values of insulation resistance and capacitance were varied arbitrary from 0 to 10^{19} ohms and 10^{6} to 10^{-12} Farads respectively during the simulations. This was done deliberately for thorough investigation of insulation variations for all possible values. The analysis procedure that was used for both transient and steady state are presented. The analysis of the models showed the following;

1) The values of insulation resistance from 10^{0} to 10^{3} ohms showed the region where the insulation changed from being perfect, deteriorating insulation and then complete failure of the insulation.

2) The values of insulation capacitance from 10^{-5} to 10^{-2} showed the variation of the insulation from perfect, deteriorating and complete failure
3) Both the regions mentioned in 1 and 2 corresponded to tan delta definition or the values in which the affected CT must be closely monitored.
4) During the transient analysis, no oscillations were observed as expected but merely glitches on the capacitance current.
5) For all the analysis done, the changes in the state variables are observable and this can assist in developing tools to monitor the changes in insulation.

5.4 Recommendations

The model developed gives the insight of the processes and phenomena leading to CT failure with insulation failure being failure mode investigated. The dissertation has presented analysis on how the insulation parameters variation can affect the state variables of the developed models. However, as is often the case in research, the work done on this dissertation have addressed some issues and uncovered further questions. Therefore, the author suggests that scope exists for further work in this area as outline below.

1) The initiative of the current transformer failures database need a continual update after this work and could lead to uncovering of issues like type of bad manufacturer and design which contribute to the failure rate and some intervention can be initiated with affected manufacturer. A revised format of the post-mortem investigation report can assist in identifying the causes of the failures and can been seen in Appendix A2. The old format of the investigation report has been attached in Appendix A3 for comparison.
2) The analysis of the model state variables was investigated under simulation conditions, a practical investigation of the model state variables under laboratory condition would be a good follow up work on this topic. Further

work on the rate at which insulation deterioration occurs can be a good contribution to the work presented in this dissertation.

3) When the voltage source overshoot was introduced, only one scenario was investigated in this work, a follow up work must investigate all other scenarios not covered in this dissertation.

4) Since the changes in state variables can be monitored and are observable, a possibility exists for the development of a condition monitoring instrumentation to detect these, and serve as means for detecting deterioration or tendency to failure earlier before it actually happens.

REFERENCES

[1] Van Bolhuis, Gulski E, Smith JJ, "Monitoring and Diagnostic of Transformer Solid Insulation" IEEE Transactions on Power Delivery,Vol 17, No 2, March 2002.

[2] Bengtsson C, "Status and Trends in Transformer Monitoring" IEEE Transactions on Power Delivery,Vol 11, No 3,July 1996.

[3] Matthiesen P, Ellis KP, "Field Experience with an On-line Gas Monitoring Device for Oil filled Instrument transformers", IEEE Transactions on Power Delivery Vol 9, No 3,July 1994, pages 1476-1478.

[4] De Klerk PJ, "Transformer Condition Monitoring, Eskom, Technology Service International Report TRR/E/95/EL107", 1995.

[5]. Cormack R, Naidoo P, Cowan P, "Eskom(RSA) experience in condition monitoring in current transformer and transformer bushings using on-line tan delta measurements", HVCT symposium, Portland, Oregon, 22-24 September 1999.

[6]. Evert R, Hoch DA, Cormack R, "Condition monitoring for high voltage current transformer in Eskom", HVCT symposium, Portland, Oregon, 22-24 September 1999.

[7] Mahlasela VS, Jimoh AA, "Condition Monitoring of HV Current Transformers in Eskom Substation", Proceedings of the 13th South African University Power System Conference,2003

[8]. Holtzhausen JP, Vosloo W, University of Stellenbosch High Voltage Engineering Notes.

[9] Alstom T&D Protection & Control LTD, "Protective Relays Application Guide" 1987

[10] AE Fitzgerald, C Kingsley Jr, SD Umans, "Electric Machinery" Metric Editions, 1992

[11] J.A Edminister, "Theory and Problems of Electric Circuits" 2nd edition, McGraw-Hill, 1985

APPENDIX A1

Current Transformer Failures Database

Station	voltage	manufacturer	type	serial no	design	d	m	y	manufactured. date	service	failure
Persus	400kV	Asea	IMBD 420		hair pin	18	8	1984	1976	8 years	porcelain shattered
Camden	400kV	Asea	IMBA 420		hair pin	17	01	1985	unknown		tank rupture
Persus	400kV	Asea	IMBE 420	10242	hair pin	2	6	1985	unknown		phase exploded
Atlas	400kV	Asea	IMBA 420	10242	hair pin	29	09	1985	unknown		white phase exploded
Carmel	132kV	Asea	IMBE 145	12565	hairpin	18	11	1985	unknown		phase exploded and caugt fire
Hendrina	400kV	Messwandler-bau	JT 400		unknown	14	03	1986	unknown		white phase exploded
Apollo	275kV	Alsthom Savouisiene	TH 300R	K70521-027	unknown	4	9	1986	unknown		Blue phase faulted
Mersey	275kV	Asea	IMBA		hair pin				unknown		star point faulted
Tutuka	400kV	Toshiba	Amr-pm400	82910258	unknown	21	06	1986	unknown		red phase faulted
Everest	132kV	Asea	IMBA		hair pin	22	06	1986	unknown		red phase faulted
Aggeneis	220kV	Haefely	Iosk 245		unknown	20	08	1986	unknown		red phase faulted

Witkop	275kV	Balteau	QDR 245		top core	21	08	1986	unknown		Blue phase faulted
Apollo	275kV	Alsthom Savouisiene			unknown	6	10	1986	unknown		white phase faulted
Gariep	275kV	Delle	Tpe 15/2/sp	105/3	unknown	26	01	1987	unknown		white phase faulted
Apollo	275kV	Alsthom Savouisiene	IE 300R-14A	K70521-027	unknown	3	2	1987	unknown		red phase faulted
Everest	275kV	Stomwandler	TMR 1275spe2	B192486	unknown	11	2	1987	unknown		white phase faulted
Pluto	275kV	Balteau	SAX 245	34529	unknown	2	3	1987	unknown		red phase faulted
Persus	275kV	Mess-Bau	JK275		unknown	21	08	1987	unknown		red phase faulted
Carmel	275kV	Balteau	sfd 123	04/01/2007	top core	16	09	1987	unknown		Blue phase faulted
Persus	275kV	Mess-Bau	JK275		unknown	3	10	1987	unknown		red phase faulted
Permbroke	220kV	Asea	IMBA245-A4	1541	hair pin	13	10	1987	unknown		white phase faulted
Alpha	400kV	Haefely	Siemens	841-279	unknown	30	11	1987	unknown		Blue phase faulted
Bernina	275kV	Balteau	Sax245	44199-67-02	top core	22	01	1988	unknown		red phase faulted
Ferrum	275kV	Delle	Tpe 15/2/sp	T31347	unknown	3	2	1988	unknown		internal fault
Kendal	400kV	Asea	IMBE 420	12641	hair pin	3	4	1988	unknown		white phase exploded
Ararat	275kV	Asea	IMBE 300	11497	hair pin	14	04	1988	unknown		internal fault
Hydra	400kV	Haefely	IOSK 420	84139	unknown	12	7	1988	unknown		exploded
Ferrum	275kV	Delle	TPE 15/29		unknown	21	09	1988	unknown		internal fault
Matimba	400kV	Asea	IMBE 420	11037	unknown	21	10	1988	unknown		white phase faulted
Muldersvlei	132kV	Conelectric	132CO	WK0774/2	unknown	3	11	1988	unknown		white phase faulted
Glochner	275kV	Balteau	QDR 245	77-53379-11	top core	3	11	1988	unknown		white phase faulted

Glochner	275kV	Balteau	QDR 246		top core	3	12	1988	unknown		white phase exploded + red phase damaged
Glochner	275kV	Balteau	QDR 247		top core	3	13	1988	unknown		white phase exploded + blue phase damaged
Bacchus	400kV	Haefely	IOSK420	840165	unknown	8	11	1988	unknown		Blue phase faulted
Komati	132kV	Asea	IMBA 145		hair pin	13	12	1988	unknown		white phase faulted
Kriel	400kV	MWB	ATS 400	77-539488	unknown	22	12	1988	unknown		blue phase faulted
Komani	132kV	Asea	IMBD 145		hair pin	24	02	1989	unknown		white phase bulged tank/ fault
Benoni	400kV	Balteau		7999	top core	14	04	1989	unknown		blue phase faulted
Grootvlei	400kV	Balteau	SEZA 400	415636804	top core	17	05	1989	unknown		blue phase faulted / fire
Acornhoek	275kV	Siemens	AKOF	WIF2155	unknown	17	11	1989	unknown		blue phase faulted/ open circuit
Arnot	275kV	Siemens	AKOF	69/22239	unknown	9	4	1990	unknown		blue phase exploded
Alpha	400kV	Haefely			unknown	1	11	1989	unknown		red phase faulted
Lepini	275kV	Asea	IMBE 300		hair pin	5	8	1990	unknown		
Marathon	132kV	Alsthom(Delle)	TPE 12D11		unknown	1	1	1991	unknown		overheating- out of service
Witkloof	132kV	Asea	IMBA 145		hair-pin	01	01	1991	unknown		exploded
Foskor	132kV	Asea	IMBA 145		hair-pin	1	1	1991	unknown		exploded and caught fire

Wildebees	132kV	Balteau	SFD 123		top core	1	1	1991	unknown		head exploded
Ruigtevlei	132kV	Asea	IMBA 145		hair-pin	13	01	1991	unknown		exploded and caught fire
Grootvlei	400kV	Balteau			top core	12	2	1991	unknown		red phase faulted
Hendrina	400kV	Asea	IMBD 420	89/14896	hair pin	5	8	1992	1983	17	red phase exploded and shattered porcelain
Grootvlei	400kV	Balteau			top core	12	2	1991	unknown		red phase exploded and caught fire
Marathon	132kV	Asea	IMBA 145		hair pin	6	4	1991	unknown		exploded and caught fire on energising
Hydra	132kV	Balteau	SFD 123		top core	28	05	1991	unknown		blue phase faulted
Bloedrivier	275kV	Balteau	QDR245	77/53379/04	top core	11	6	1991	1977	14	white phase exploded
Alpha	400kV	Haefely	IOSK420	841-281	unknown	6	12	1991	unknown		blue phase faulted
Beta	400kV	Haefely	IOSK421	841-283	unknown	8	7	1991	unknown		blue phase faulted/ acetelyn absent
Hydra	132kV	Balteau	sfd 123		top core	4	8	1991	unknown		blue phase faulted
Impala	275kV	Balteau	SAX 245	54679/10	top core	17	08	1991	unknown		blue phase faulted
Kriel	400kV	Mess-Bau		74-469520	unknown	11	10	1991	unknown		red phase faulted

Glochner	275kV	Balteau	SAX 245		top core	3	11	1991	unknown		white phase faulted
Inchandu	132kV	Asea	IMBA 145		hair pin	11	12	1991	unknown		tornado
Buffalo	132kV	Balteau	SGD 123	236/32/4	top core	24	03	1991	unknown		blue phase faulted
Normadie	132kV	Conelectric	132 CO	wk0524-11	hair pin	7	4	1992	unknown		blue phase exploded and caught fire
Trans Alloy	132kV	Asea	IMBA 145		hair pin	4	6	1992	unknown		Red phase exploded and caught fire
Olympus	132kV	Asea	IMBA 145 A4	3415	hair pin	20	07	1992	1975	25	blue phase faulted and exploded due to insulation failure
Hendrina	400kV	Asea	IMBD 420	89/14896	hair pin	5	8	1992	1989	3	red phase exploded and caught fire
Normadie	132kV	Conelectric	132 CO	wk0524-11	hair pin	7	8	1992	unknown		blue phase faulted
Aliwal North	132kV	Balteau		0551/2267	top core	16	03	1993	unknown		
Mersey	400kV	Balteau	TDX 420	82-52635-12	top core	17	07	1997	1982	11	insulation failure in bend point of hair pin
Ulco	132kV	Mess-Bau			unknown	17	08	1993	unknown		red phase faulted
Impala	275kV	Balteau	SAX 245	54679/11	top core	21	09	1993	1972	21	red phase faulted

Lyndenburg	132kV	Balteau	SCD 132		top core	29	09	1993	unknown		blue phase faulted and exploded
Gariep	275kV	Delle	TPE 15/2/2	1H 300	unknown	1	11	1993	unknown		red phase exploded and caught fire
Vaalkraal	132kV	Balteau	SCD 132		top core	24	01	1994	unknown		blue phase faulted
Kudu	132kV	Balteau	SCD 132		top core	30	03	1994	unknown		red phase faulted exploded and caught fire
Welkom	132kV	Balteau	288/23/7		top core	20	04	1994	unknown		red phase faulted and healthy
Incandu	132kV	Asea	IMBA 145	2060	hair-pin	5	8	1994	1972	22	red phase exploded and caught fire
Incadu	400kV	Asea	IMBA 145 A4	2060	hair pin	5	8	1994	1972	28	red phase exploded and shattered porcelain
Incandu	400kV	Asea	TDX 420	81/52622-01	hair pin	19	01	1995	1981	13	blue phase exploded
Grootvlei	400kV	Balteau	SEZA 400	415606803	top core	29	11	1995	unknown		blue phase exploded
Muldersvlei	400kV	Asea	IMBD 420	88/14529	hair pin	15	12	1995	1988	12	red phase faulted and exploded due hv insuation failure

Athene	132kV	**BBT**	**IMBE 145**		**hair pin**	22	06	**1995**	**1995**	**0**	exploded on energising
Grootvlei	400kV	Balteau	SEZA 400	415616802	top core	6	7	1996	1969	31	red phase exploded and caught fire
Camden	400kV	Asea	IMBD 420	82/9771	hair-pin	1	2	1996	1982	14	HV insulation b/n core and earthed screen on sec fail
Spitskop	132kV	Balteau/ GEC SA	SFD 123	12/01/5423	top core	24	05	1996	1981	15	overstressed hv insulation
Marathon	275kV	Balteau	SAX 245	30793/02	top core	28	02	1997	1970	27	hv insulation failure
Impala	275kV	Balteau	SAX 245		top core	5	5	1997	unknown		white phase exploded (head)
Hydra	400kv	Balteau	TDX 420	83/53015	top core	28	06	1997	1989	8	hv insulation failure above P1 terminal
Makala	88kV	Balteau	SCD 82	5868	top core	9	9	1997	1976	24	insulation failure
Arnot	400kV	Siemens	AKOF 275	69/22231	top core	11	9	1997	1969	31	insulation failure
Buffalo	132kV	Balteau	SGD 123	236/38/1	top core	6	1	1998	1984	14	insulation failure
Impala	132kV	ABB	IMBA 145 cu6	97/19**703**	hair pin	6	10	1998	1997	1	during repositioning unit was accidentaly tripped and fell
Matla	275kV	Asea	IMBE 300 A6	5800	hair pin	28	07	1998	1978	20	degradation of primary

											ins. In the hair pin bend
Watershed	88kV	**Balteau GEC SA**	**SCD 82**		**hair pin**	22	05	**1998**	**1982**	**16**	insulation breakdown and crack spreading
Ferrum	275kV	Asea	IMBE 300 A6	4418	hair pin	14	03	1999	1977	22	breakdownof ins. In the porcelain area
Grassridge	132kV	Balteau GEC SA	SGD 123	288/23/50	top core	18	02	1999	1989	10	degradation of insulation in the porcelain area
Kruispunt	132kV	Asea	IMBA 120 A4		hair pin	22	03	2000	1964	36	thermal runaway
Watershed	132kV	Conelectric	132CO	wk 4136/1	unknown	4	1	2000	1996	4	primary insulation failure

APPENDIX A2

Modified Investigation Report

Title of the Report

Author/s of the report

1. Introduction
2. Details of the CT
3. Site/Visual inspection
4. Strip Down Results
5. Conclusion
6. Contributory Causes
7. Root Cause of failure
8. Recommendations

APPENDIX B

1 Specification of model parameters.

The specification of CT used for practical determination of the model parameters was as follows

2. Apparatus

2 Ammeter (0-1A) Yokogawa Manufacturer

1 Ammeter (0-10A) Yokogawa Manufacturer

1 Voltmeter (0-750V) Yokogawa Manufacturer

Variac(0-1000V)

3. Calculation of parameters

The following table demonstrates result open during short circuit test

$I_{primary}$(A)	$V_{primary}$(V)	$I_{secondary}$(A)
3.6	0.985	0.018
6.7	1.83	0.031
8	2.27	0.037

The above results were obtained when 200/1 ratio was used. There were other results obtained during short circuit when different secondary cores were used but same effect was observed.

The following table demonstrates result open during short circuit test

$V_{secondary}$(V)	$I_{secondary}$(A)	$V_{primary}$(V)
730	0.031	1.218

The above results were obtained when 600/1 ratio was used although some tests were performed on the other secondary cores.

The following assumptions were used after consultation with Eskom Design Department

$X_{secondary}$ is about 100 times less than $R_{secondary}$

$X_{magnetising}$ is about 100 times greater than $R_{magnetising}$

$X_{primary}$ is about 100 times less than $R_{primary}$

X_{burden} is about 100 times less than R_{burden}

The following values were obtained with short circuit result

$R_{primary} = 0.985/3.6 = 0.274\ \Omega$

$X_{primary} = 0.00274\ \Omega$

$R_{secondary} = n*R_{primary} = 54.8\ \Omega$

$X_{secondary} = 0.548\ \Omega$

From the open circuit test results the following parameters were calculated as follows

$X_{magnetising} = 730/0.031 = 23548.39\ \Omega$

$R_{magnetising} = 235.48\ \Omega$

$V_{breakdown} = V_{rated}*(I_{insulation}/I_{insulationmax})$

Where V_{rated} is the primary voltage of the current transformer

$I_{insulationmax}$ is the maximum insulation current

APPENDIX C

Sample of Matlab programs

1. Programs when one component of insulator was varied

```
Rm = 235.48;
Xm = 23 458;
Rp = 0.274;
Cins = 0.000006;
Xp = 0.00274;
Rs = 54.8;
Xs = 0.548;
Rb = 10;
Xb = 0.01;
w= 314;
n=0;
count=0;
Ip=1+ j*0;
pi= 3.14;
M = 0;
  for i = 1:19
    Rins(i) = 10^M ;
    M = M+1;
  Xins = 1/(j*w*Cins);
  Zins(i) = Rins(i)*Xins/(Rins(i) + Xins);
  Zp = Rp + j*Xp;
  Zs = Rs+ j*Xs;
  Zm = Rm *j*Xm / (Rm+j*Xm);
  Zburden = Rb + j*Xb;
  Zsb = Zs + Zburden;
  Zsbm = Zm*Zsb/(Zm+Zsb);
  Zeffective = Zsb + n*Zp;
  Zpeffective(i) = n*Zp*Zins(i)/(n*Zp+Zins(i));
  Ztotal(i) = Zeffective + Zpeffective(i);
  Vp(i) = Ztotal(i)*Ip;
  Is= Ip*Zm/(Zm+Zsb);
  Im = Ip*Zsb/(Zm+Zsb);
  Iins(i) = Ip*n*Zp/(n*Zp+Zins(i));
  Iburden = Is;

End
```

```
Rm = 235.48;
Xm = 23 458;
```

```
Rp = 0.274;
Rins = 1000;
Xp = 0.00274;
Rs = 54.8;
Xs = 0.548;
Rb = 10;
Xb = 0.01;
w= 314;
n=0;
count=0;
Ip=1+ j*0;
pi= 3.14;
M = -12;
  for i = 1:19
    Cins(i) = 10^M ;
    M = M+1;
  Xins(i) = 1/(j*w*Cins(i));
  Zins(i) = Rins*Xins(i)/(Rins + Xins(i));
  Zp = Rp + j*Xp;
  Zs = Rs+ j*Xs;
  Zm = Rm *j*Xm / (Rm+j*Xm);
  Zburden = Rb + j*Xb;
  Zsb = Zs + Zburden;
  Zsbm = Zm*Zsb/(Zm+Zsb);
  Zeffective = Zsb + n*Zp;
  Zpeffective(i) = n*Zp*Zins(i)/(n*Zp+Zins(i));
  Ztotal(i) = Zeffective + Zpeffective(i);
  Vp = Ztotal(i)*Ip;
  Is= Ip*Zm/(Zm+Zsb);
  Im = Ip*Zsb/(Zm+Zsb);
  Iins(i) = Is*n*Zp/(n*Zp+Zins(i));
  Iburden = Is;

End
```

2. Program when both components of insulator were varied

```
Rm = 235.48;
Xm = 23 458;
Rp = 0.274;
Xp = 0.00274;
Rs = 54.8;
Xs = 0.548;
Rb = 10;
Xb = 0.01;
w= 314;
n=0;
count=0;
Ip=1+ j*0;
pi= 3.14;
M = 0;

    for i = 1:19
    Rins(i) = 10^M ;
    M = M+1;
    h = -12;
    for  k = 1:19
    Cins(k) = 10^h;
    h = h+1;
  Xins(k) = 1/(j*w*Cins(k));
  Zins(i,k) = Rins(i)*Xins(k)/(Rins(i) + Xins(k));
  Zp = Rp + j*Xp;
  Zs = Rs+ j*Xs;
  Zm = Rm *j*Xm / (Rm+j*Xm);
  Zburden = Rb + j*Xb;
  Zsb = Zs+Zburden;
  Zsbm = Zm*Zsb/(Zm+Zsb);
  Zeffective = Zsb + 0.5*Zp;
  Zpeffective(i,k) = 0.5*Zp*Zins(i,k)/(0.5*Zp+Zins(i,k));
  Ztotal(i,k) = Zeffective + Zpeffective(i,k);
  Vp(i,k) = Ztotal(i,k)*Ip;
  Is= Ip*Zm/(Zm+Zsb);
  Im = Ip*Zsb/(Zm+Zsb);
  Iins(i,k) = Is*0.5*Zp/(0.5*Zp+Zins(i,k));
  Iburden = Is;


end
end
```

APPENDIX D

Steady State Analysis

1.Insulation Failure between Primary winding and Ground

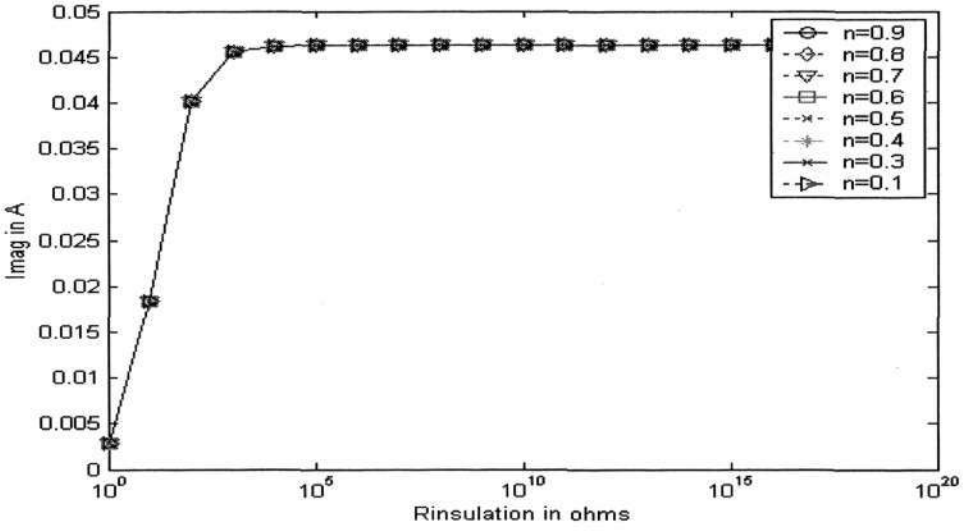

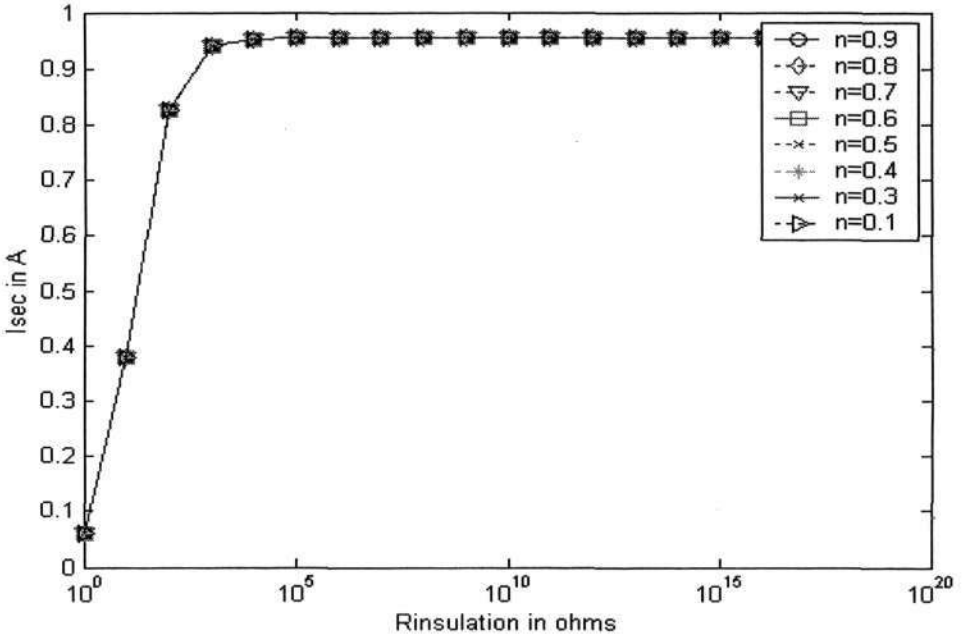

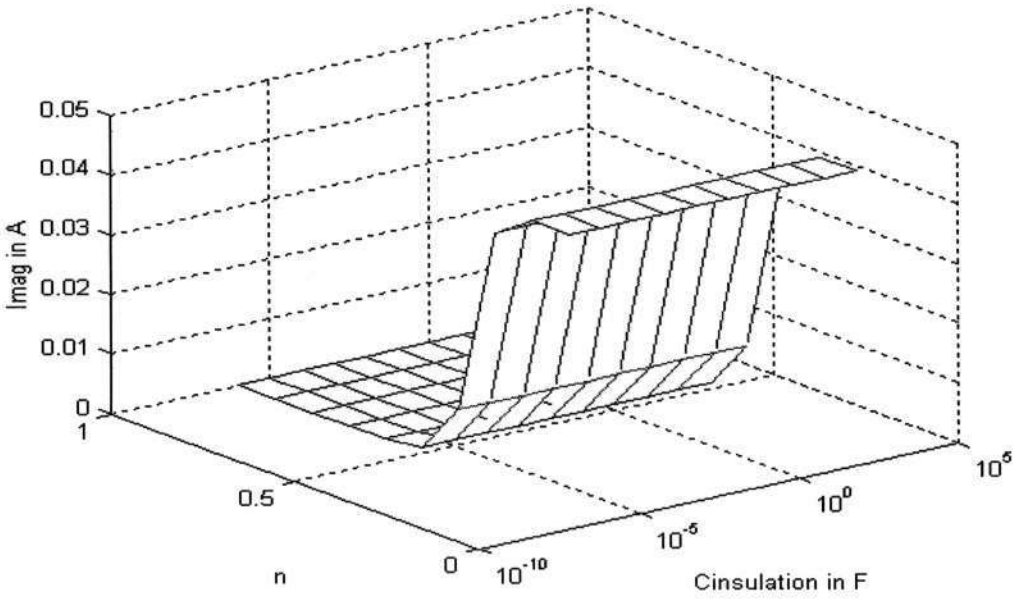
0.05
0.04
0.03
0.02
0.01
0
Imag in A
1
0.5
0
n
10^{-10}
10^{-5}
10^{0}
10^{5}
Cinsulation in F

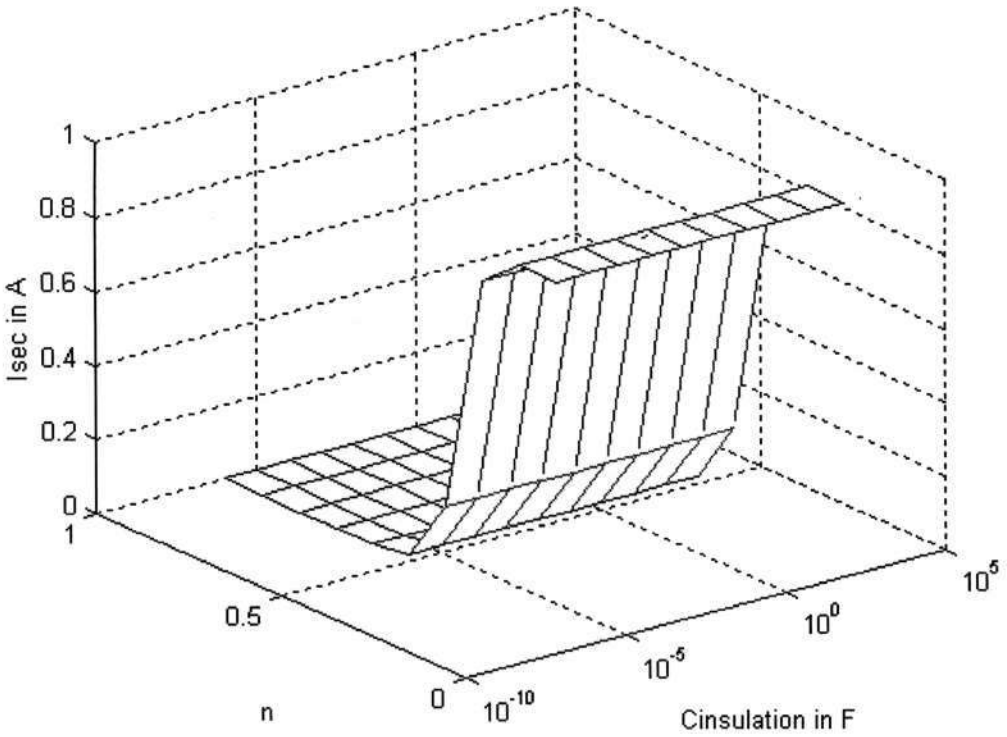
1
0.8
0.6
0.4
0.2
0
Isec in A
1
0.5
0
n
10^{-10}
10^{-5}
10^{0}
10^{5}
Cinsulation in F

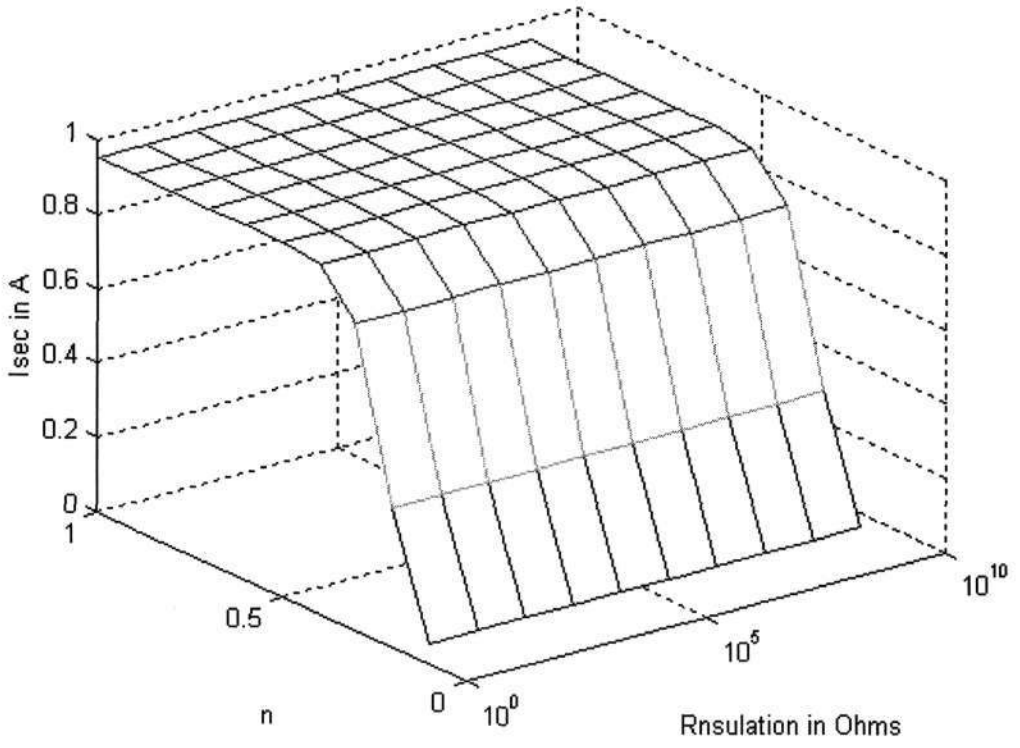
1
0.8
0.6
0.4
0.2
0
Isec in A
1
0.5
0
n
10^0
10^5
10^{10}
Rnsulation in Ohms

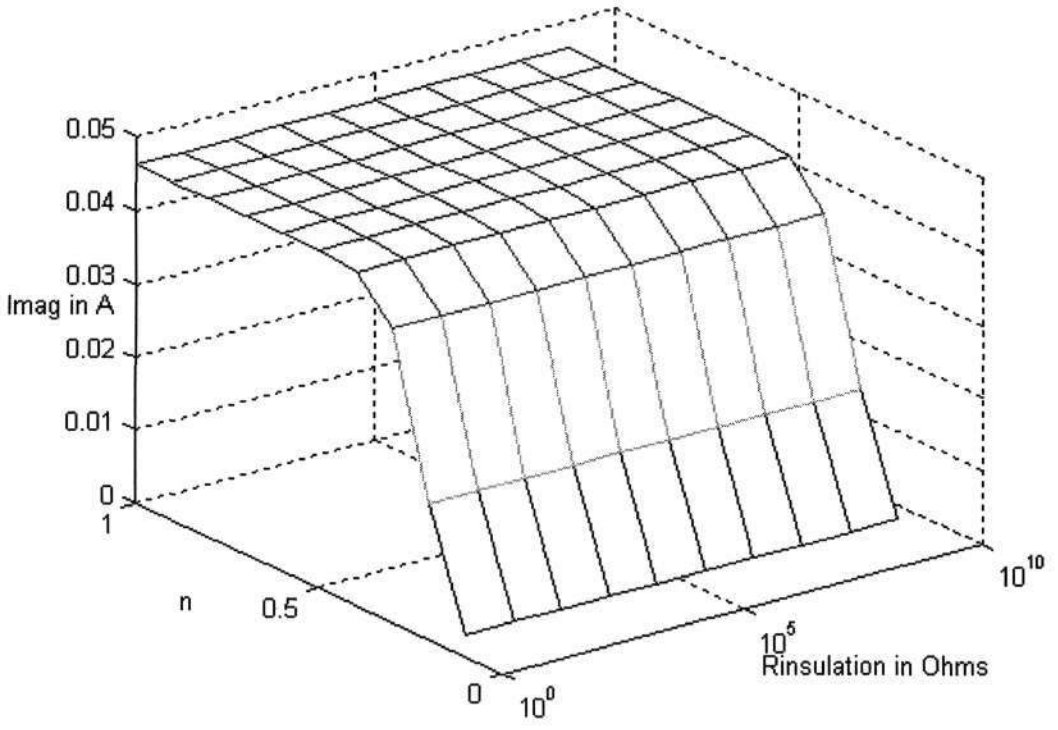
0.05
0.04
0.03
0.02
0.01
0
Imag in A
1
0.5
0
n
10^0
10^5
10^{10}
Rinsulation in Ohms

2. Insulation Failure between the Secondary Winding

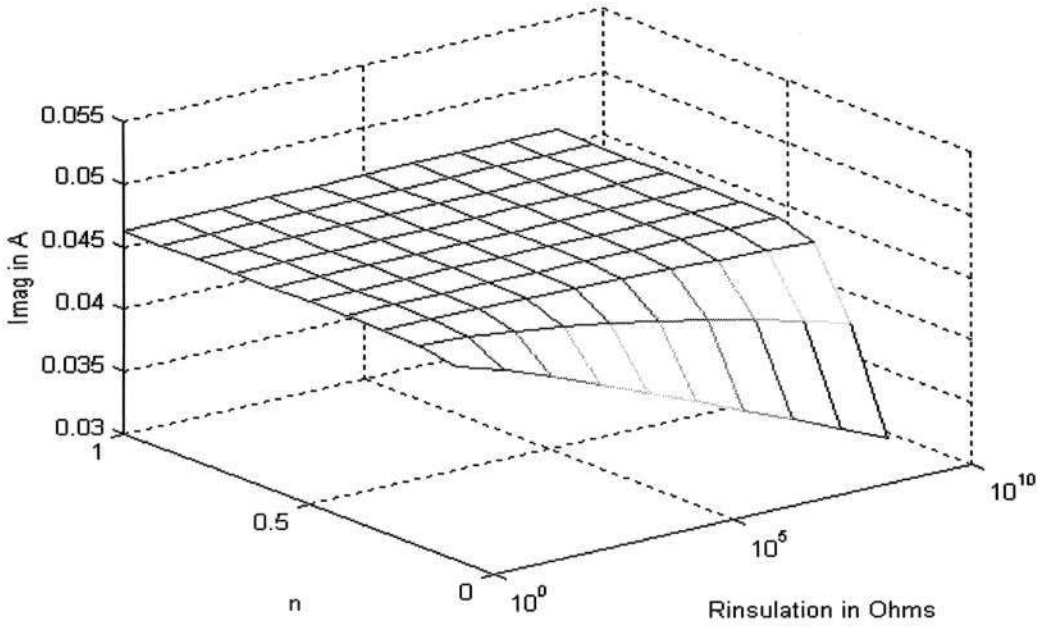

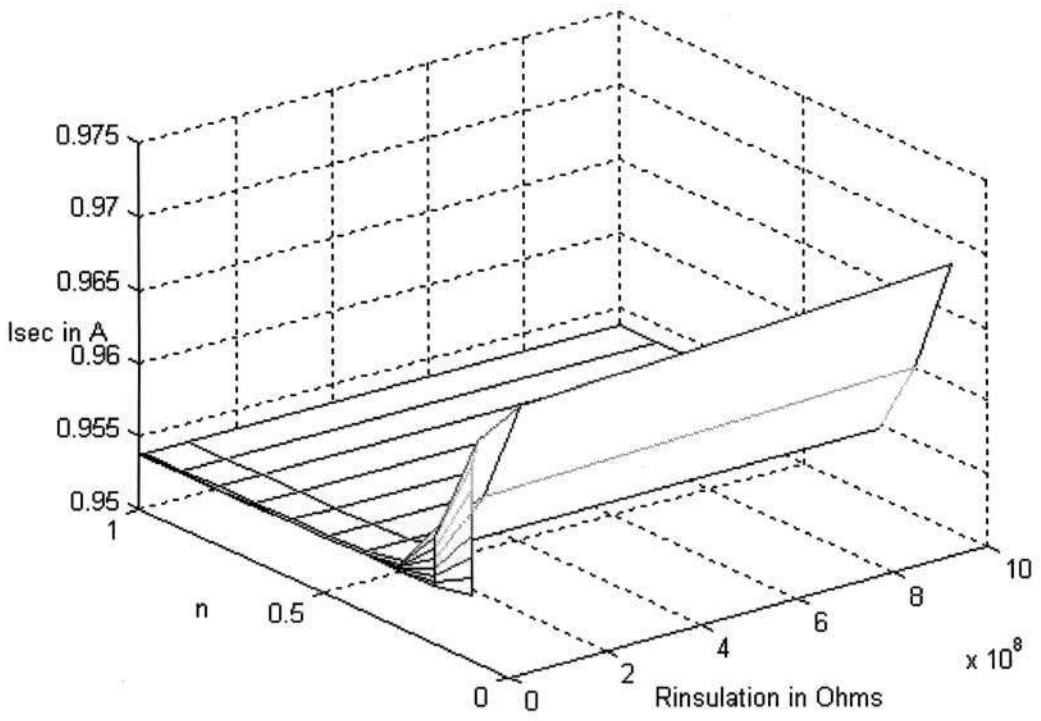

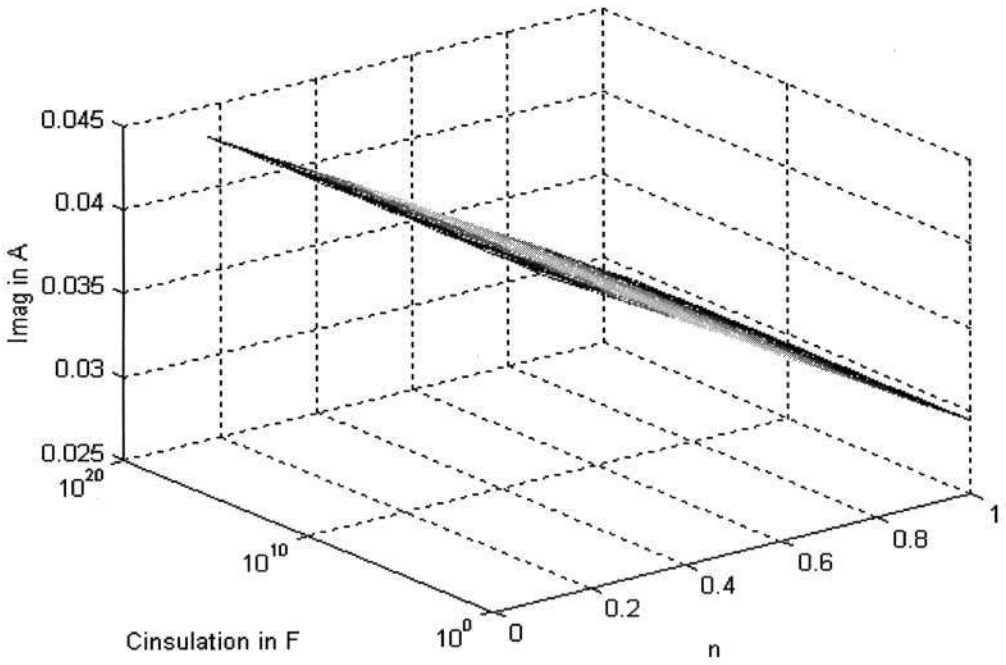
0.045
0.04
0.035
0.03
0.025
Imag in A
10^{20}
10^{10}
10^{0}
Cinsulation in F
0
0.2
0.4
0.6
0.8
1
n

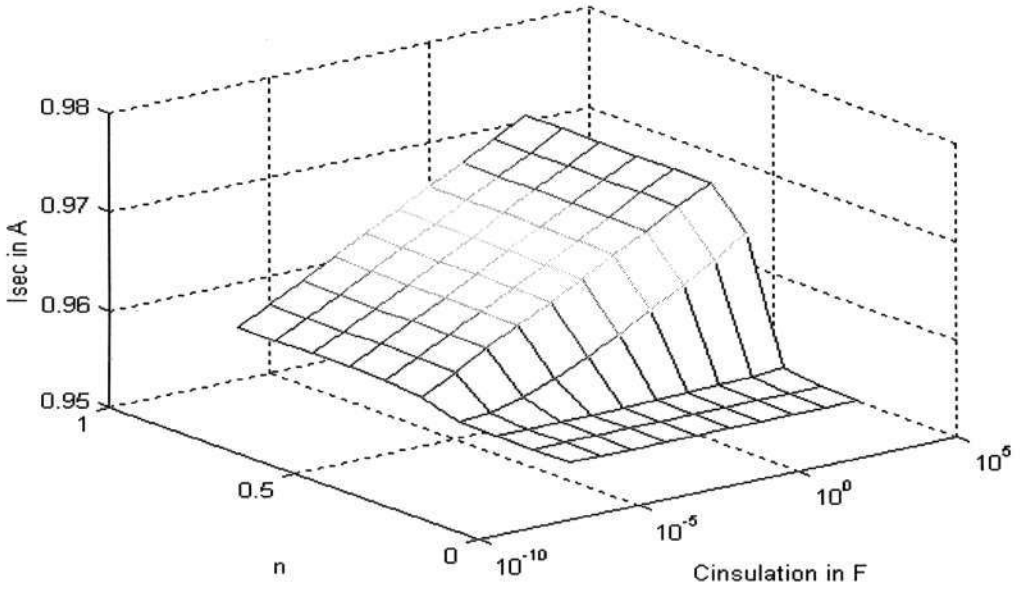
0.98
0.97
0.96
0.95
Isec in A
1
0.5
0
n
10^{-10}
10^{-5}
10^{0}
10^{5}
Cinsulation in F

3. Insulation Failure between Secondary and Primary Windings

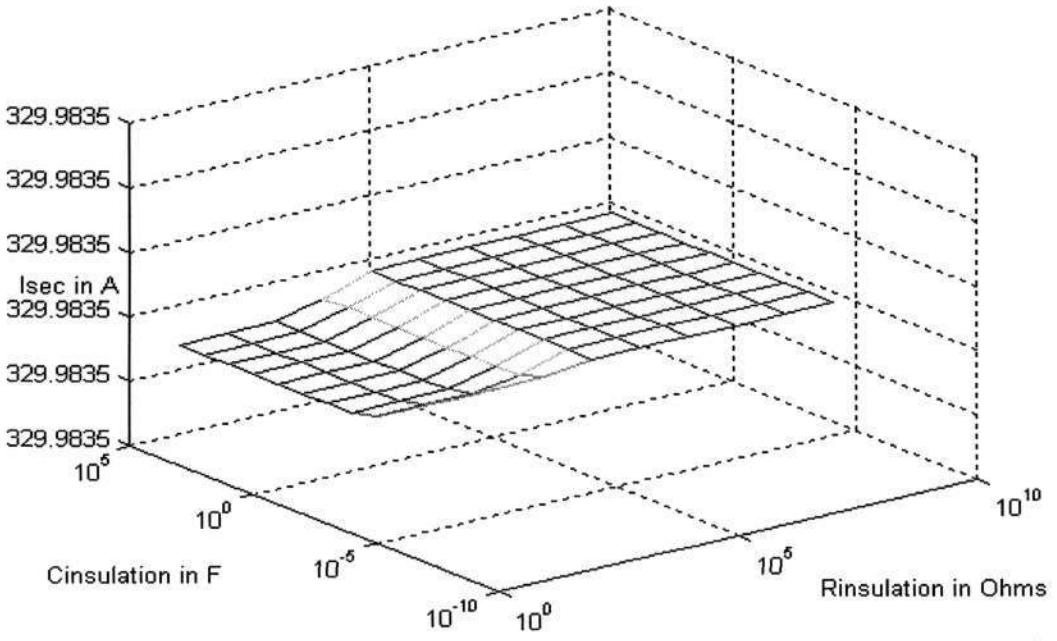

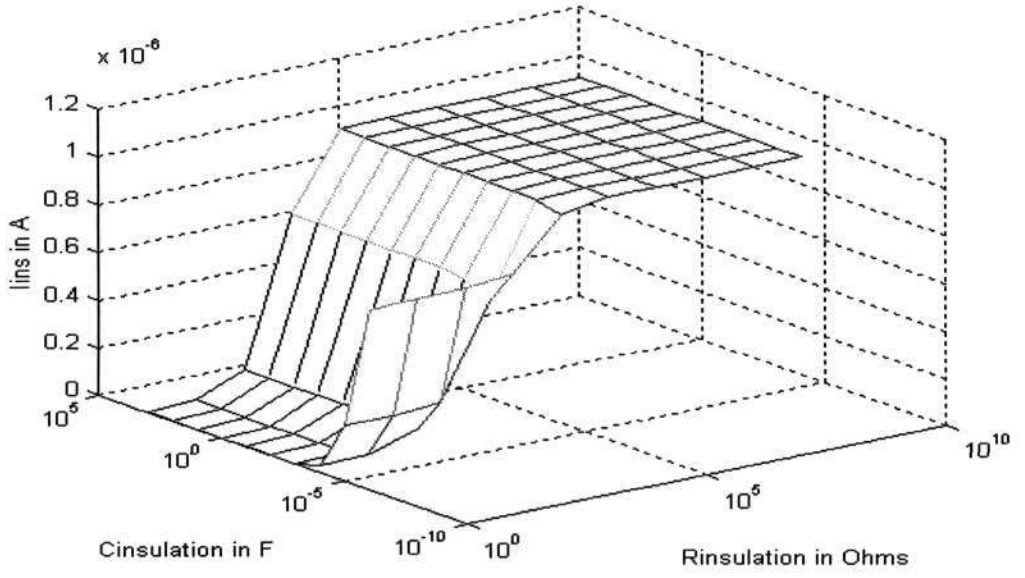

4. Insulation Failure between Secondary Winding and Ground

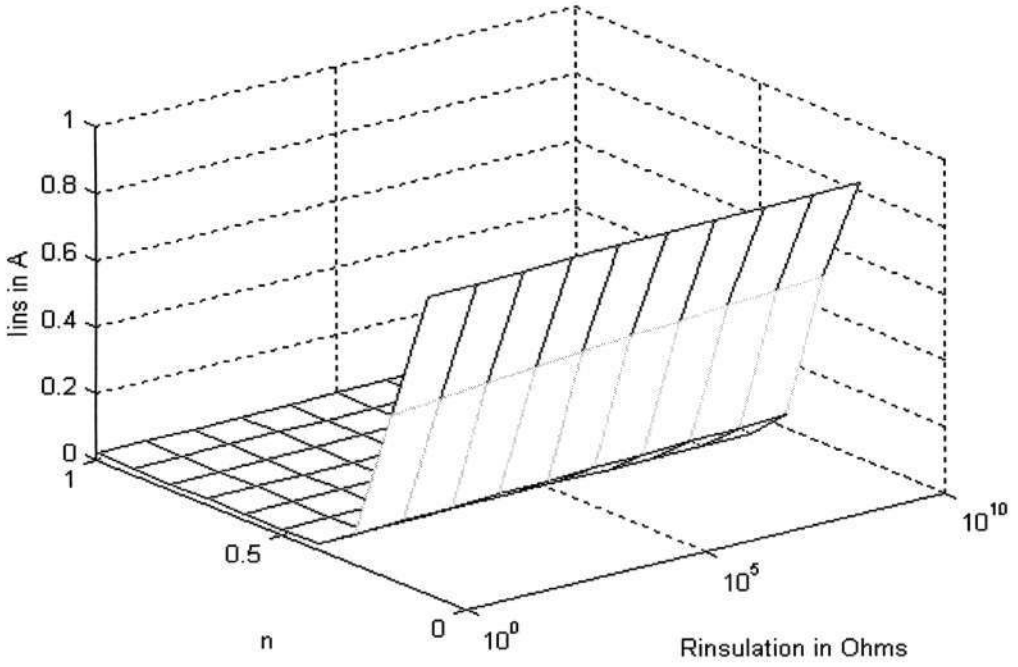

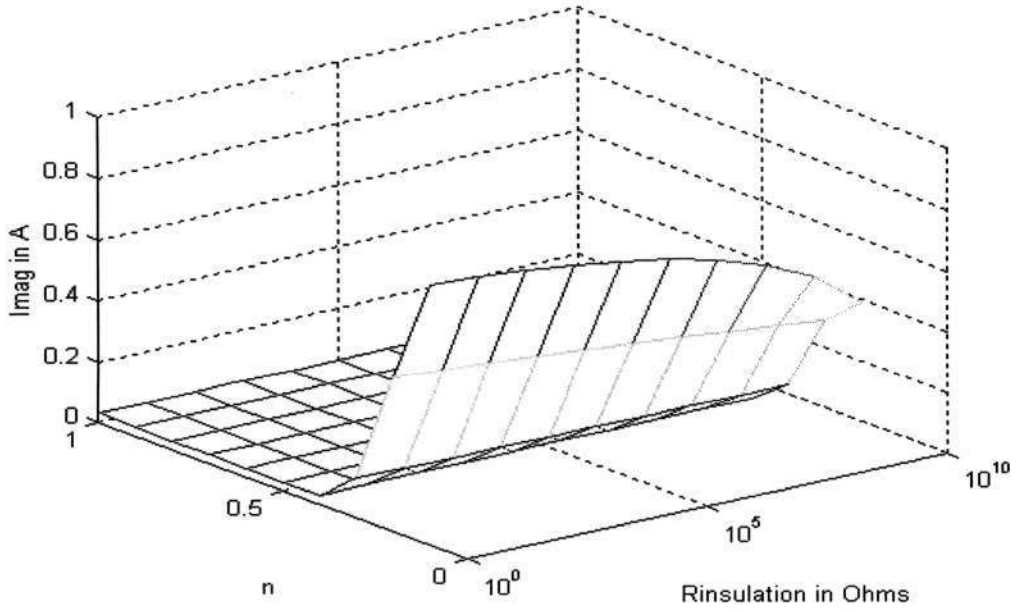

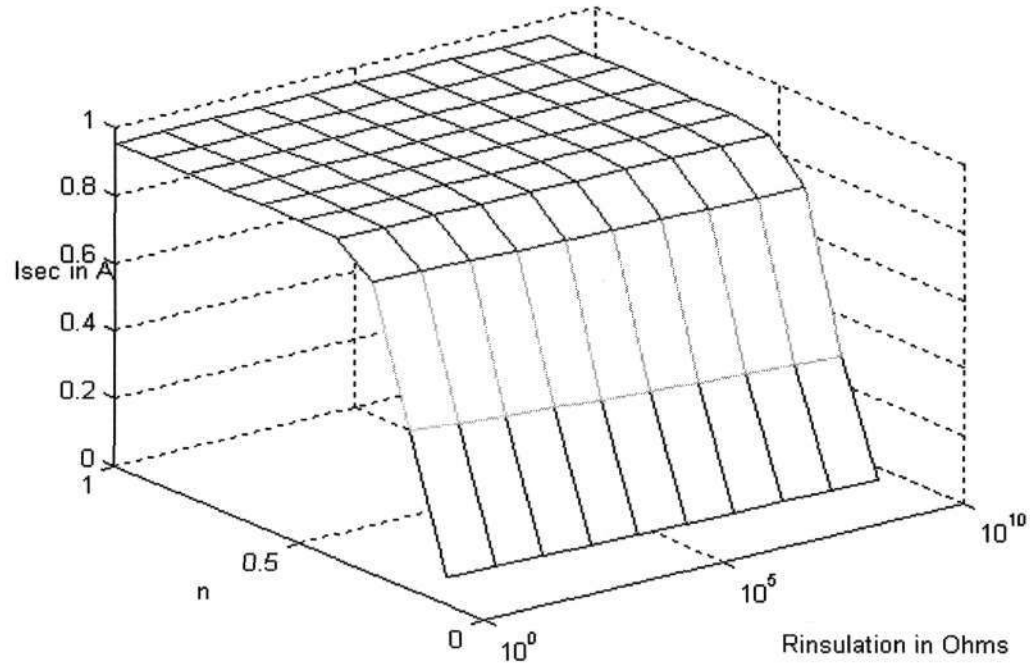
1
0.8
0.6
Isec in A
0.4
0.2
0
1
0.5
n
0
10^{0}
10^{5}
10^{10}
Rinsulation in Ohms

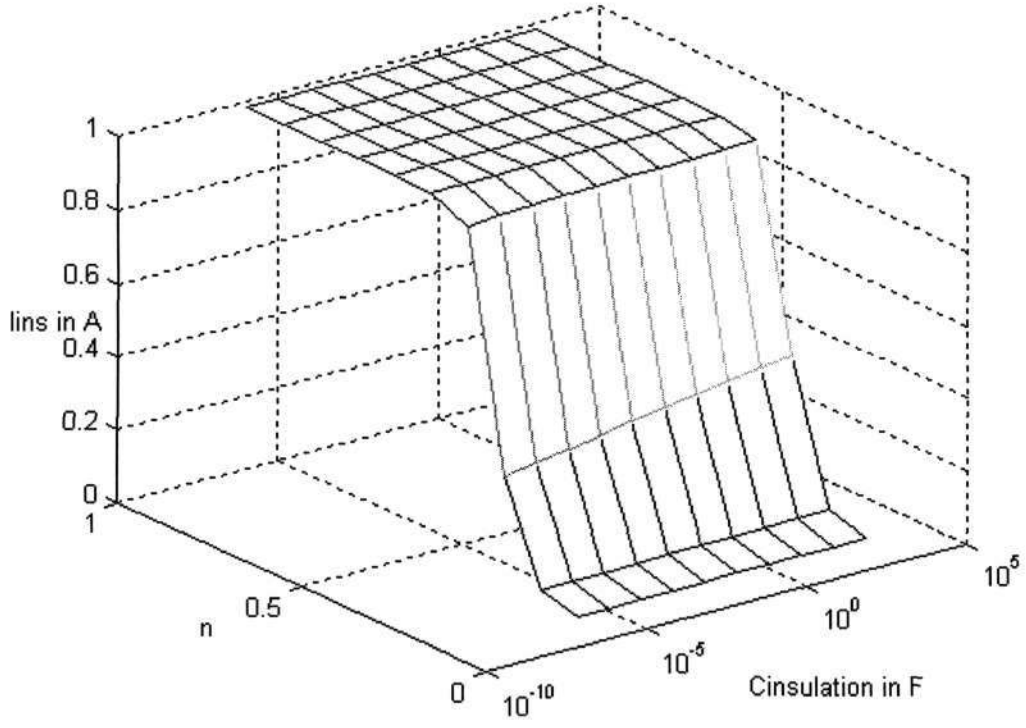
1
0.8
0.6
Iins in A
0.4
0.2
0
1
0.5
n
0
10^{-10}
10^{-5}
10^{0}
10^{5}
Cinsulation in F

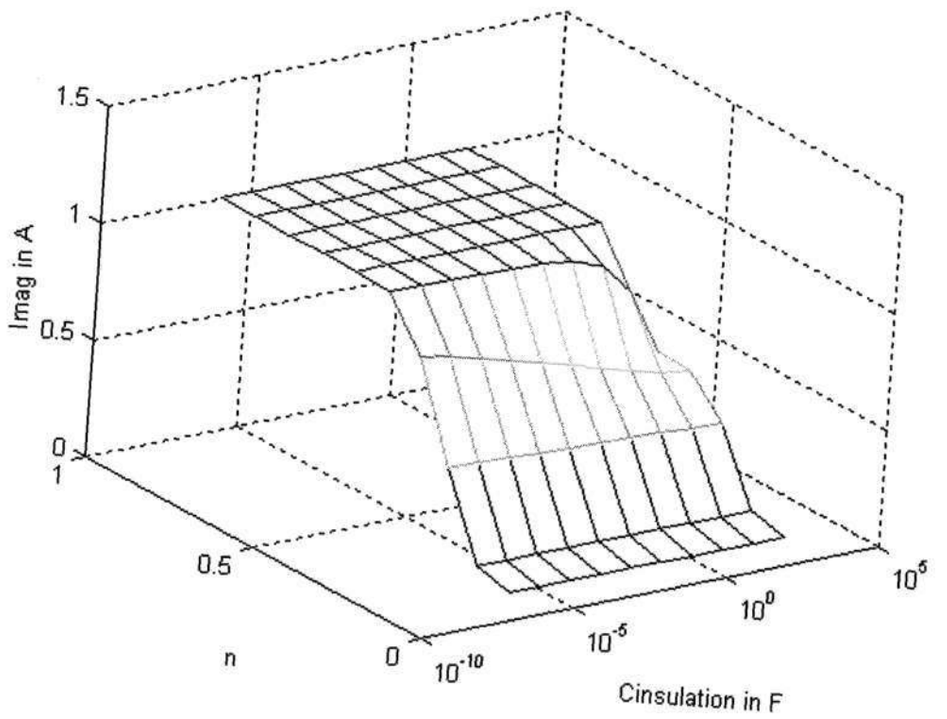
1.5
1
0.5
0
Imag in A
1
0.5
0
n
10^{-10}
10^{-5}
10^{0}
10^{5}
Cinsulation in F

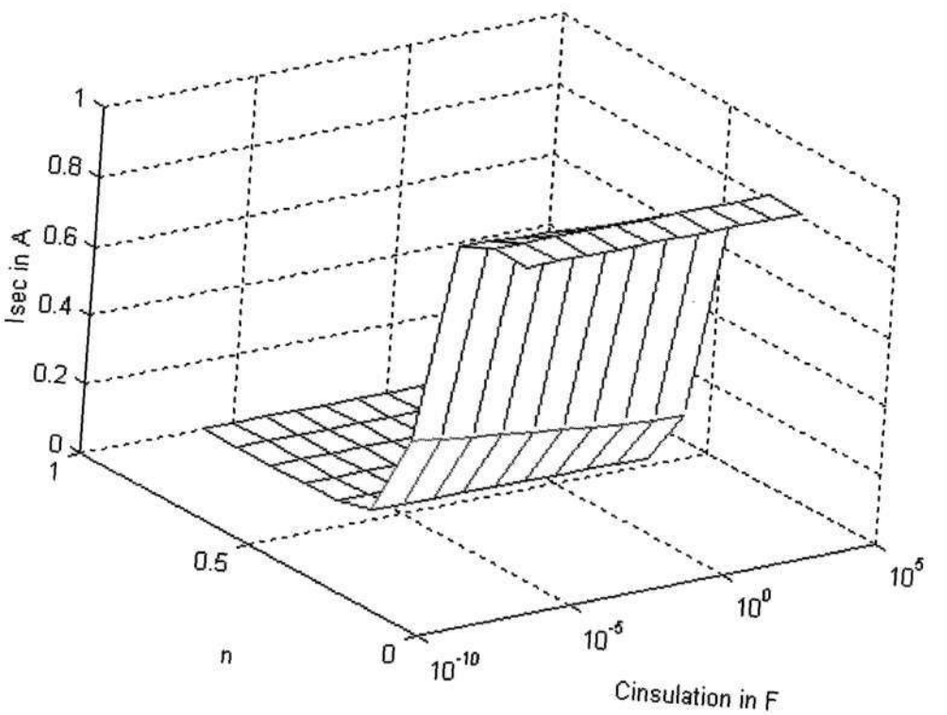
1
0.8
0.6
0.4
0.2
0
Isec in A
1
0.5
0
n
10^{-10}
10^{-5}
10^{0}
10^{5}
Cinsulation in F

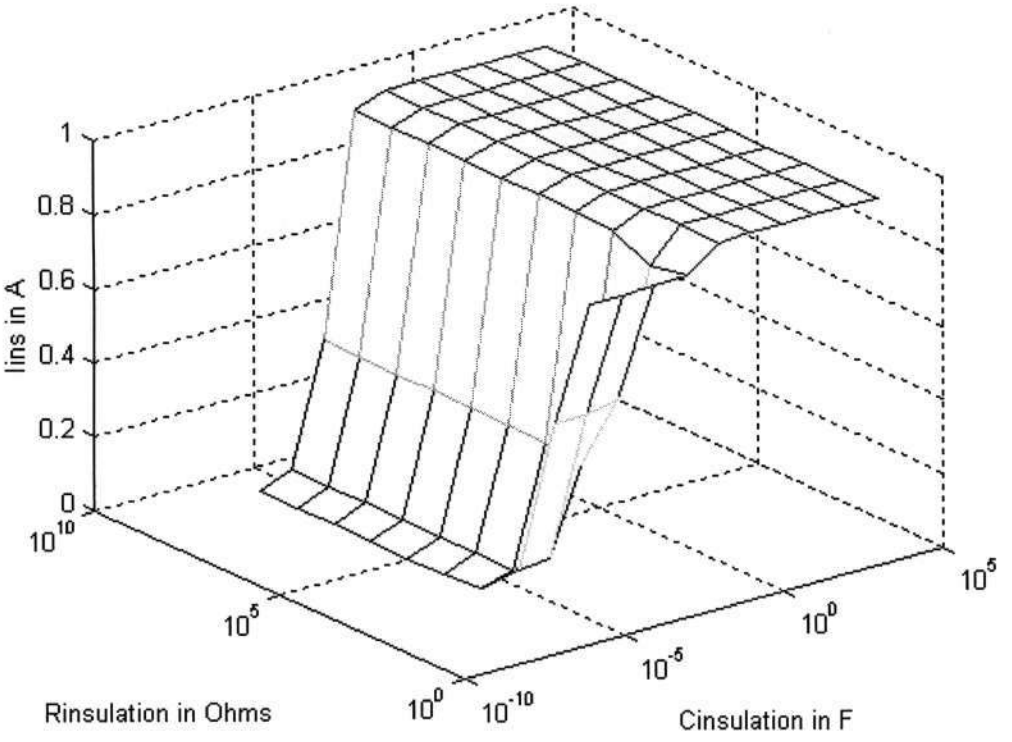
1
0.8
0.6
0.4
0.2
0
Iins in A
10^{10}
10^{5}
10^{0}
Rinsulation in Ohms
10^{-10}
10^{-5}
10^{0}
10^{5}
Cinsulation in F

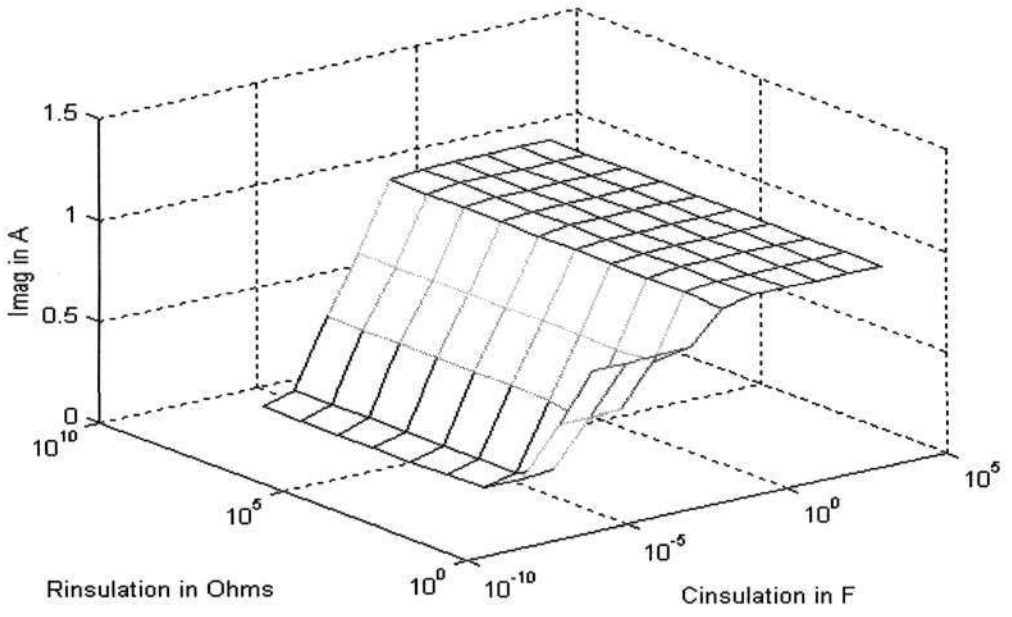
1.5
1
0.5
0
Imag in A
10^{10}
10^{5}
10^{0}
Rinsulation in Ohms
10^{-10}
10^{-5}
10^{0}
10^{5}
Cinsulation in F

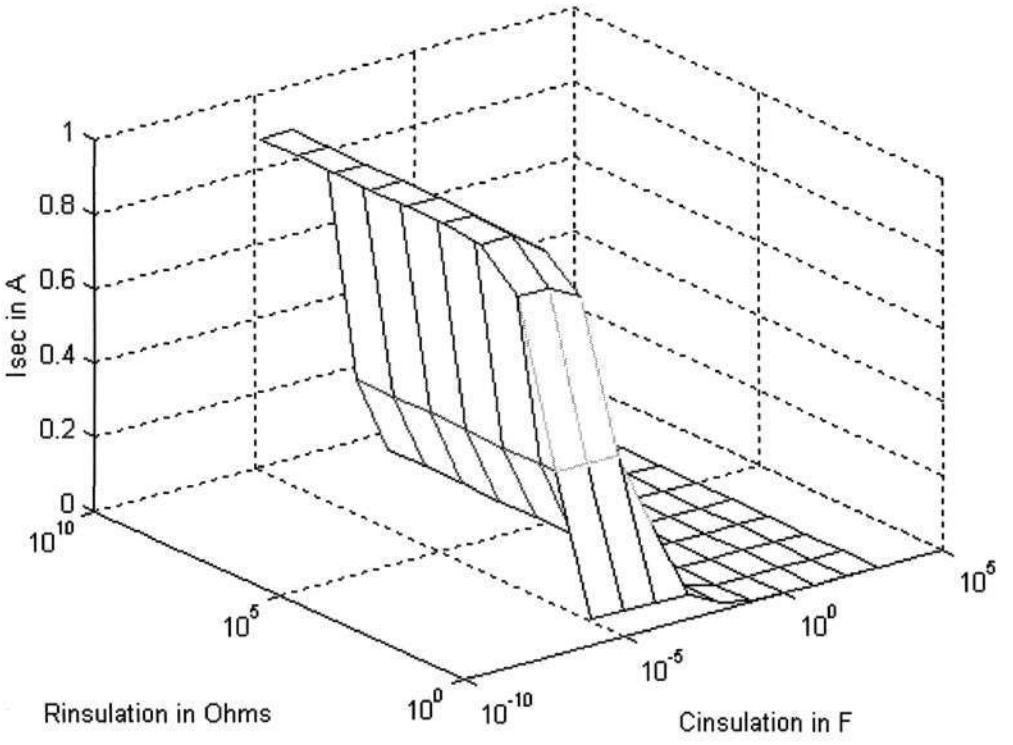

5. Insulation Failure between the Core and Ground

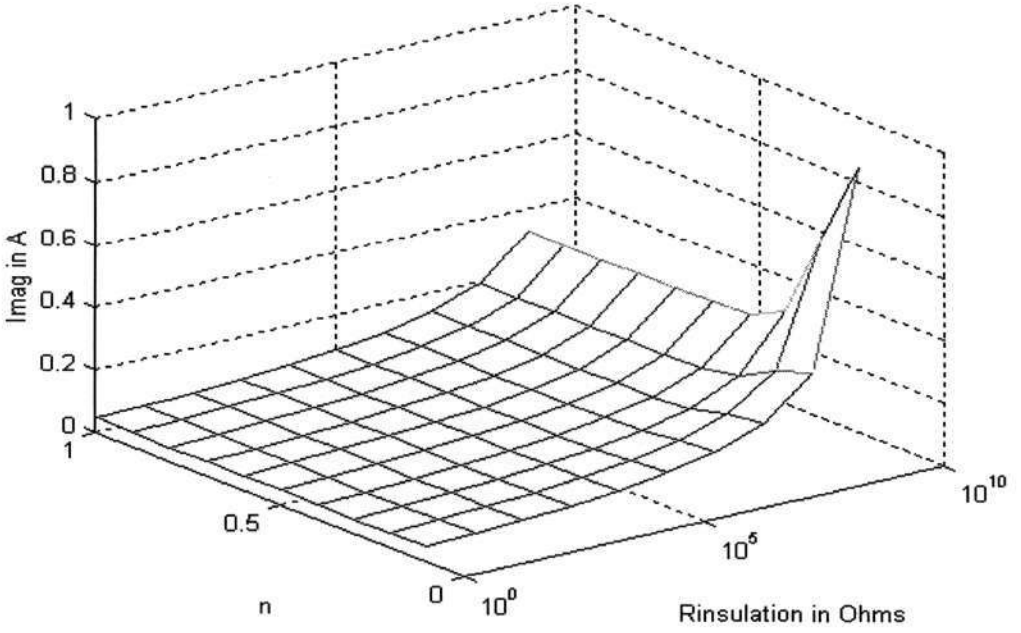

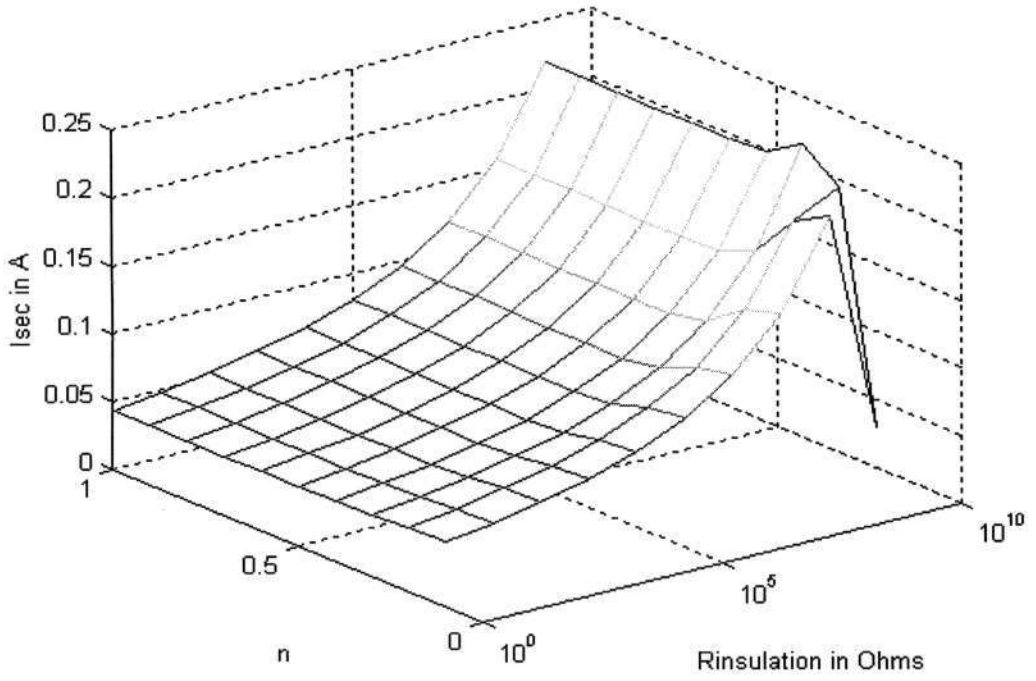
0.25
0.2
0.15
0.1
0.05
0
Isec in A
1
0.5
0
n
10^{0}
10^{5}
10^{10}
Rinsulation in Ohms

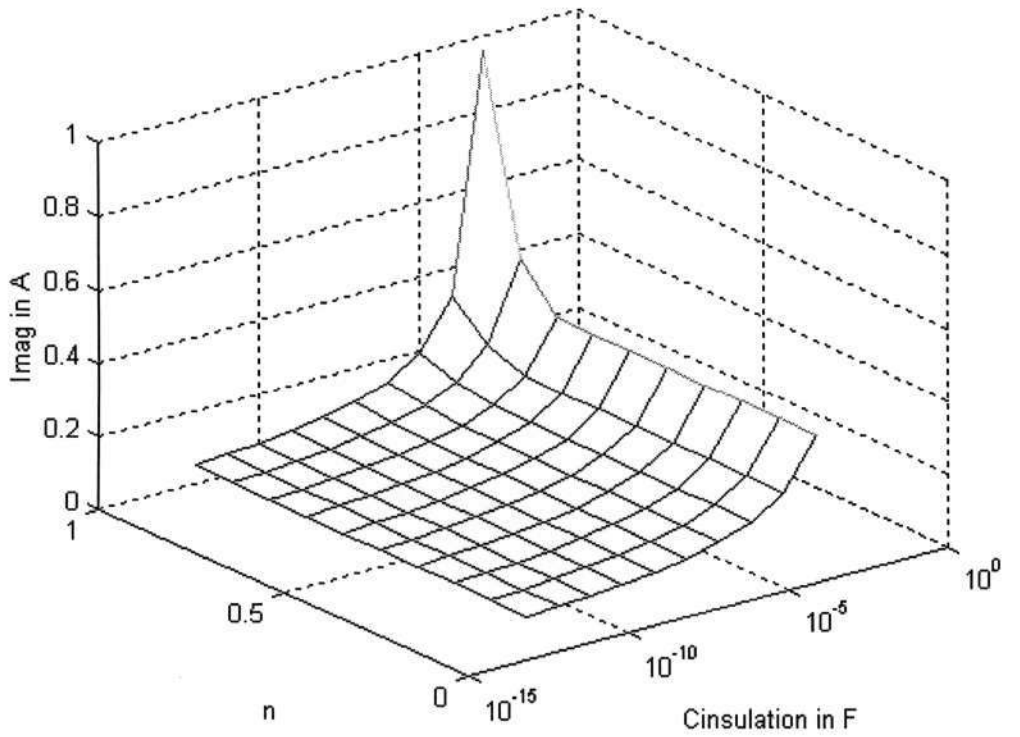
1
0.8
0.6
0.4
0.2
0
Imag in A
1
0.5
0
n
10^{-15}
10^{-10}
10^{-5}
10^{0}
Cinsulation in F

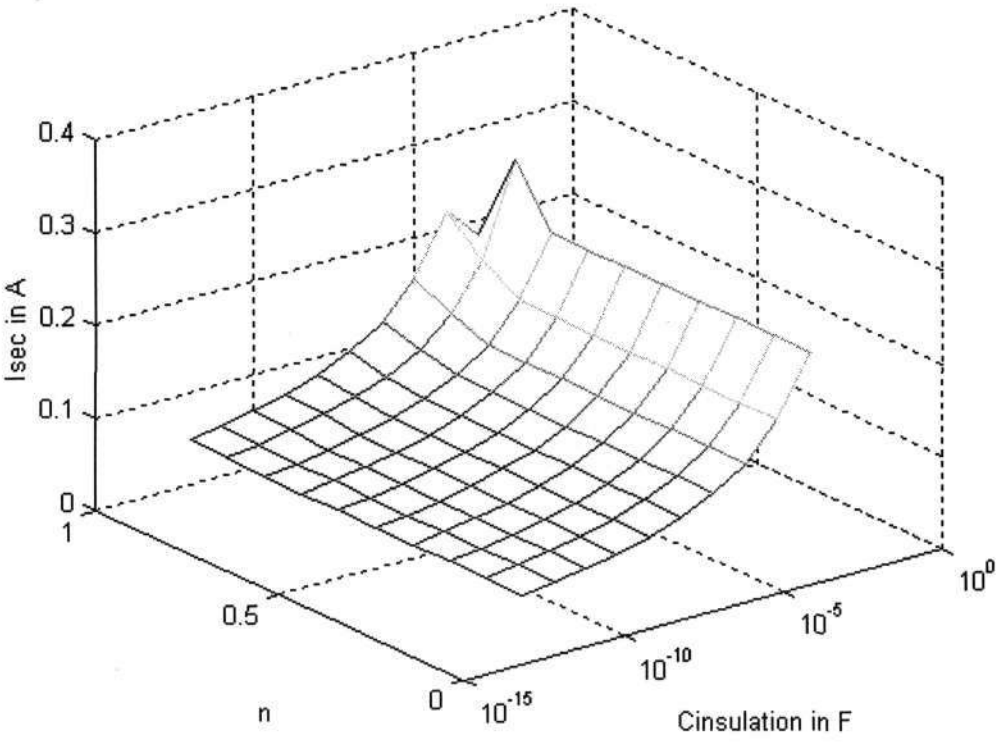

Transient State Results

1.Insulation Failure between Primary Winding and Ground

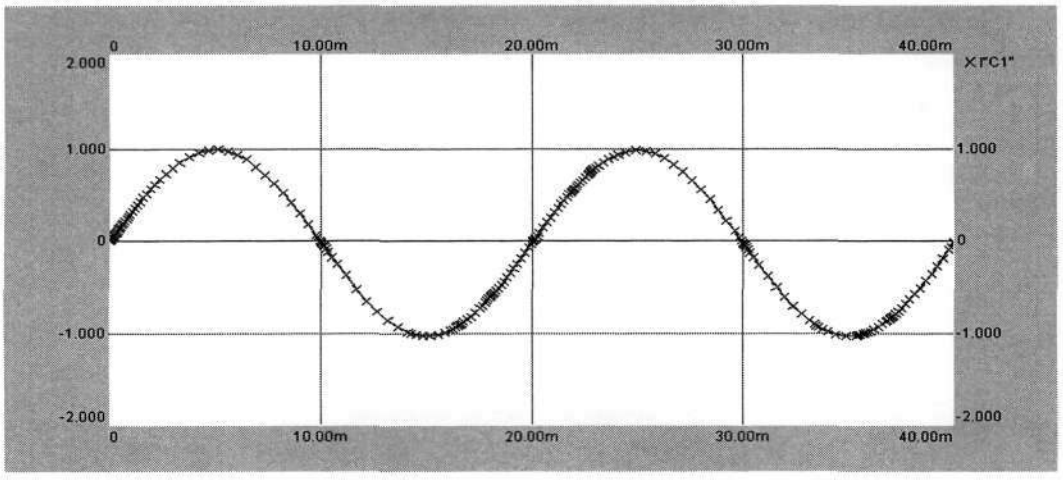

2. Insulation Failure between Primary and Secondary Windings

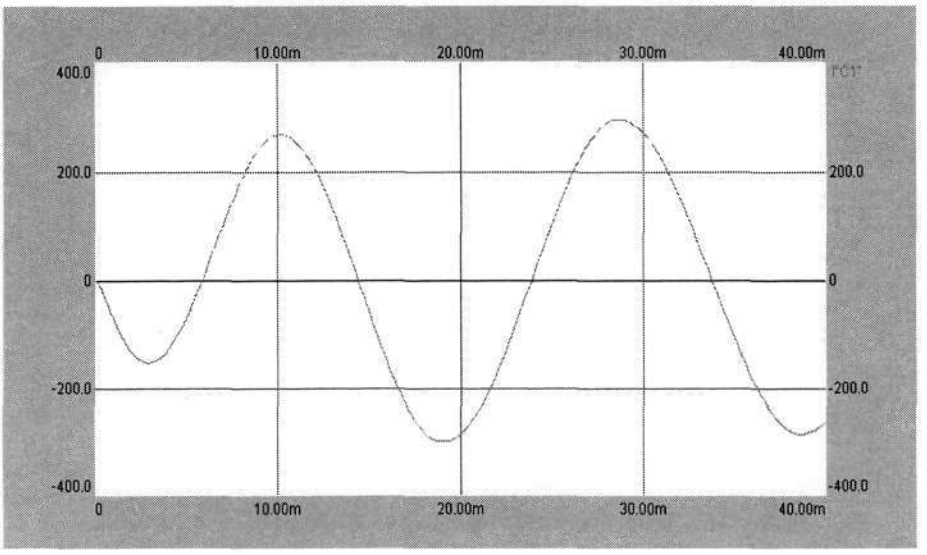

3. Insulation Failure between Secondary Winding

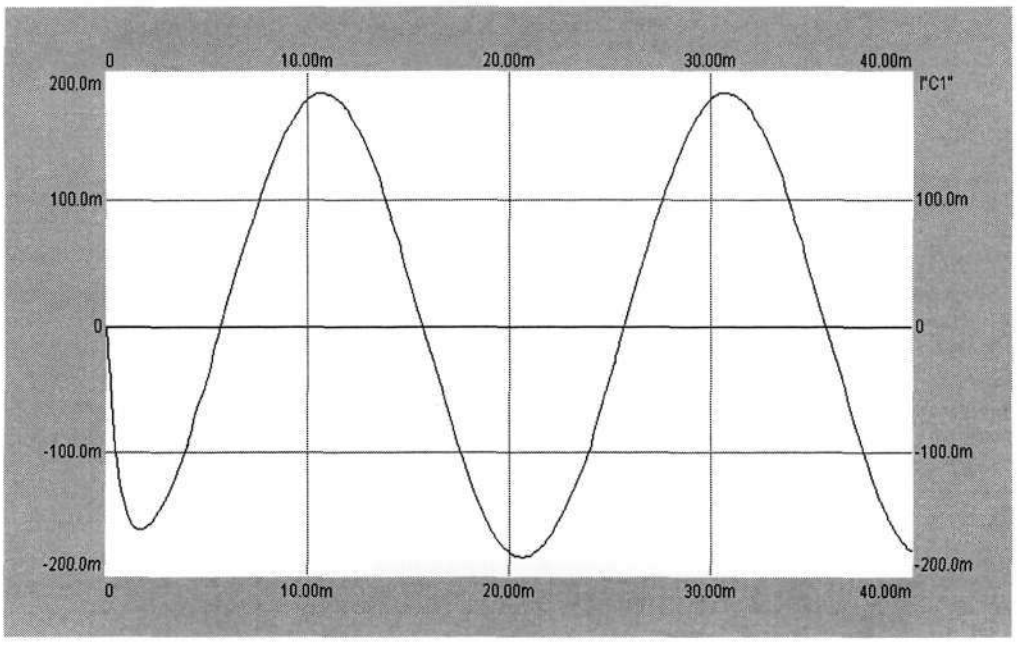

4. Insulation Failure between the Core and Ground

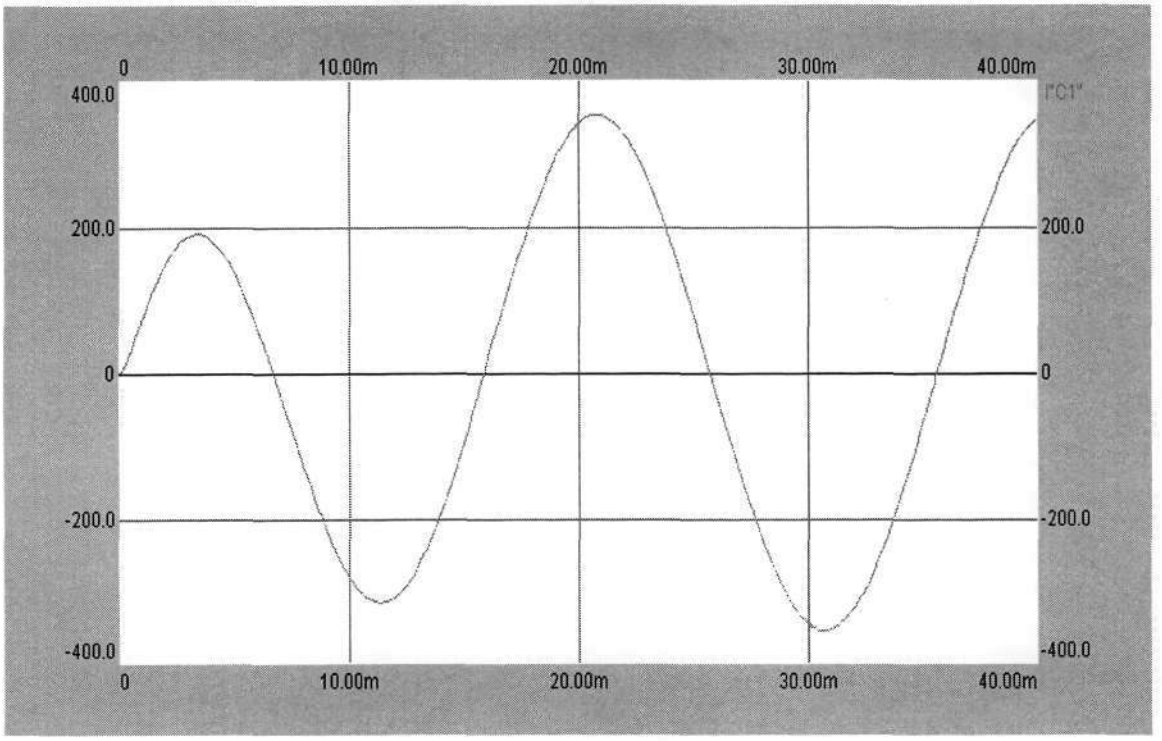

APPENDIX E

APPENDIX E1

Sample of circuits used for transient implementation in Simplorer

1. Insulation failure within Primary Windings only

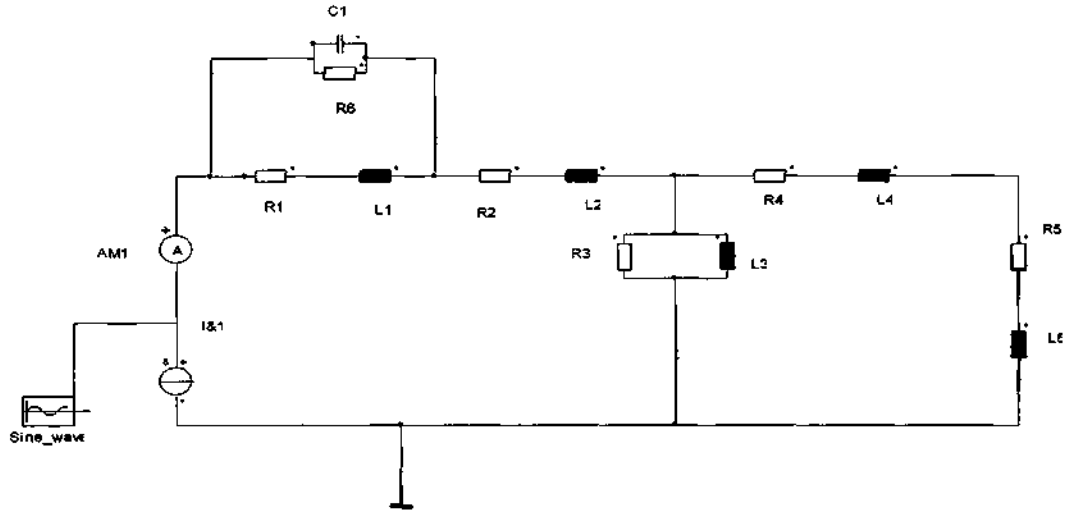

2. Insulation failure between Primary Windings and Ground